Electronic Supporting Information

Far-Red/Near-Infrared Emitting, Two-Photon Absorbing, and Bio-Stable Amino-Si-Pyronin Dyes

Kyeong Hwan Kim,[a] Subhankar Singha,*[a] Yong Woong Jun,[a] Ye Jin Reo,[a] Hye Rim Kim,[a] Hye Gun Ryu,[a] Snehasis Bhunia[b] and Kyo Han Ahn*[a]

[a.] Department of Chemistry, Pohang University of Science and Technology (POSTECH), 77 Cheongam-Ro, Nam-Gu, Pohang, Gyungbuk 37673, Republic of Korea. E-mail: subhankar@postech.ac.kr, ahn@postech.ac.kr
[b.] National Institute for Nanomaterials Technology (NINT), Pohang University of Science and Technology, 77 Cheongam-Ro, Nam-Gu, Pohang, Gyungbuk 37673, Republic of Korea.

Contents **Page No**

Supporting tables and figures S2-S15
Experimental procedures S16-S27
General methods
One-photon spectroscopic analysis
Fluorescence assays with the probe **ASiP^{i}-H_2O_2**
Quantum yield measurement
Two-photon property measurement
Preparation of cell samples and their confocal microscopic imaging
Two-photon microscopic imaging of cells
Cell viability assay
Synthetic procedures for the dyes
References
^{1}H NMR and ^{13}C NMR spectra S28-S51
HR Mass data (ESI^{+}) S52-S62
LCMS analysis data for selected compounds S63-S64

Supporting tables and figures

Table S1 Structure and photophysical properties of ASiP[a] **4**–**10** dyes

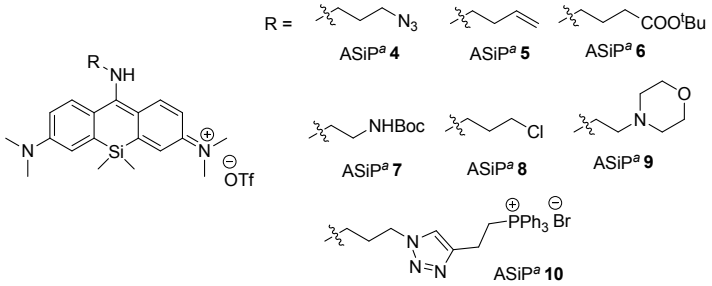

Comp.	λ_{abs} (nm)[a]	λ_{em} (nm)[b]	Φ_F[c]
ASiP[a] 4	459	612	0.36
ASiP[a] 5	459	613	0.53
ASiP[a] 6	462	608	0.26
ASiP[a] 7	462	606	0.59
ASiP[a] 8	462	612	0.53
ASiP[a] 9	464	617	0.31
ASiP[a] 10	469	609	n.d.[d]

[a]The maximum absorption wavelength and [b]the maximum emission wavelength in PBS (pH 7.4). [c]Fluorescence quantum yields determined in ethanol using rhodamine 101 as reference dye (Φ = 0.915 in ethanol). [d]n.d. = not determined.

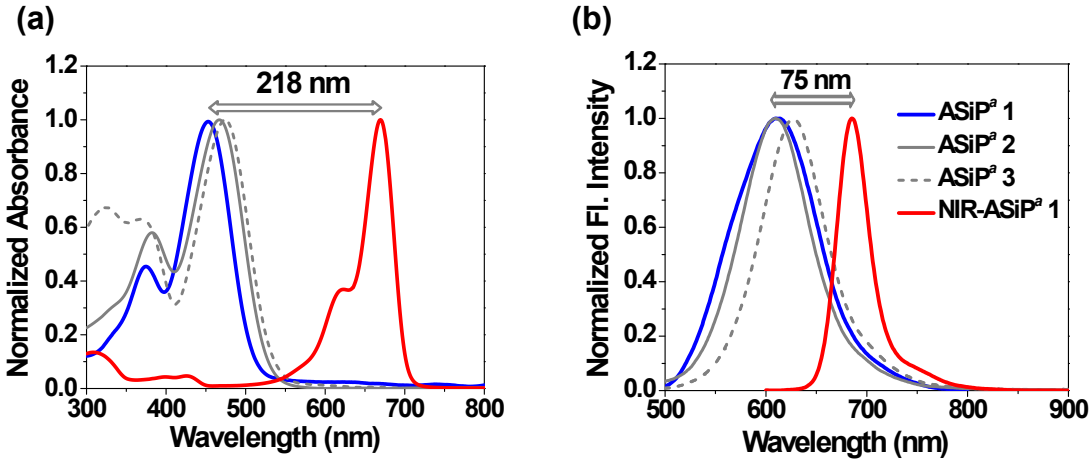

Fig. S1 Normalized (a) absorption and (b) emission spectra of ASiP[a] **1** (blue line), ASiP[a] **2** (gray solid line), ASiP[a] **3** (gray dash line) and NIR-ASiP[a] **1** (red line) in PBS (pH 7.4) containing 1% DMSO. The emission spectra were obtained by excitation at the maximum absorbance wavelength of each dye.

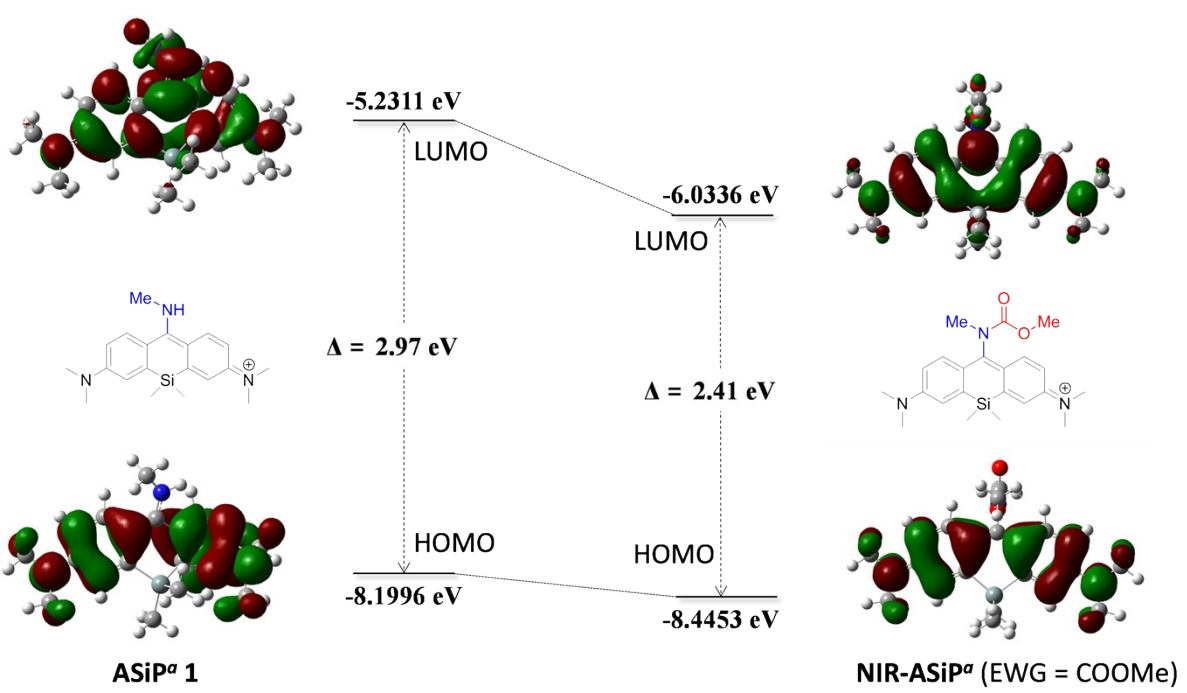

Fig. S2 Calculated HOMO-LUMO energy levels and the corresponding electronic distribution of ASiP^a **1** and a simplified NIR-ASiP^a (EWG = -CO_2Me**)**. The calculations were performed using Gaussian 09 (B3LYP method).

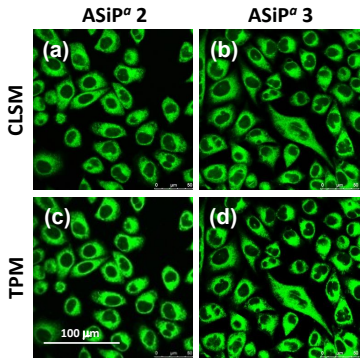

Fig. S3 (a, b) Confocal laser-scanning microscopic (CLSM) images of HeLa cells incubated with ASiP^a **2** and ASiP^a **3**, respectively. The emissions were collected in the range of 498–800 nm upon excitation at 488 nm. (c, d) Two-photon microscopic (TPM) images of HeLa cells treated with ASiP^a **2** and ASiP^a **3**, respectively. The emissions were collected in the range of 500–675 nm upon two-photon excitation at 900 nm. The HeLa Cells were incubated with 10 μM of each ASiP^a dye for 30 min.

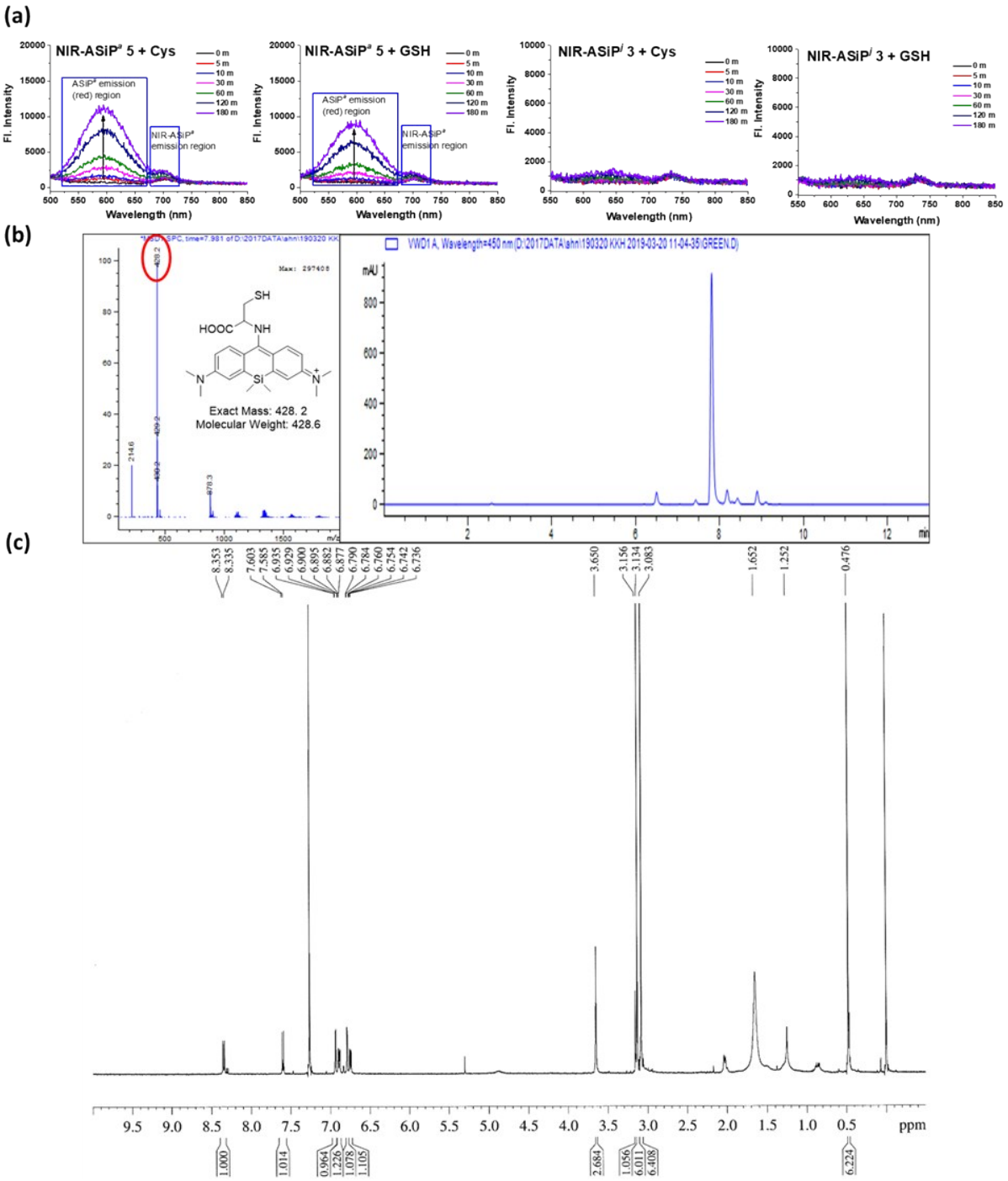

Fig. S4 (a) Time-dependent (up to 30 min) fluorescence spectral changes of NIR-ASiP^a **5** (10 μM) and NIR-ASiP^j **3** (10 μM) upon addition of glutathione (GSH, 500 μM) and cysteine (Cys, 500 μM), respectively, in 1:1 PBS/dioxane (v/v) at 37 °C. The spectral changes suggest that NIR-ASiP^a **5** underw substitution with these thiols. In the case of Cys, NIR-ASiP^a **5** was converted into the corresponding ASiP^a-type adduct through thiol addition followed by intramolecular amine substitution. Such amine adducts emit in the shorter wavelength (around 600 nm) region under excitation at 460 nm. The julolidine-derived analogue NIR-ASiP^j **3** that contains the same amine and electron-withdrawing moiety exhibited little response toward Cys and GSH. (b) LCMS data of a mixture of NIR-ASiP^a **5** (10

μM) and Cys (500 μM) in 1:1 water/dioxane (v/v) stirred at 36 °C for 24 h, showing the formation of the Cys-substituted ASiP^a as the major product with mass peak (*m*/*z*) at 428.2 under the reverse-phase chromatogram (with absorption at 450 nm). (c) ^{1}H NMR ($CDCl_3$, 500 MHz, 298 K) spectrum of the Cys-substituted ASiP^a **5** (Experimental: a mixture of NIR-ASiP^a **5** (0.03 mmol) and Cys (50 equiv.) in 1:1 water/dioxane (v/v) was stirred at 36 °C for 24 h. The Cys-adduct was formed as the major product, which was isolated by HPLC): δ 8.35 (d, J = 9.0 Hz, 1H), 7.60 (d, J = 9.0 Hz, 1H), 6.94 (d, J = 9.0 Hz, 1H), 6.90 (dd, J = 9.0, 3.0 Hz, 1H), 6.79 (d, J = 9.0 Hz, 1H), 6.76 (dd, J = 9.0, 3.0 Hz, 1H), 3.66 (s, 2H), 3.16 (s, 1H), 3.13 (s, 6H), 3.08 (s, 6H), 0.48 (s, 6H).

Analysis methods: HPLC and LCMS were performed on an Agilent system with C18 reversed phase column (Eclipse XDB, 3.5 μm, 4.6 mm × 150 mm). The signals were recorded at 450 nm as a function of retention time. A mixed solvent of H_2O (eluent A)/acetonitrile (eluent B) was used with a linear gradient elution profile: 0 min, 90% A; 7 min, 0% A; 13 min, 0% A was used as the mobile phase. The column temperature was maintained at 25 ºC and the flow rate of the mobile phase was 0.7 mL/min.

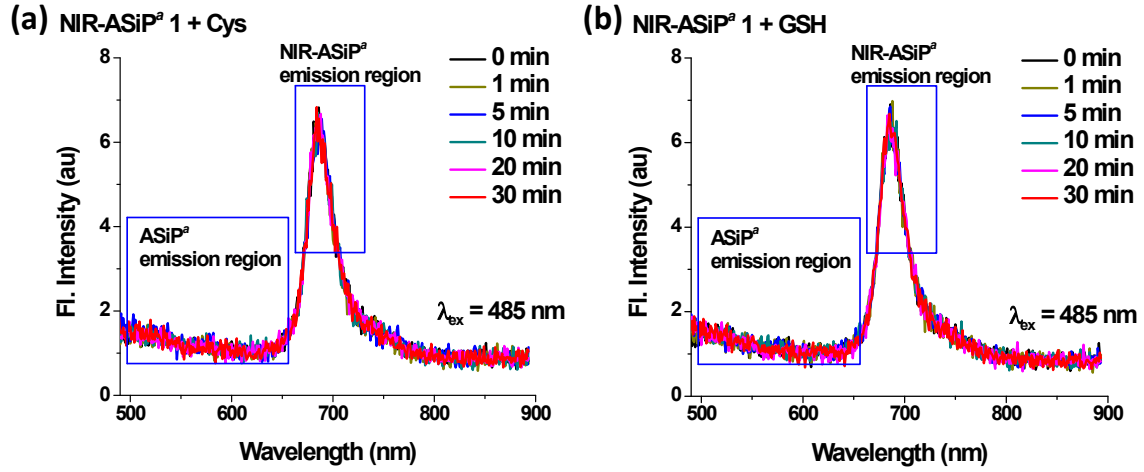

Fig. S5 Time dependent (up to 30 min) fluorescence spectral changes of NIR-ASiP^a **1** (10 μM) upon addition of (a) Cys (250 μM) and (b) GSH (10 mM) in PBS containing 1% DMSO. The emissions were collected upon excitations at shorter wavelength of 485 nm, to observe any emissions in the short wavelength region. The fluorescence spectral studies show that NIR-ASiP^a **1** containing less electron-withdrawing carbamate moiety at the C-10 amine does not react with biothiols (Cys or GSH) in only PBS buffer, as there appear no appreciable signals in the shorter wavelength (around 600 nm) region, except the desired NIR emission region.

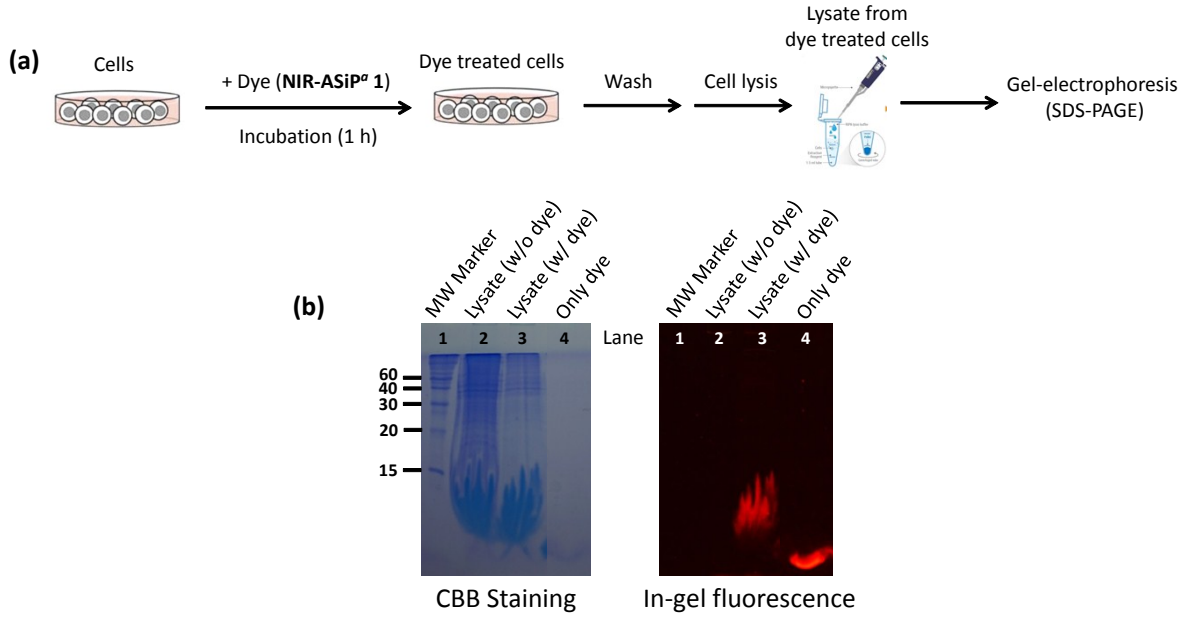

Fig. S6 Gel-electrophoresis analysis of cell lysate. (a) A549 cells were incubated with NIR-ASiP^a **1** dye (10 μM) for 1 h, washed with PBS buffer, and lysed with RIPA (RadioImmunoPrecipitation Assay) lysis buffer; the lysate was used for the gel-electrophoresis analysis. (b) Coomassie Brilliant Blue (CBB) staining and in-gel fluorescence imaging of the SDS-PAGE gel after electrophoresis analysis (18% PAA, 120 V, 90 min) show that the dye-treated cell lysate provides strong fluorescence due to labeling of cellular proteins. Lane 1: molecular weight marker (in kDa). Lane 2: lysate of cells without dye treatment. Lane 3: lysate of dye treated cells. Lane 4: only dye (1.0 μM).

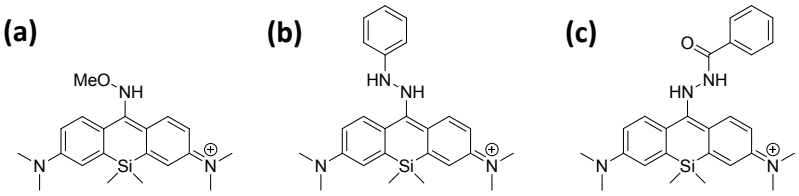

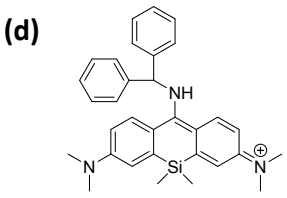

Fig. S7 (a–c)The structures of the ASiP^a analogues containing different amine substituents (methoxyamine, phenylhydrazine and benzhydrazide). (d) The structure of the ASiP^a analogue containing sterically hindered benzhydrylamine substituent.

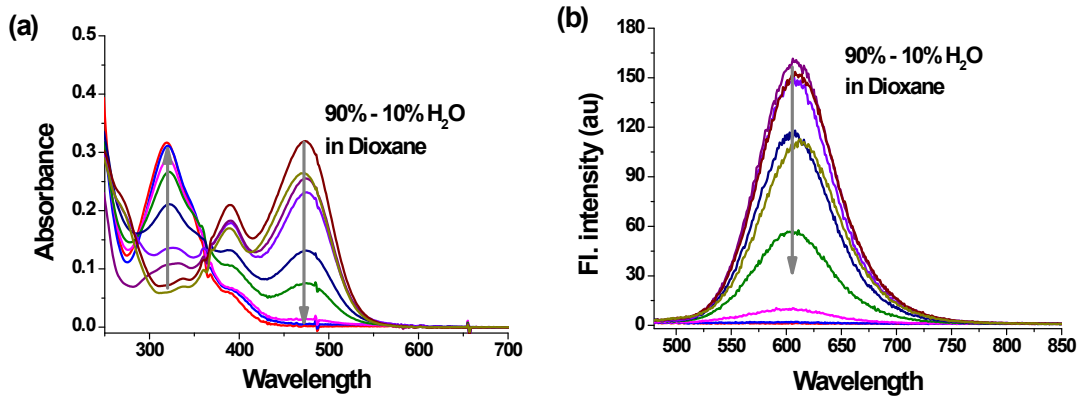

Fig. S8 (a) Absorption and (b) emission spectral changes of tetramethylamino analogue ASiP^{a} **2** (10 μM) in a mixture of water–dioxane with varying water content (90–10%). In accordance with the increasing dioxane content (thus, decreasing solvent polarity), the corresponding absorption spectra show a gradual decrease of absorbance at 472 nm (corresponding to fluorescent enamine form) and an increase at 320 nm (corresponding to non-fluorescent imine form); whereas the corresponding emission intensity gradually decreases with decreasing solvent polarity.

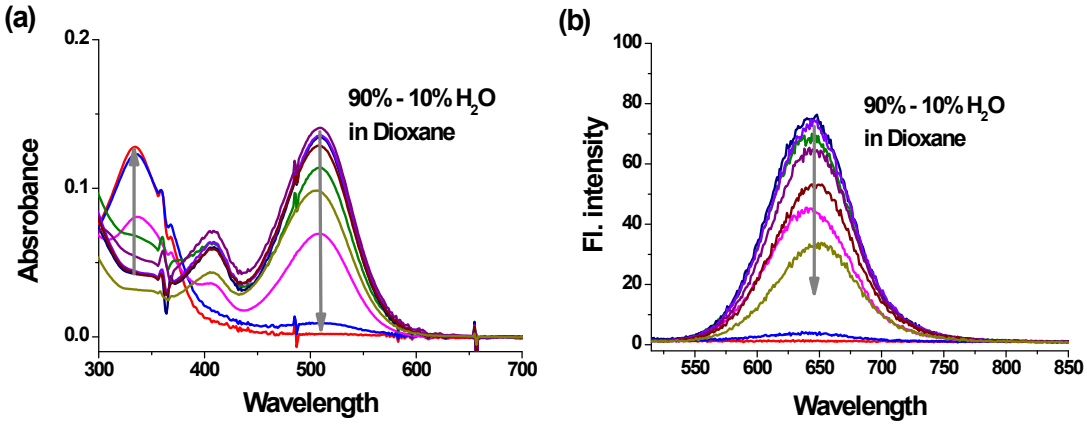

Fig. S9 (a) Absorption and (b) emission changes of julolidine derived ASiP^{j} **2** (10 μM) in a mixture of water–dioxane with varying water content (90–10%). In accordance with the increasing dioxane content (thus, decreasing solvent polarity), the corresponding absorption spectra show a gradual decrease of absorbance at 507 nm (corresponding to the fluorescent enamine form) and an increase at 335 nm (corresponding to the non-fluorescent imine form); whereas the corresponding emission intensity gradually decreases with decreasing solvent polarity.

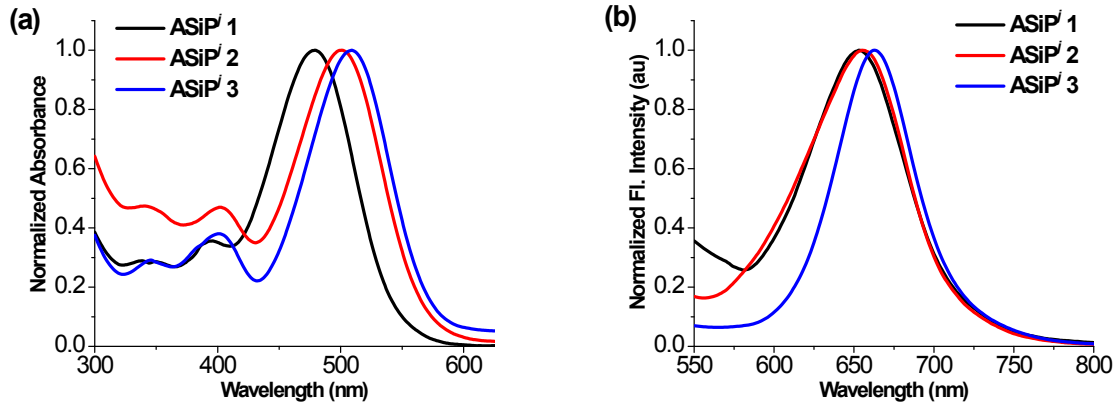

Fig. S10 Normalized (a) absorption and (b) emission spectra of ASiP^j **1** (black line), ASiP^j **2** (red line) and ASiP^j **3** (blue line) in *PBS buffer (pH 7.4)* containing 1% DMSO, with dye concentration at 1.0 µM. The emission spectra were collected by excitation at the corresponding maximum absorbance wavelength for each dye.

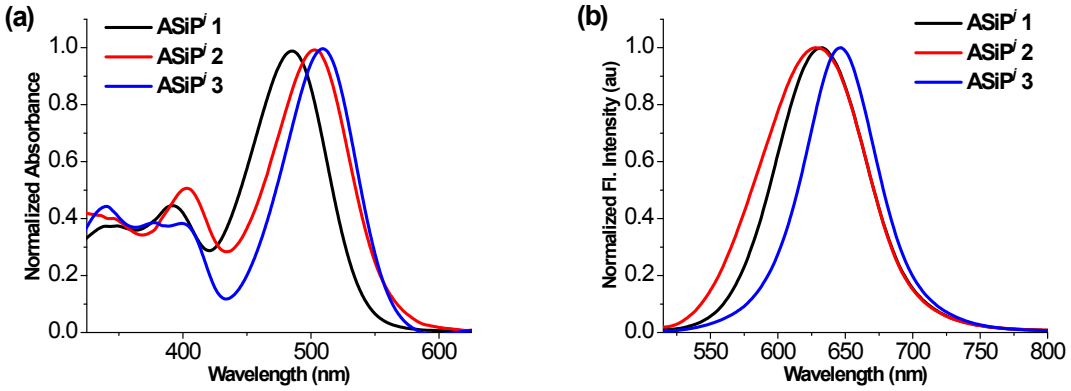

Fig. S11 Normalized (a) absorption and (b) emission spectra of ASiP^j **1** (black line), ASiP^j **2** (red line) and ASiP^j **3** (blue line) in ethanol (EtOH), obtained for each dye at 10 µM concentration. The emission spectra were collected by excitation at the corresponding maximum absorbance wavelength for each dye.

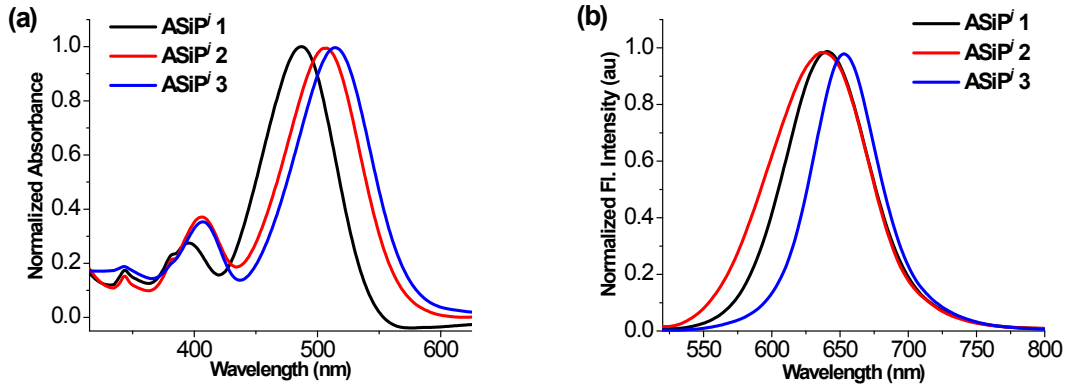

Fig. S12 Normalized (a) absorption and (b) emission spectra of ASiP^j **1** (black line), ASiP^j **2** (red line) and ASiP^j **3** (blue line) in *acetonitrile (CH_3CN)*, obtained for each dye at 10 µM concentration. The

emission spectra were collected by excitation at the corresponding maximum absorbance wavelength for each dye.

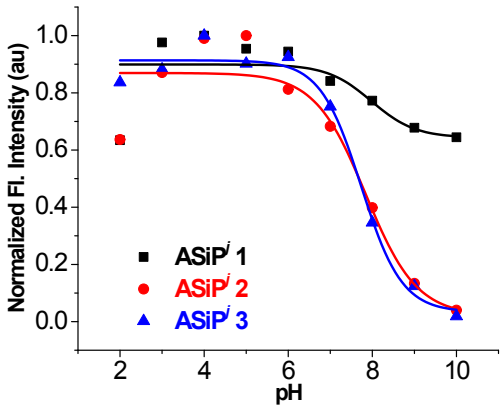

Fig. S13 pH-Dependent fluorescence intensity changes of ASiP^j **1** (black line), ASiP^j **2** (red line) and ASiP^j **3** (blue line). The emission spectra were monitored at the corresponding maximum emission wavelength by excitation at the corresponding maximum absorbance wavelength for each dye (10 μM).

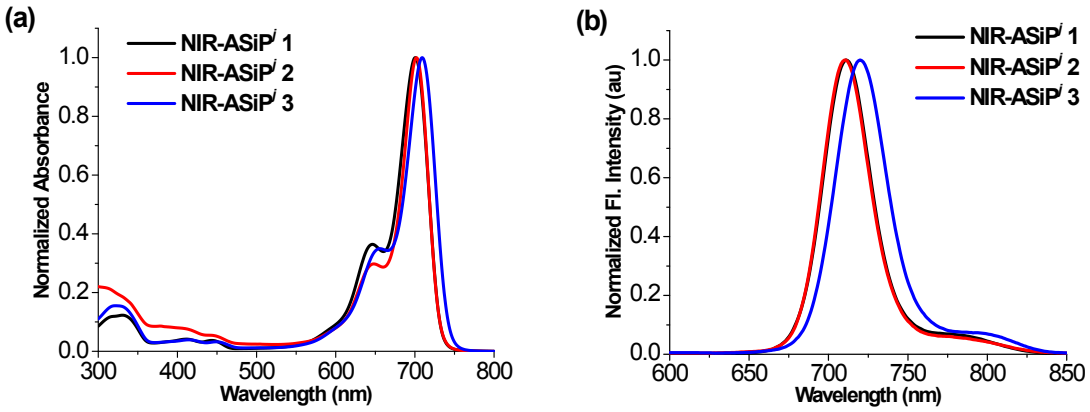

Fig. S14 Normalized (a) absorption and (b) emission spectra of NIR-ASiP^j **1** (black line), NIR-ASiP^j **2** (red line) and NIR-ASiP^j **3** (blue line) in *PBS buffer (pH 7.4)* with 1% DMSO, obtained for each dye at 10 μM concentration. The emission spectra were collected by excitation at the corresponding maximum absorbance wavelength for each dye.

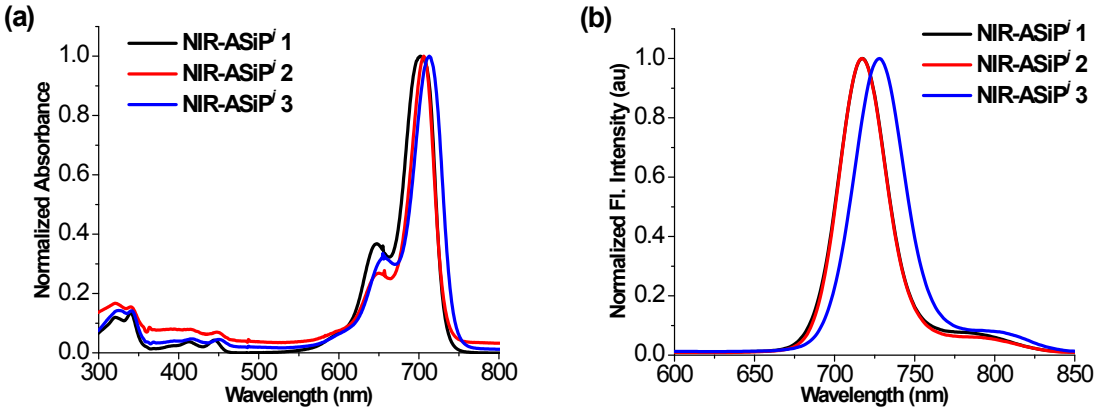

Fig. S15 Normalized (a) absorption and (b) emission spectra of NIR-ASiP^j **1** (black line), NIR-ASiP^j **2** (red line) and NIR-ASiP^j **3** (blue line) in *ethanol (EtOH)*, obtained with each dye at 10 μM concentration. The emission spectra were collected by excitation at the corresponding maximum absorbance wavelength for each dye.

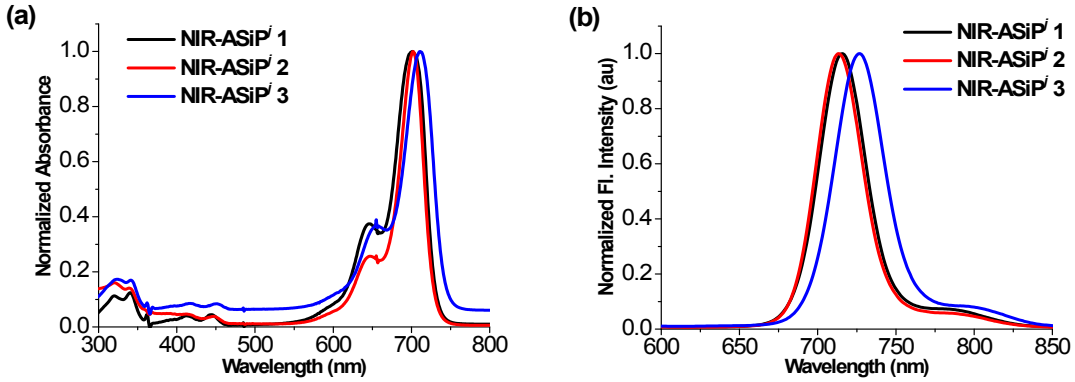

Fig. S16 Normalized (a) absorption and (b) emission spectra of NIR-ASiP^j **1** (black line), NIR-ASiP^j **2** (red line) and NIR-ASiP^j **3** (blue line) in *acetonitrile* (*CH_3CN*), obtained for each dye at 10 μM concentration. The emission spectra were collected by excitation at the corresponding maximum absorbance wavelength for each dye.

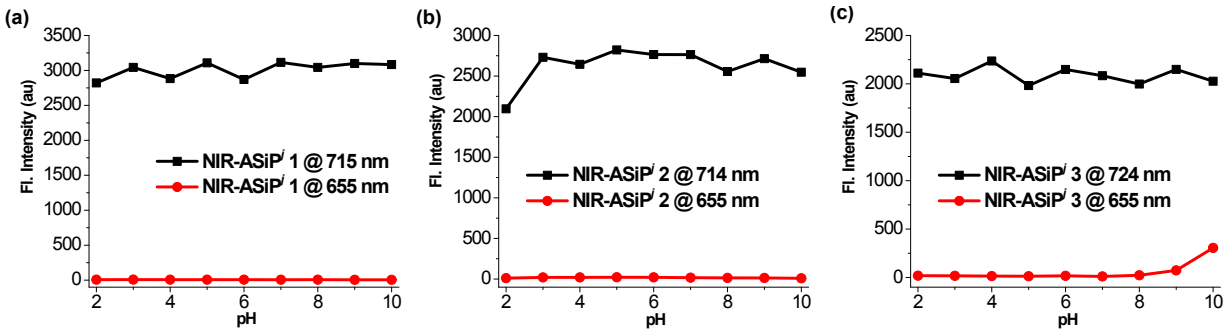

Fig. S17 pH-Dependent fluorescence intensity changes of (a) NIR-ASiP^j **1**, (b) NIR-ASiP^j **2** and (c) NIR-ASiP^j **3**. The corresponding emission spectrum of each dye (10 μM) was monitored at two

wavelengths—NIR emission (black lines; upon excitation at the corresponding maximum absorbance wavelength for each dye) and red emission wavelengths (red lines; upon excitation at 480 nm). The strong electron-withdrawing trifluoroacetamide containing NIR-ASiP^j **3** shows a little interference only at the highly basic medium (pH = 9–10) when observed in the red emission wavelength.

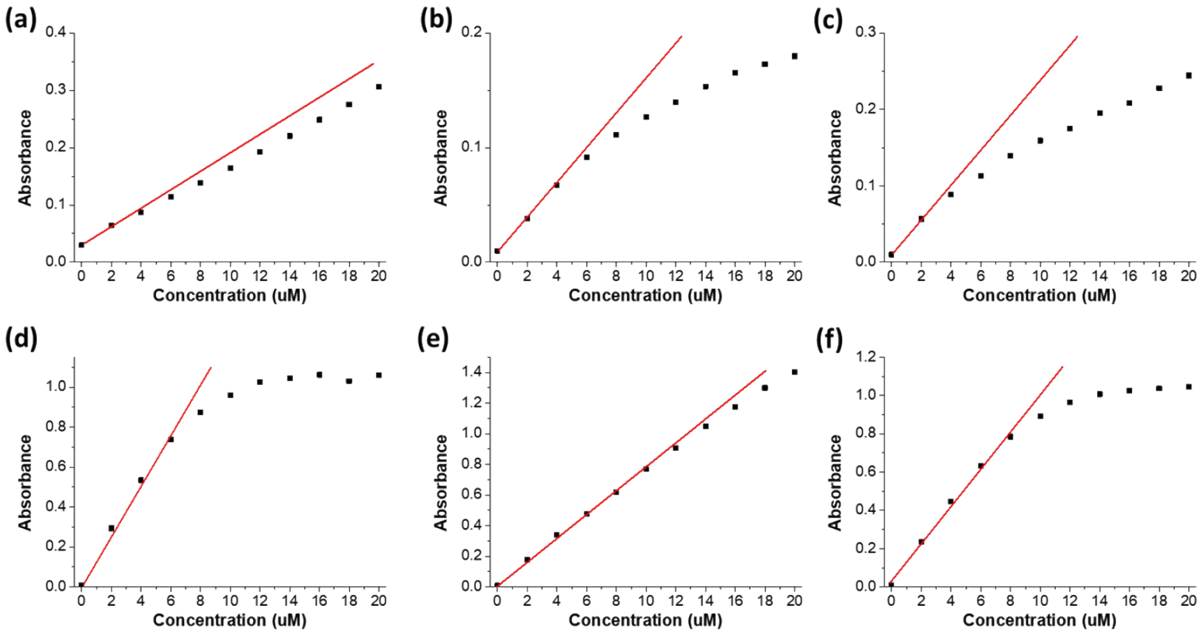

Fig. S18 Evaluation of aggregation behaviour of the dyes. Maximum absorbance values of (a) ASiP^j **1**, (b) ASiP^j **2**, (c) ASiP^j **3**, (d) NIR-ASiP^j **1**, (e) NIR-ASiP^j **2**, and (f) NIR-ASiP^j **3**, plotted against different concentrations (0–20 μM) in PBS buffer (pH 7.4) at 25 ℃. The data show that the ASiP^j and NIR-ASiP^j dyes show slight aggregation tendency at or above 10 μM in in PBS (pH 7.4) at 25 ℃. For cellular imaging, however, use of 10 μM of the dyes would cause little aggregation because of the higher temperature of incubation (36 ℃) and the less hydrophilic nature of the cellular environment compared to that of PBS.

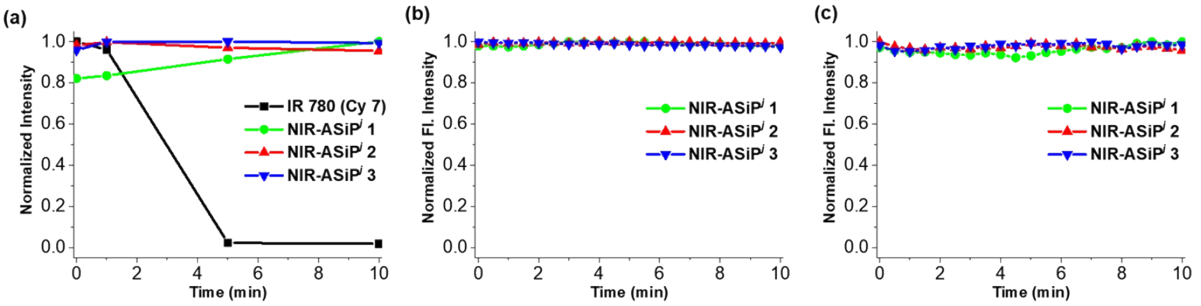

Fig. S19 Normalized time-dependent fluorescence intensity changes of NIR-ASiP^j **1**–**3** and a cyanine dye (Cy 7; IR 780) in pH 7.4 PBS buffer (containing 1% DMSO), observed by continuously irradiating at (a) 254 nm (300 μW/cm^2), (b) 633 nm (22 μW/cm^2), usual CLSM imaging conditions, (c) 900 nm (145 mW/cm^2), harsh two-photon imaging conditions for 10 min at 10 μM dye concentration..

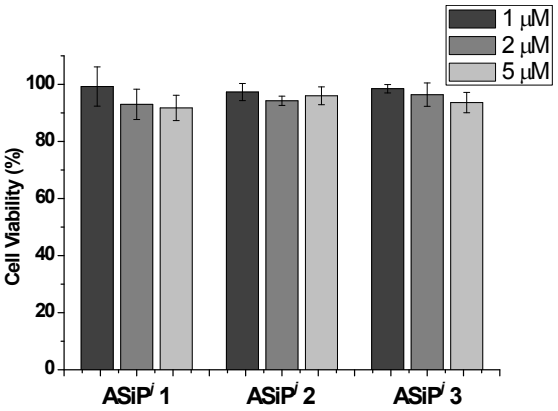

Fig. S20 Viability of HeLa cells incubated with ASiP^j **1**–**3** at various concentrations (1.0, 2.0, and 5.0 μM) for 24 h at 37 °C. The cell viability was assessed by measuring their ability to metabolize CCK-8 (Cell Counting Kit-8) in HeLa cell line.

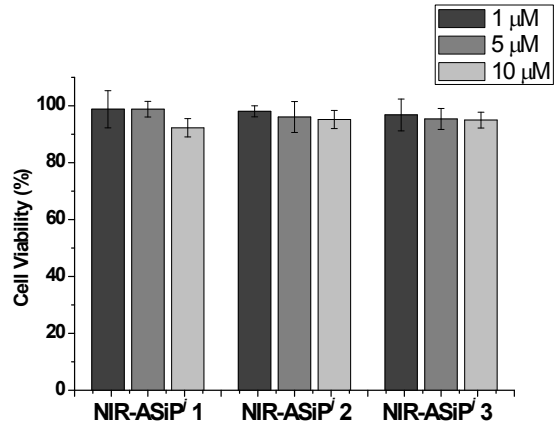

Fig. S21 Viability of HeLa cells incubated with NIR-ASiP^j **1**–**3** at various concentrations (1.0, 5.0, and 10 μM) for 24 h at 37 °C. The cell viability was assessed by measuring their ability to metabolize CCK-8 (Cell Counting Kit-8) in HeLa cell line.

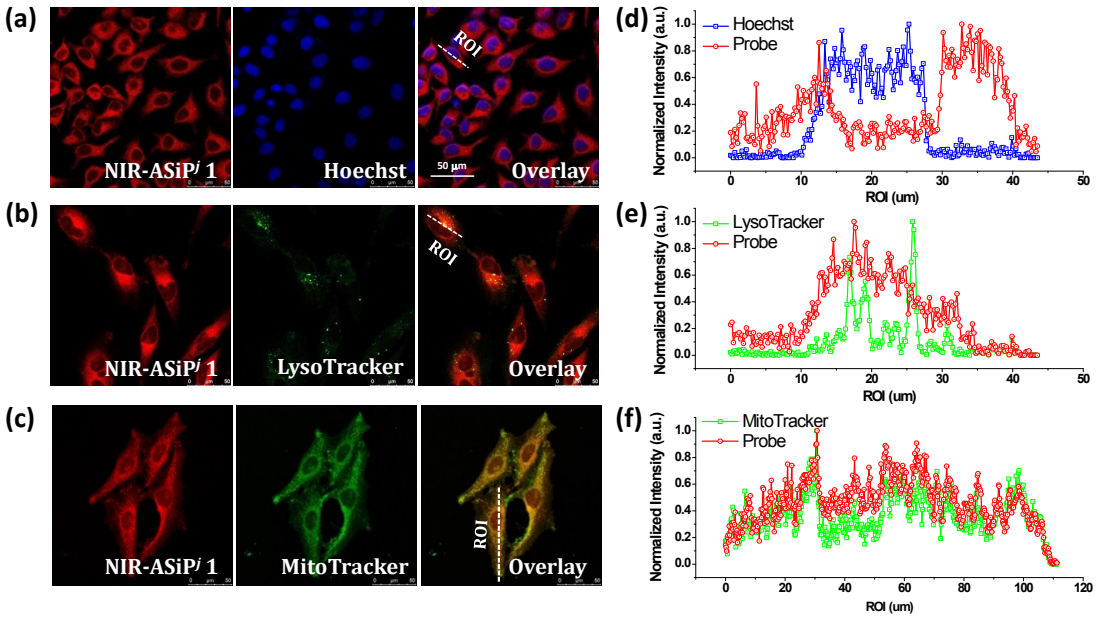

Fig. S22 Confocal microscopic images of cells co-incubated with NIR-ASiP^j **1** (5.0 μM) and (a) Hoechst (10 mg/mL), (b) LysoTracker Green (200 nM), and (c) MitoTracker Green (1.0 μM), respectively, for 20 min at 37 °C. The images were collected in various emission channels corresponding to Hoechst (λ_{em} = 415–500 nm; λ_{ex} = 405 nm), LysoTracker Green (λ_{em} = 500–550 nm; λ_{ex} = 488 nm), MitoTracker Green (λ_{em} = 500–550 nm; λ_{ex} = 488 nm) and NIR-ASiP^j **1** (λ_{em} = 650–700 nm; λ_{ex} = 633 nm). (d,e,f) The corresponding intensity profiles measured across the region of interest (ROI) in the respective overlay images. The corresponding Pearson's correlation co-efficient (PCC) values were calculated as follows: Hoechst/NIR-ASiP^j **1** = −0.30; LysoTracker/NIR-ASiP^j **1** = 0.54; MitoTracker/NIR-ASiP^j **1** = 0.73.

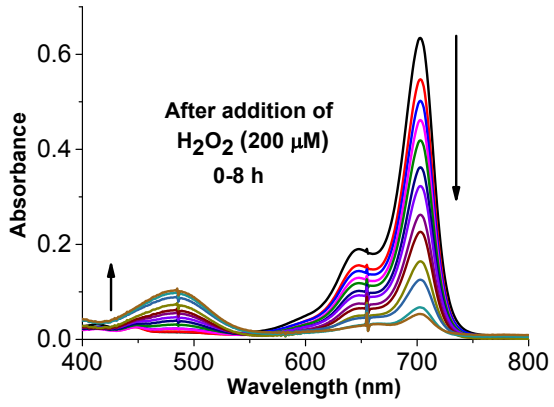

Fig. S23 Time dependent (0–8 h) absorption changes of **ASiP^j-H_2O_2** in the presence of H_2O_2 (200 μM), showing a gradual decrease of absorbance at 702 nm and a gradual increase of absorbance at 481 nm. The spectra were recorded after mixing at 25 °C in PBS buffer (pH = 7.4) containing 1% DMSO.

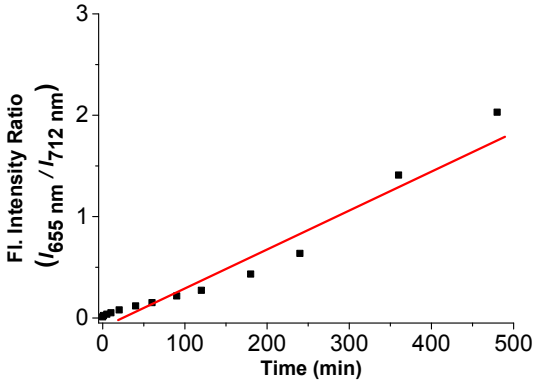

Fig. S24 Time dependent (0–8 h) emission intensity ratio ($I_{655\ nm}$/ $I_{712\ nm}$) changes of **ASiP^{i}-H_2O_2** in presence of H_2O_2 (200 μM). The spectra were recorded after mixing at 25 °C in PBS buffer (pH = 7.4) containing 1% DMSO.

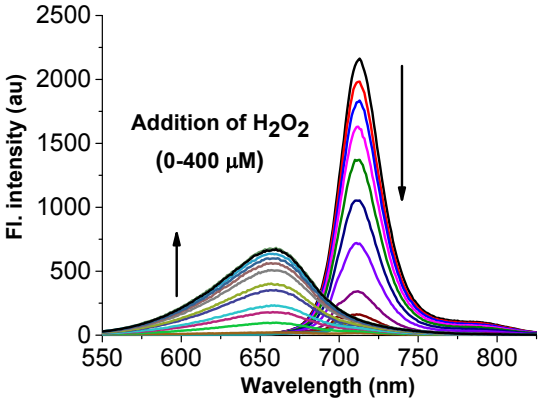

Fig. S25 The fluorescence changes of **ASiP^{i}-H_2O_2** (10 μM) with increasing concentrations of H_2O_2 (0–400 μM), showing a gradual decrease of NIR intensity with maxima at 712 nm (under excitation at 702 nm) and a gradual increase of far-red intensity with maxima at 655 nm (under excitation at 481 nm). The spectra were recorded after mixing at 25 °C for 3 h in PBS buffer (pH = 7.4) containing 1% DMSO.

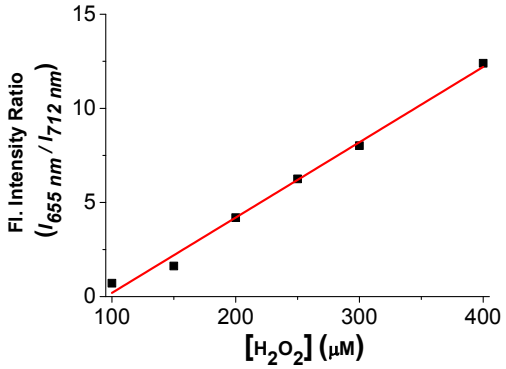

Fig. S26 The emission intensity ratio ($I_{655\ nm}$/ $I_{712\ nm}$) changes of **ASiP^{i}-H_2O_2** (10 μM) depending on [H_2O_2] in the higher concentration region (100–400 μM) in PBS (pH 7.4) containing 1% DMSO. The spectra were recorded after mixing at 25 °C for 3 h, under excitation at 481 nm and 702 nm, respectively.

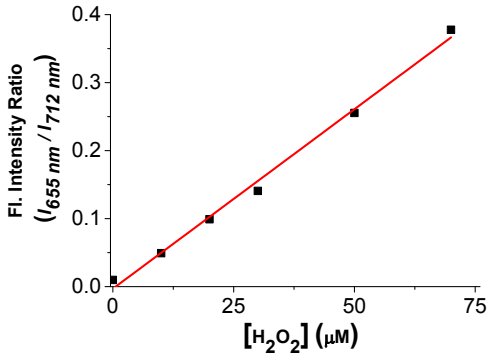

Fig. S27 The emission intensity ratio ($I_{655\ nm}$/ $I_{712\ nm}$) changes of **ASiP^j-H_2O_2** (10 μM) depending on [H_2O_2] at the low concentration region (0–75 μM) in PBS (pH 7.4) containing 1% DMSO. The spectra were recorded after mixing at 25 °C for 3 h, under excitation at 481 nm and 702 nm, respectively. On the basis of this plot, the detection limit (LOD) was calculated to be 9.0 nM by the equation: LOD = 3σ/k,

Where σ is the standard deviation of three blank measurements = 2.93×10^{-4}, k is the slope of the linear plot of the fluorescence intensity ratios changes ($I_{655\ nm}$/$I_{712\ nm}$) in the lower H_2O_2 concentration region (0–75 μM) = 9.85×10^{-2}.

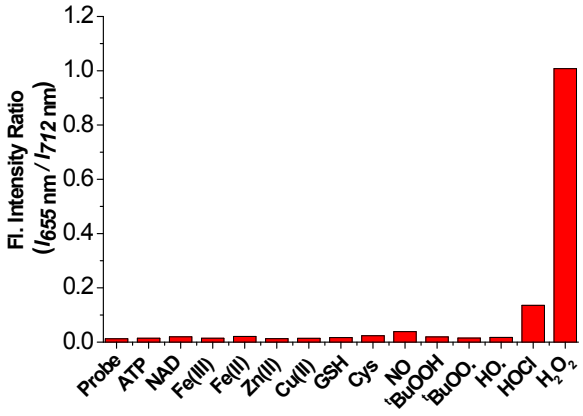

Fig. S28 The ratiometric fluorescence response ($I_{655\ nm}$/ $I_{712\ nm}$) of **ASiP^j-H_2O_2** (10 μM) in the presence of H_2O_2 (100 μM) and various biologically relevant analytes (ATP, NAD, Fe(III), Fe(II), Zn(II) and Cu(II), each at 50 μM), biothiols (GSH at 1 mM and Cys at 200 μM), reactive oxygen species (such as nitric oxide (NO•), *t*-butyl hydroperoxide (^{t}BuOOH), *t*-butyl peroxide radical (^{t}BuOO•), hydroxyl radical (HO•) and hypochlorous acid (HOCl), each at 100 μM). The spectra were recorded in PBS buffer (pH 7.4) containing 1% DMSO after incubation at 25 °C for 3 h, under excitation at 481 nm (for 655 nm emission) and at 702 nm (for 712 nm emission), respectively.

Experimental procedures

One-photon optical property measurement

Absorption spectra were measured using a HP Agilent 8453 spectrophotometer. Fluorescence spectra were recorded on a Photon Technical International Fluorescence system using a 1.0 mL quartz cuvette (10 mm light path). The excitation and emission wavelength band paths were both set at 2 nm. Stock solutions of each dye were prepared in DMSO (1 mM) and it was added to the various solvents by keeping the concentration of DMSO within 1% of the total volume for measurement of photophysical properties of the dyes. Final titrant volume is the same (1.0 mL) for all the measurements. MilliQ water was used to prepare all aqueous solutions. All measurement were performed at 25 °C. All pH measurements were made with a Thermo scientific, Orion 2 star pH benchtop.

Fluorescence assays with NIR-ASiP^{j} based ratiometric H_2O_2 probe, ASiP^{j}-H_2O_2

All of the solvents used were of analytical grade. A stock solution of H_2O_2 (10 mM) was prepared by addition of commercially available H_2O_2 (30 % (w/w) in H_2O in DI water. The concentration of H_2O_2 was determined from the absorption at 240 nm (ε = 43.6 M^{-1} cm^{-1}). Solutions of other biologically relevant analytes were prepared by dissolving each of the corresponding reagents in distilled water. A stock solution of probe was prepared in DMSO at a concentration of 1.0 mM. For spectroscopic measurement, the probe stock solution was diluted to 10 μM in 10 mM PBS buffer solutions of pH 7.4, which was treated with an analyte solution and then kept at 25 °C. After specified time, a required amount of the mixed solution was transferred to a cuvette (1.0 mL) for spectroscopic measurement. One-photon fluorescence spectra were recorded on a Photon Technical International Fluorescence system using a 1.0 mL quartz cuvette (10 mm light path).

Quantum yield measurement

Fluorescence quantum yields for the synthesized dyes were determined using Rhodamine 101 (Φ_F = 0.915 in ethanol), fluorescein (Φ = 0.95 in 0.1 *M* NaOH) or Nile blue (Φ = 0.27 in ethanol) as the reference dye. The quantum yield was calculated using the following equation:

$$\Phi_{F(X)} = \Phi_{F(S)}(A_S F_X / A_X F_S)\,(n_X/n_S)^2$$

Where Φ_F is the fluorescence quantum yield, *A* is the absorbance at the excitation wavelength, *F* is the area under the corrected emission curve, and *n* is the refractive index of the solvents used. Subscripts $_S$ and $_X$ refer to the standard and to the unknown, respectively.

Two-photon property measurement

Two-photon absorption cross-section (TPACS) values were measured by following the known method.[1] Two equations are referred from the references as below.

$$\frac{\langle F(t)\rangle_{\mathrm{cal}}}{\langle F(t)\rangle_{\mathrm{new}}} = \frac{\phi_{\mathrm{cal}}\eta_{2\mathrm{cal}}\sigma_{2\mathrm{cal}}C_{\mathrm{cal}}\langle P_{\mathrm{cal}}(t)\rangle^2 n_{\mathrm{cal}}}{\phi_{\mathrm{new}}\eta_{2\mathrm{new}}\sigma_{2\mathrm{new}}C_{\mathrm{new}}\langle P_{\mathrm{new}}(t)\rangle^2 n_{\mathrm{new}}}, \quad (4)$$

The equation (4) is the main equation that calculates TPACS using a reference dye and equation (5) could be extracted from equation (4).

$$\sigma_{2\mathrm{new}}(\lambda)\eta_{2\mathrm{new}} = \frac{\phi_{\mathrm{cal}}\eta_{2\mathrm{cal}}\sigma_{2\mathrm{cal}}(\lambda)C_{\mathrm{cal}}}{\phi_{\mathrm{new}}C_{\mathrm{new}}} \frac{\langle P_{\mathrm{cal}}(t)\rangle^2}{\langle P_{\mathrm{new}}(t)\rangle^2} \frac{\langle F(t)\rangle_{\mathrm{new}}}{\langle F(t)\rangle_{\mathrm{cal}}} \frac{n_{\mathrm{cal}}}{n_{\mathrm{new}}}. \quad (5)$$

(σ_2 = two-photon absorption cross section; η = quantum efficiency; σ_{TPE} (Two-photon sction cross section = $\sigma\eta$; <F(t)> = time averaged fluorescence emission; C = fluorophore concentration; <P(t)> = time averaged laser power; n = reflective index of sample; Φ = fluorescence collection efficiency).

Φ_{cal} and Φ_{new} are the identical value in the same experimental setup, and $<P_{cal}(t)>$, $<P_{new}(t)>$ are also identical when the same laser has been applied. TPACS values of samples could be calculated by adding values of known TPACS (Two-Photon Action Cross Section) ($\sigma\eta$), concentration (C), detected emission (<F(t)>), and known reflective index (n).

Rhodamine B in methanol (1.0 μM or 10 μM) was used as a reference, and 10 μM of ASiP*j* dyes in acetonitrile were used for the measurement. Each reflective index of a given solvent was applied (assuming that the reflective index of sample is almost the same as that of pure solvent). 100 μL of each sample was loaded in a well slide and covered with a cover glass. The edge of cover glass was coated with transparent manicure to prevent the evaporation of solvent and then mounted on a vibration isolation table. Two-photon excitation was performed with a Ti-sapphire laser (Chameleon Vision II, Coherent) at 140 fs pulse width and 80 MHz pulse repetition rate. The emission intensity was collected through an HCX APO 10× objective lens (Leica, Germany) of a two-photon microscopy (TCS SP5 II, Leica, Germany) equipped with HyD detector (Leica, Germany), in the range of 400–665 nm.

Preparation of cell samples and their confocal microscopic imaging

HeLa and A549 human cancer cells were obtained from Korean Cell Line Bank. The cells were incubated in DMEM supplemented with 10% (*v*/*v*) fetal bovine serum (FBS) and 1% (*v*/*v*) penicillin-streptomycin (PS) at 37 °C in a humidified atmosphere of 5% of CO_2 in the air. Cells were passaged when they reached approximately 80% confluence. Cells were seeded onto a cell culture dish at a density of 1.0×10^5 cells, which was incubated at 37 °C overnight under 5% CO_2 in the air. For imaging experiments with the dyes, cells were incubated with the corresponding dye (1.0 μM or 10 μM) in DMEM containing for 30 min and washed with PBS (phosphate buffered saline) three times to remove the remaining dye. For imaging experiments with the H_2O_2 probe, the cells were incubated in DMEM

containing the probe (10 μM) for 30 min, washed with PBS three times to remove the remaining probe. In the positive control experiment with an exogenous H_2O_2 source, the cells were incubated in DMEM containing the probe (10 μM) for 30 min and washed with PBS (phosphate buffered saline) three times to remove the remaining probe and then incubated further with H_2O_2 (50 or 200 μM) for further 30 min. Fluorescent cellular images were recorded by confocal microscopy, using Leica TCS SP5 II Advanced System equipped with multiple visible laser lines (405, 458, 476, 488, 496, 514, 561, 594, and 633 nm) and a 40× objective lens (obj. HCX PL APO 40×/ 1.10 W CORR CS, Leica, Germany). Acquired images were processed using LAS AF Lite (Leica, Germany).

Two-photon microscopic imaging of cells

The above mentioned stained cell samples were placed on a slide glass flatway. Fluorescence images of the cells were recorded by two-photon microscopy (TPM). TPM imaging was performed using a Ti-Sapphire laser (Chameleon Vision II, Coherent) at 140 fs pulse width and 80 MHz pulse repetition rate (TCS SP5 II, Leica, Germany) and a 20× objective lens (obj. HCX PL APO 20×/ 1.10 W CORR CS, Leica, Germany). The two-photon excitation wavelength was tuned to 900 nm. Each emission light was spectrally resolved into multi-channels as mentioned for each image. The excitation laser power was approximately 9.3 mW. The images were consisted of 1024×1024 pixels, and the scanning speed was maintained as 100 MHz during the entire imaging.

Cell viability assay

Cell viability was assessed by measuring their ability to metabolize CCK-8 (Cell Counting Kit-8) in HeLa cell line.[2] Cells were seeded onto 96-well plates at a density of about 5×10^3 cells per well in the growth medium and incubated until about 70–80% confluency. Following the probe treatment at various concentrations as indicated, 10 μL of the CCK-8 solution (from Dojindo Molecular Technologies, Inc.) was added to each well and cells were maintained for 1 h at 37 °C. After being incubated for 24 h at 37 °C, absorbance at 450 nm was measured.

Synthetic procedures of the dyes

General methods. The chemical reagents were purchased from Sigma-Aldrich or Alfa-Aesar and used as received. All solvents were purified and dried by standard methods prior to use. Deionized water was used to prepare all aqueous solutions. All reactions were performed under argon atmosphere unless otherwise mentioned. Analytical TLC was performed on Merck silica gel (60 F_{254}) plates (0.25 mm) and visualized with UV light. Preparative HPLC was performed with column: Zorbax XBD-C18, 5 μm, 21.2 × 150 mm; solvent A: acetonitrile + 0.1% v/v TFA, solvent B: H_2O + 0.1% v/v TFA; solvent gradient 30/70–100/0 A:B over 40 min, flow rate = 20 mL/min; temperature 25 °C; detection at 254 nm. ^1H and ^{13}C NMR spectra were measured with a Bruker DPX-300 spectrometer. Coupling constants

(*J* value) are reported in Hertz. The chemical shifts (δ) are shown in ppm, multiplicities are indicated by s (singlet), d (doublet), t (triplet) and m (multiplet). All chemical shifts are reported in the standard notation of parts per million (ppm) using residual solvent protons as the internal standard. Spectra are referenced to residual chloroform (7.26 ppm, ^{1}H; 77.23 ppm, ^{13}C) or CD_3OD (3.31 ppm, ^{1}H; 49.17 ppm, ^{13}C). Mass spectroscopic data were obtained from the Korea Basic Science Institute (Daegu) using a JEOL JMS 700 high resolution mass spectrometer.

Scheme S1. Synthetic scheme of ASiP^a **1**–**9** and **11**.

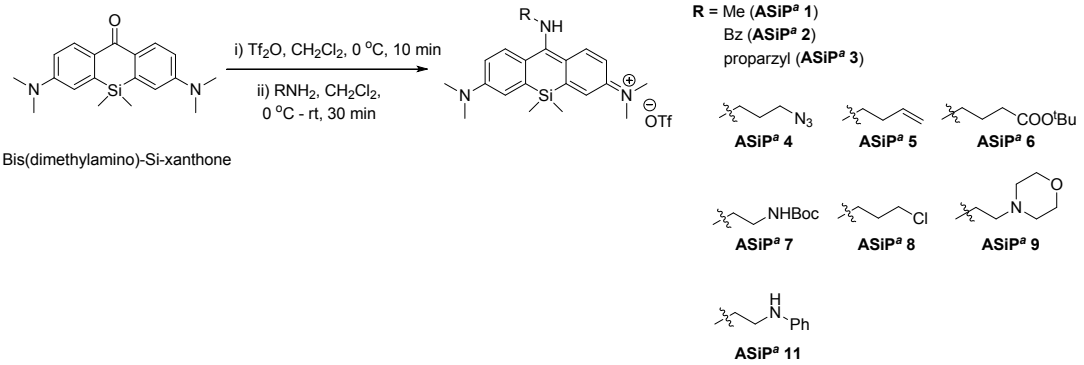

Synthesis of ASiP^a 1–9 and 11.

Trifluoromethanesulfonic anhydride (39 μL, 0.231 mmol) was added drop-wise to a solution of bis(dimethylamino)-Si-xanthone (prepared according to the reported procedure[3]: 50 mg, 0.154 mmol) in anhydrous CH_2Cl_2 (5 mL) at 0 °C. The resulting intense blue reaction mixture was stirred at 0 °C for 10 min and then each of various amines (3 equiv.) was added at the same temperature. The reaction mixture was further stirred for 30 min at room temperature, and then directly loaded onto silica gel for flash chromatography (eluent: MeOH/CH_2Cl_2 = 5/95) to afford the pure ASiP^a dyes as orange coloured solids.

ASiP^a 1: A solution of methylamine in THF (2.0 M, 231 μL, 0.462 mmol) was used as the amine source. Yield = 41 mg (78%). ^{1}H NMR ($CDCl_3$, 500 Hz, 298 K) δ 8.00 (d, J = 9.0 Hz, 1H), 7.60 (d, J = 9.0 Hz, 1H), 6.94 (d, J = 2.5 Hz, 1H), 6.84–6.75 (m, 2H), 3.62 (s, 3H), 3.14 (s, 6H), 3.08 (s, 6H), 0.48 (s, 6H); ^{13}C NMR (125 MHz, $CDCl_3$, 298 K) δ 173.5, 152.0, 151.8, 143.1, 139.0, 131.8, 129.8, 125.1, 122.1, 119.6, 119.4, 116.5, 115.3, 113.7, 111.3, 40.1, 37.6, 29.8, 0.1, -1.9; HRMS (ESI$^+$): calcd for $C_{20}H_{28}N_3Si^+$ $[M]^+$ 338.2053; found 338.2055.

ASiP^a 2: Benzylamine (51 μL, 0.462 mmol) was used as the amine source. Yield = 52 mg (82%). ^{1}H NMR ($CDCl_3$, 300 Hz, 298 K) δ 7.96 (d, J = 8.7 Hz, 1H), 7.40–7.38 (m, 2H), 7.34–7.29 (m, 5H), 7.23–7.19 (m, 2H), 6.96 (d, J = 2.7 Hz, 1H), 6.84 (d, J = 2.4 Hz, 1H), 6.82 (dd, J = 8.7, 2.7 Hz, 1H), 6.66 (dd, J = 8.7, 2.7 Hz, 1H), 5.04 (s, 2H), 2.99 (s, 6H), 2.97 (s, 6H), 0.48 (s, 6H); ^{13}C NMR ($CDCl_3$, 75 MHz, 298 K): δ 167.9, 150.2, 149.8, 141.2, 139.9, 136.3, 135.5, 129.7, 128.6, 128.5, 127.6, 127.3, 127.0, 126.8, 126.6, 116.1, 114.9, 113.9, 111.4, 56.8, 40.6, 40.3, −2.2; HRMS (ESI$^+$): calcd for

$C_{26}H_{32}N_3Si^+$ $[M]^+$ 414.2366; found 414.2362.

ASiP^a 3: Propargylamine (30 µL, 0.462 mmol) was used as the amine source. Yield = 40 mg (71%). ^{1}H NMR (300 Hz, $CDCl_3$, 298 K): δ 7.54 (d, J = 8.4 Hz, 1H), 7.44 (d, J = 8.7 Hz, 1H), 6.93 (dd, J = 8.7, 2.4 Hz, 2H), 6.76 (dd, J = 8.7, 2.7 Hz, 1H), 6.70 (dd, J = 8.4, 2.7 Hz, 1H), 6.11 (s, 1H), 5.50 (t, J = 5.4 Hz, 1H), 4.01–3.99 (m, 2H), 2.99 (d, J = 4.2 Hz, 12H), 2.14 (t, J = 2.1 Hz, 1H), 0.47 (s, 6H); ^{13}C NMR ($CDCl_3$, 125 MHz, 298 K): δ168.5, 149.9, 149.5, 139.6, 136.6, 135.8, 129.4, 128.2, 127.3, 116.1, 114.7, 113.9, 111.4, 83.1, 70.7, 43.6, 40.5, 40.2, −2.4; HRMS (ESI$^+$): calcd for $C_{22}H_{28}N_3Si^+$ $[M]^+$ 362.2053; found 362.2050.

ASiP^a 4: 3-Azidopropylamine (prepared according to reported procedure[4]; 47 mg, 0.462 mmol) was used as the amine source. Yield = 61 mg (73%)^{1}H NMR ($CDCl_3$, 300MHz, 298K): δ 7.81 (d, J = 8.7 Hz, 1H), 7.38 (d, d, J = 8.7 Hz, 1H), 6.98 (d, J = 2.7 Hz 1H), 6.87 (d, J = 2.7 Hz, 1H), 6.83 (dd, J = 8.7, 2.7 Hz, 1H), 6.75 (dd, J = 8.7, 2.7 Hz, 1H), 3.90 (t, J = 6.3 Hz, 2H), 3.46 (t, J = 6.3 Hz, 2H), 3.04 (s, 6 H), 3.00 (s, 6H), 2.08 (m, 2H)), 0.49 (s, 6H). ^{13}C NMR ($CDCl_3$, 75 MHz, 298 K): δ166.7, 150.0, 149.5, 139.7, 136.4, 136.0, 129.7, 128.0, 127.6, 115.9, 114.9, 113.9, 111.3, 50.8, 49.7, 40.6, 40.3, 31.1, −2.3.

ASiP^a 5: But-3-en-1-amine (42 µL, 0.462 mmol) was used as the amine source. Yield = 63 mg (80%) ^{1}H NMR ($CDCl_3$, 500MHz, 298K): δ 8.06 (d, J = 8.5 Hz, 1H), 7.51 (d, J = 8.5 Hz, 1H), 6.92 (s, 1H), 6.83 (m, 3H), 5.66 (m, 1H), 5.07 (m, 2H), 4.07 (t, J = 6.5 Hz, 2H), 3.13 (s, 6H), 3.07 (s, 6H), 2.67 (q, J = 6.5 Hz, 2H), 0.47 (s, 6H). ^{13}C NMR ($CDCl_3$, 125 MHz, 298K) δ 173.72, 151,8, 151,6, 142.4, 138.7, 133.3, 131.6, 129.4, 125.1, 123.8, 122.0, 119.7, 119.4, 118.4, 116.3, 115.1, 113.5, 111.2, 49.7, 39.9, 33.1, 0.0, −2.2.

ASiP^a 6: *tert*-Butyl 4-aminobutanoate (55 mg, 0.462 mmol) was used as the amine source. Yield = 52 mg (60%). ^{1}H NMR ($CDCl_3$, 500MHz, 298K): δ 8.00 (d, J = 9.0 Hz, 1H), 7.64 (d, J = 9.0 Hz, 1H), 6.92 (d, J = 2.0 Hz, 1H), 6.86 (m, 3H), 4.06 (t, J = 6.5 Hz, 2H), 3.13 (s, 6H), 3.07 (s, 6H), 2.40 (t, J = 6.5 Hz, 2H), 2.17 (t, J = 6.5 Hz, 2H), 1.33 (s, 9H), 0.48 (s, 6H). ^{13}C NMR ($CDCl_3$, 125 MHz, 298K): δ 173.3, 172.9, 151.9, 151.7, 142.4, 138.8, 132.1, 129.3, 125.0, 119.3, 116.2, 115.2, 113.6, 111.5, 81.2, 50.2, 40.0, 39.9, 32.7, 27.9, 24.2, 0.0, −2.0.

ASiP^a 7: *tert*-Butyl 2-aminoethylcarbamate (prepared according to the reported procedure[5]: 74 mg, 0.462 mmol) was used as the amine source. Yield = 65 mg (70%). ^{1}H NMR ($CDCl_3$, 500MHz, 298K): δ 7.84 (d, J = 8.5 Hz, 1H), 7.59 (d, J = 9.0 Hz, 1H), 6.90 (d, J = 2.0 Hz, 1H), 6.82 (m, 3H), 4.09 (t, J = 4.5 Hz, 2H), 3.59 (q, J = 4.5 Hz, 2H), 3.12 (s, 6H), 3.09 (s, 6H) 1.33 (s, 9H), 0.47 (s, 6H). ^{13}C NMR ($CDCl_3$, 125 MHz, 298 K): δ173.9, 158.0, 152.0, 151.9, 142,7, 139.2, 132.2, 129.4, 125.0, 122.0, 119.5, 119.2, 116.4, 115.4, 113.3, 111.6, 80.1, 77.4, 52.5, 40.0, 39.7, 28.3, 0.0, −2.0.

ASiP^a 8: 3-Chloropropylamine hydrochloride (60 mg, 0.462 mmol) was used as the amine source. Yield = 58 mg (70%). ^{1}H NMR ($CDCl_3$, 300MHz, 298K): δ 7.87 (d, J = 8.4 Hz, 1H), 7.41 (d, J = 8.4 Hz, 1H), 6.95 (d, J = 2.7 Hz, 1H), 6.84 (m, 2H), 6.73 (dd, J = 9.0, 2.7 Hz, 1H), 3.99 (t, J = 6.3 Hz, 2H), 3.69 (t,

J = 6.3 Hz, 2H), 3.04 (s, 6H), 3.00 (s, 6H), 2.29 (m, 2H), 0.48 (s, 6H). ^{13}C NMR ($CDCl_3$, 75 MHz, 298 K): δ 168.2, 150.3, 149.9, 140.3, 136.5, 134.5, 130.1, 128.4, 126.4, 116.0, 115.0, 113.9, 111.3, 50.2, 43.3, 40.5, 40.3, 34.1, −2.3.

ASiP^a 9: 4-(2-Aminoethyl)morpholine (61 μL, 0.462 mmol) was used as the amine source. Yield = 65 mg (72%). ^{1}H NMR ($CDCl_3$, 300MHz, 298K): δ 8.51 (d, J = 9.0 Hz, 1H), 7.63 (d, J = 9.0 Hz, 1H), 6.91 (m, 2H), 6.78 (d, J = 2.4 Hz, 1H), 6.72 (dd, , J = 9.0, 2.4 Hz, 1H), 4.18 (t, , J = 6.0 Hz, 2H), 3.56 (t, J = 6.0 Hz, 4H), 3.10 (s, 6H), 3.06 (s, 6H), 2.41 (s, 4H), 0.47 (s, 6H). ^{13}C NMR ($CDCl_3$, 125 MHz, 298 K): δ 173.8, 151.9, 151.5, 142.1, 138.6, 131.3, 131.0, 125.6, 121.0, 116.3, 115.0, 113.5, 111.3, 66.8, 57.0, 53.6, 47.0, 40.1, −1.9.

ASiP^a 11: *N*-(2-(2,2′-Dipicolylamino)ethyl)aniline (prepared according to the reported procedure[6]: 63 mg, 0.462 mmol) was used as the amine source. Yield = 49 mg (83%). ^{1}H NMR ($CDCl_3$, 500MHz, 298K): δ 8.00 (d, J = 8.5 Hz, 1H), 7.56 (d, J = 9.0 Hz, 1H), 7.07 (t, J = 8.5 Hz, 1H), 6.87 (m, 3H), 6.67 (m, 4H), 4.19 (t, J = 5.5 Hz, 2H), 3.67 (t, J = 5.5 Hz, 2H), 3.11 (s, 6H), 3.07 (s, 6H), 0.41 (s, 6H). ^{13}C NMR ($CDCl_3$, 125 MHz, 298 K): δ 174.3, 152.0, 151.8, 147.3, 142.4, 139.0, 131.6, 129.8, 129.5, 129.3, 125.3, 122.1, 119.9, 117.6, 116.3, 115.3, 113.7, 112.9, 111.5, 77.4, 49.5, 42.6, 40.1, 40.0, −2.14.

Scheme S2. Synthetic scheme of ASiP^a **10**.

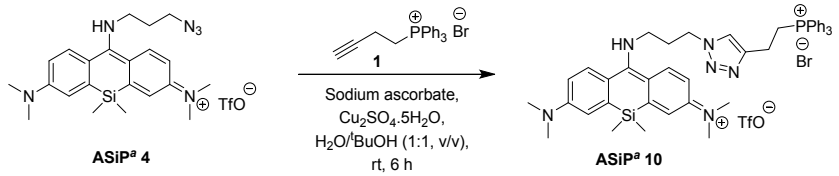

Synthesis of ASiP^a 10.

To a mixture of ASiP^a **4** (56 mg, 0.10 mmol) and alkyne **1** (40 mg, 0.10 mmol) was added ^{t}BuOH (3 mL) and H_2O (3 mL), and then a separately prepared 1.0 M solution of sodium ascorbate (100 μL, 0.10 mmol) was added to the reaction mixture, followed by $CuSO_4.5H_2O$ (2.5 mg, 0.01 mmol). After being stirred for 6 h at room temperature, the reaction mixture was diluted with dichloromethane (30 mL) and washed with water (30 mL). The organic layer was evaporated and the residue was subjected to flash column chromatography (CH_2Cl_2/MeOH = 99/1) to obtain the pure product (52 mg, 54%) as a red solid. ^{1}H NMR ($CDCl_3$, 500MHz, 298K): δ 8.47 (s, 1H), 8.44 (d, J = 9.0 Hz, 1H), 7.81 (m, 9H), 7.68 (m, 6H), 7.46 (d, J = 8.5 Hz, 1H), 6.86 (s, 1H), 6.81 (d, J = 8.5 Hz, 1H), 6.75 (s, 2H), 4.38 (t, J = 6.0 Hz, 2H), 4.05 (m, 4H), 3.13 (m, 2H), 3.07 (s, 6H), 3.02 (s, 6H), 2.66 (t, J = 6.5 Hz, 2H), 0.43 (s, 6H). ^{13}C NMR ($CDCl_3$, 125 MHz, 298 K): δ 173.6, 151.9, 151.7, 144.3, 144.2, 142.3, 139.1, 135.4, 135.3, 133.9, 133.8, 131.5, 131.0, 130.7, 124.9, 124.2, 119.9, 118.1, 117.4, 116.4, 115.2, 113.3, 111.9, 47.6, 47.2, 40.1 (d), 29.8, 23.0, 22.6, 19.4 (d), −1.9.

Scheme S3. Synthetic scheme of NIR-ASiP^a **1**.

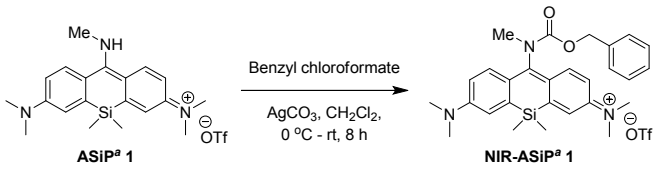

Synthesis of NIR-ASiP^{a} 1.

A solution of ASiP^{a} **1** (49 mg, 0.1 mmol) in anhydrous dichloromethane (5 mL) at 0 °C was treated with benzyl chloroformate (141 µL, 1.0 mmol) and Ag_2CO_3 (276 mg, 1.0 mmol). After keeping the reaction mixture at room temperature, it was allowed to stir for 8 h, and then it was diluted with dichloromethane and washed with 1 *N* HCl. The organic layer was evaporated and the residue was subjected to flash coloumn chromatography (eluent, CH_2Cl_2/MeOH = 95/5) to collect the product, which was further purified by preparative HPLC to obtain the pure product (22 mg, 35%) as a deep blue coloured solid which was used for spectroscopic analysis. ^{1}H NMR (CD_3CN, 500 MHz, 298 K): δ7.62–7.21 (d, J = 10 Hz, 2H), 7.23–7.18 (m, 4H), 7.01 (d, J = 6.5 Hz, 2H), 6.85 (dd, J = 9.5, 2.5 Hz, 2H), 5.01 (s, 2H), 3.32 (s, 12H), 3.27 (s, 3H), 0.53 (s, 3H), 0.49 (s, 3H); ^{13}C NMR (CD_3OD, 125 MHz, 298 K): δ156.7, 156.2, 150.1, 138.8, 137.5, 129.5, 129.3, 128.9, 126.6, 122.7, 116.5, 69.1, 41.2, 39.7, −0.9, −1.5; HRMS (ESI$^+$): calcd for $C_{28}H_{34}N_3O_2Si^+$ $[M]^+$ 472.2420; found 472.2422.

Scheme S4. Synthetic scheme of NIR-ASiP^{a} **2**–**4**.

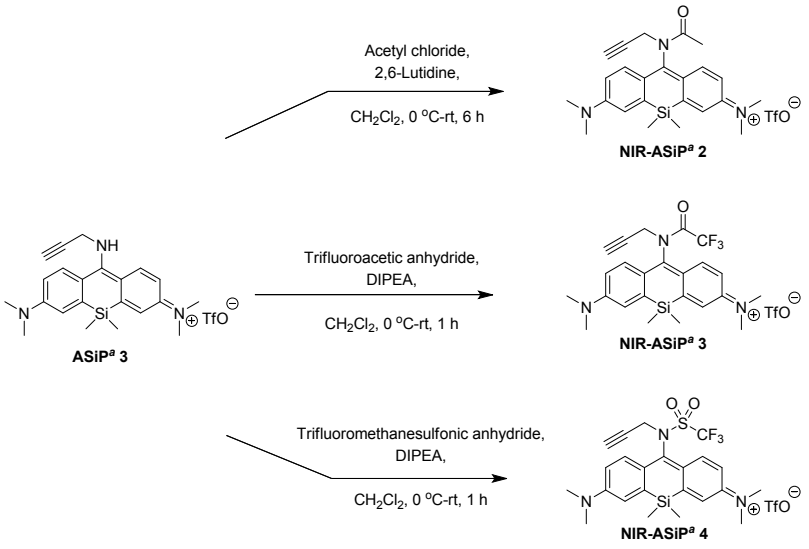

Synthesis of NIR-ASiP^{a} 2.

A solution of ASiP^{a} **3** (51 mg, 0.1 mmol) in anhydrous dichloromethane (5 mL) at 0 °C was treated with 2,6-lutidine (87 µL, 0.75 mmol), and the resulting mixture was stirred for 5 min at 0 °C and then treated with acetyl chloride (36 µL, 0.5 mmol). The resulting mixture, after being stirred at room temperature for 6 h, was diluted with dichloromethane and washed with 1 *N* HCl. The organic layer was evaporated and the residue was subjected to column chromatography (eluent: CH_2Cl_2/MeOH = 95/5) to afford the pure dye NIR-ASiP^{a} **2** (41 mg, 63%) as a green solid. ^{1}H NMR (500 Hz, CD_3OD,

298 K): δ 7.75 (d, 9.5 Hz, 2H), 7.38 (d, 2.5 Hz, 2H), 7.07 (dd, 10.0, 3.0 Hz, 2H), 4.57 (d, 2.5 Hz, 2H), 3.42 (s, 12H), 2.75 (d, 2.5 Hz, 1H), 1.89 (s, 3H), 0.60 (s, 3H), 0.56 (s, 3H); ^{13}C NMR (CD_3OD, 125 MHz, 298 K): δ 171.7, 156.2, 149.8, 139.4, 126.9, 123.3, 116.7, 78.4, 76.1, 41.3, 41.0, 22.1, −0.7, −1.5.

Synthesis of NIR-ASiP^a 3.

A solution of ASiP^a **3** (51 mg, 0.1 mmol) in anhydrous dichloromethane (5 mL) at 0 °C was treated with diisopropylethylamine (88 µL, 0.5 mmol) followed by trifluoroacetic anhydride (42 µL, 0.3 mmol). The resulting mixture, after being stirred at room temperature for 1 h, was diluted with dichloromethane and washed with 1 *N* HCl. The organic layer was evaporated and the residue was subjected to column chromatography (eluent: CH_2Cl_2/MeOH = 95/5) to afford the pure dye NIR-ASiP^a **3** (44 mg, 72%) as a green solid. ^{1}H NMR (500 Hz, CD_3OD, 298 K): δ 7.78 (d, J = 10 Hz, 2H), 7.429 (d, J = 3 Hz, 2H), 7.104 (dd, J = 9.5, 2.5 Hz, 2H), 4.731 (d, J = 3 Hz, 2H), 3.46 (s, 12 H), 2.96 (s, 1H), 0.645 (m, 3H), 0.571 (m, 3H); ^{13}C NMR (CD_3OD, 125 MHz, 298 K): δ 155.4, 154.6, 147.9, 137.7, 125.4, 123,6, 115.0, 76.7, 75.3, 42.4, 39.9, −2.2, −3.0.

Synthesis of NIR-ASiP^a 4.

A solution of ASiP^a **3** (51 mg, 0.1 mmol) in anhydrous dichloromethane (5 mL) at 0 °C was treated with diisopropylethylamine (88 µL, 0.5 mmol) followed by trifluoromethanesulfonic anhydride (84 µL, 0.5 mmol). The resulting mixture, after being stirred at room temperature for 1 h, was diluted with dichloromethane and washed with 1 *N* HCl. The organic layer was evaporated and the residue was subjected to column chromatography (eluent: CH_2Cl_2/MeOH = 95/5) to afford the pure dye NIR-ASiP^a **4** (48 mg, 75%) as a green solid. ^{1}H NMR (500 Hz, CD_3OD, 298 K): δ 7.97 (d, J = 10 Hz, 2H), 7.37 (d, J = 3 Hz, 2H), 7.121 (dd, J = 10, 2.0 Hz, 2H), 4.86 (d, J = 4.0 Hz, 2H), 3.44 (s, 12H),3.10 (q, J = 2.5 Hz,1H) 0.60 (s, 6H), 0.53 (s, 6H); ^{13}C NMR (CD_3OD, 125 MHz, 298 K): δ 154.5, 148.0, 138.4, 126.3, 122.1, 114.6, 78.2, 75.2, 45.2, 39.8, −2.0, −3.3.

Scheme S5. Synthetic scheme of NIR-ASiP^a **5**.

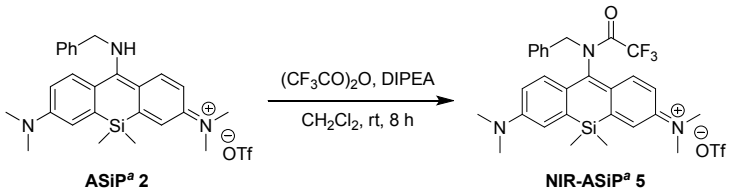

ASiP^a 2 **NIR-ASiP^a 5**

Synthesis of NIR-ASiP^a 5.

A solution of ASiP^a **2** (56 mg, 0.1 mmol) in anhydrous dichloromethane (5 mL) at 0 °C was treated with diisopropylethylamine (174 µL, 1.0 mmol) followed by trifluoroacetic anhydride (69 µL, 0.5 mmol). The resulting mixture, after being stirred at room temperature for 3 h, was diluted with dichloromethane and washed with 1 *N* HCl. The organic layer was evaporated and the residue was subjected to column chromatography (eluent: CH_2Cl_2/MeOH = 95/5) to afford the pure dye NIR-ASiP^a **5** (51 mg, 78%) as a green solid. ^{1}H NMR (500 Hz, CD_3OD, 298 K): δ 7.93 (m, 9H), 6.86 (dd, J = 10, 2.5 Hz, 2H), 5.09 (s, 2H), 3.41 (s, 12H), 0.56 (s, 3H), 0.54 (s, 3H); ^{13}C NMR (CD_3OD, 125 MHz, 298 K): δ 155.5, 147.8, 137.8, 133.4, 130.9, 128.7, 128.2, 125.4, 121.7, 114.5, 78.1, 56.9, 39.8, −2.5, −2.9.

Scheme S6. Synthetic scheme of NIR-ASiP^a **6**.

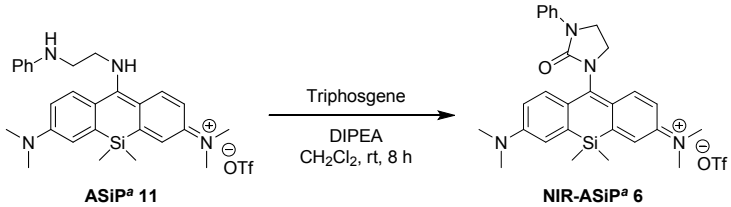

ASiP^a 11 **NIR-ASiP^a 6**

A solution of ASiP^a **11** (59 mg, 0.1 mmol) in anhydrous dichloromethane (5 mL) was treated with diisopropylethylamine (174 µL, 1.0 mmol) at 0 °C. Triphosgene (89 mg, 0.3 mmol) in 0.5 mL dichloromethane was added drop-wise to the mixture, which was allowed to stir for 8 h at room temperature. The reaction mixture was diluted with dichloromethane, washed with 1 *N* HCl, and the organic layer was evaporated. The residue was subjected to flash coloumn chromatography (eluent, CH_2Cl_2/MeOH = 95/5) to afford the pure dye NIR-ASiP^a **6** (44 mg, 72%) as a green solid. ^{1}H NMR (500 Hz, CD_3OD, 298 K): δ 7.90 (d, J = 9.5 Hz, 2H), 7.65 (d, J = 7.5 Hz, 2H), 7.40 (t, J = 7.5 Hz, 2H), 7.34 (d, J = 2.5 Hz, 2H), 7.14 (t, J = 7.5 Hz, 1H), 7.05 (dd, J = 9.5, 3.0 Hz, 2H), 4.35 (q, J = 6.5 Hz, 2H), 4.05 (q, J = 6.5 Hz, 2H), 3.40 (s, 12H), 0.58 (s, 6H); ^{13}C NMR (CD_3OD, 125 MHz, 298 K): δ 156.2, 139.2, 130.1, 124.8, 122.8, 119.8, 116.4, 56.0, 49.6, 49.4, 43.9, 41.2, 18.8, 17.4, 13.2, −1.03.

Scheme S7. Synthetic scheme of julolidine derived ASiP^j **1**–**3** dyes.

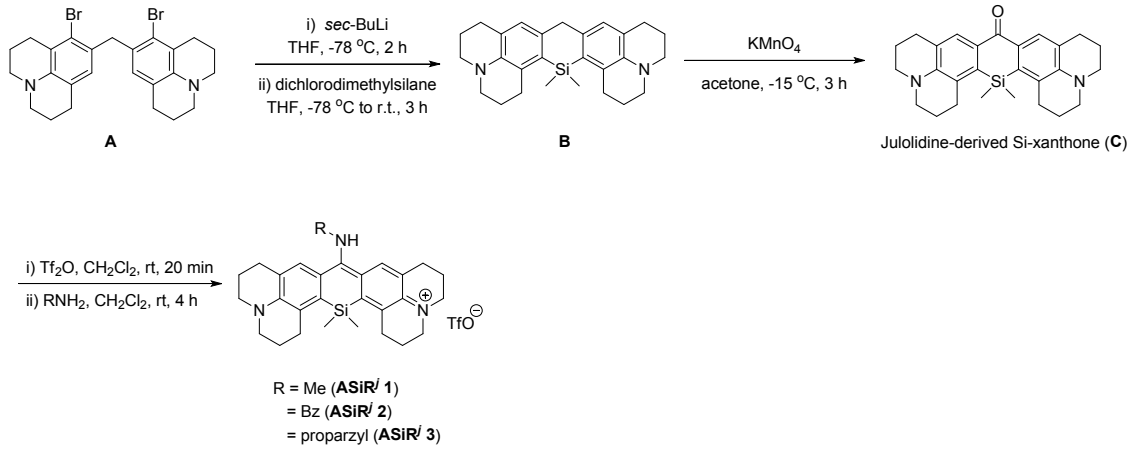

Synthesis of julolidine-derived Si-xanthone (C).

A solution of dibromide **A** (prepared according to the reported procedure[7]; 200 mg, 0.39 mmol) in anhydrous THF (15 mL) at −78 °C was treated with *sec*-BuLi (1.4 M, 0.84 mL. 1.17 mmol) under Ar-atmosphere, and the resulting mixture was further stirred at −78 °C for 2 h. The reaction mixture was treated with dichloromethylsilane (85 µL, 0.7 mmol) at −78 °C and then stirred at room temperature for 3 h before quenching with 1 *N* HCl. After neutralization with saturated $NaHCO_3$, the mixture was extracted with dichloromethane (2 × 10 mL), and the organic layer was washed with brine followed by drying over anhydrous Na_2SO_4. The organic solvent was evaporated to obtain the crude product **B**, which was used for the next step without further purification.

A solution of the compound **B** in acetone (15 mL) at −15 °C was treated with $KMnO_4$ (185 mg, 1.17 mmol) portionwise over 30 min, and the resulting mixture was stirred for 2 h 30 min at −15 °C. The reaction mixture was diluted with dichloromethane (15 mL) and then filtered through Celite. The filtrate was concentrated and the residue was purified with coloumn chromatography (eluent, CH_2Cl_2/EtOAc = 97/3) to give the julolidine-derived Si-xanthone **C** (33 mg, 20%) as a yellow solid. ^{1}H NMR ($CDCl_3$, 300 MHz, 298K): δ 8.07 (s, 2H), 3.29–3.27 (m, 8H), 2.91-2.80 (m, 8H), 2.03–1.96 (m, 8H), 0.59 (s, 6H); ^{13}C NMR ($CDCl_3$, 125 MHz, 298 K): δ 185.74, 145.5, 136.1, 129.8, 128.5, 124.1, 122.8, 50.6, 50.1, 28.9, 28.3, 22.0, 21.7, 0.3.

Synthesis of ASiP^j 1–3.

Trifluoromethanesulfonic anhydride (21 µL, 0.123 mmol) was added dropwise to a solution of julolidine-derived Si-xanthone **C** (35 mg, 0.082 mmol) in anhydrous CH_2Cl_2 (3 mL) at 0 °C. The resulting intense green reaction mixture was stirred for 20 min at room temperature and then each of the various amines (3 equivalents) was added at the same temperature. The reaction mixture was further stirred for 4 h at room temperature and then directly loaded onto silica gel for flash chromatography (eluent: MeOH/CH_2Cl_2 = 3/97), affording the pure dyes ASiP^j **1**–**3** as deep-red coloured solids.

ASiP^j 1: Methylamine in THF (2 M, 123 µL, 0.246 mmol) was used as the amine source. Yield = 34

mg (70%). ^{1}H NMR ($CDCl_3$, 500 MHz, 298K): δ 9.82 (s, br, 1H), 7.53 (br, 1H), 7.12 (br, 1H), 3.47 (d, J = 5.0 Hz, 3H), 3.33 (s, br, 8H), 2.83 (s, br, 8H), 1.97 (s, br, 8H), 0.56 (s, 6H); ^{13}C NMR ($CDCl_3$, 125 MHz, 298 K): δ 175.1, 146.6, 129.4, 127.0, 124.7, 122.2, 119.6, 50.7, 50.1, 37.9, 29.9, 29.4, 28.0, 26.7, 21.5, 21.2, 0.2, 0.1, −0.1, −0.3; HRMS (ESI$^+$): calcd for $C_{28}H_{36}N_3Si^+$ [M]$^+$ 442.2679; found 442.2678.

ASiP^j 2: Benzylamine (27 µL, 0.246 mmol) was used as the amine source. Yield = 43 mg (85%). ^{1}H NMR ($CDCl_3$, 500MHz, 298K): δ 7.38 (m, 5H), 7.30 (s, br, 2H), 4.93 (s, 2H), 3.35–3.30 (m, 8H), 2.85–2.82 (m, br, 8H), 2.02–1.98 (m, 8H), 0.56 (s, 6H); ^{13}C NMR ($CDCl_3$, 75 MHz, 298 K): δ 176.1, 146.8, 137.3, 129.2, 128.1, 127.7, 126.3, 122.9, 118.7, 53.7, 50.7, 50.2, 29.9, 29.4, 27.9, 21.5, 21.1, 0.2, −0.1; HRMS (ESI$^+$): calcd for $C_{34}H_{40}N_3Si^+$ [M]$^+$ 518.2992; found 518.2989.

ASiP^j 3: Propargylamine (16 µL, 0.246 mmol) was used as the amine source. Yield = 39 mg (78%). ^{1}H NMR ($CDCl_3$, 300MHz, 298K): δ 7.59 (s, 2H), 4.44 (d, J = 1.8 Hz, 2H), 3.36–3.34 (m, 8H), 2.85–2.81 (m, 8H), 2.53 (s, 1H), 2.03–1.96 (m, 8H), 0.56 (s, 6H); ^{13}C NMR ($CDCl_3$, 125 MHz, 298 K): δ 175.4, 147.0, 128.6, 126.5, 123.0, 122.1, 119.6, 78.4, 74.5, 50.8, 50.2, 39.9, 29.9, 29.4, 27.9, 21.5, 21.1, 0.2, −0.1; HRMS (ESI$^+$): calcd for $C_{30}H_{36}N_3Si^+$ [M]$^+$ 466.2679; found 466.2677.

Scheme S8. Synthetic scheme of NIR-ASiP^j **1-3** and the probe **ASiP^j-H_2O_2**.

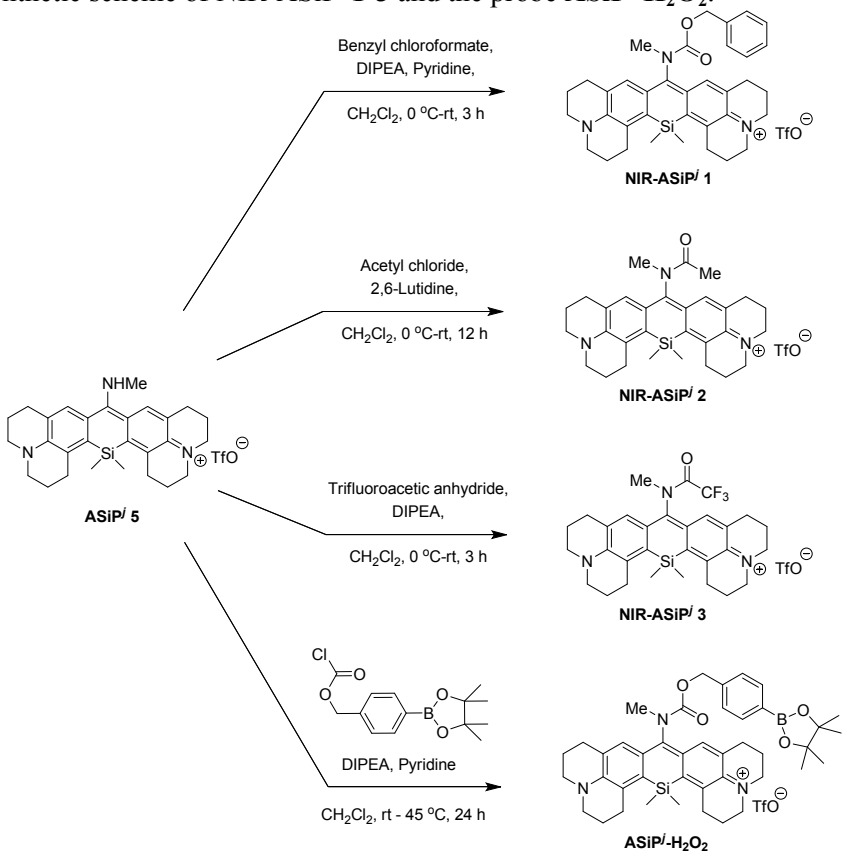

Synthetic procedures of NIR-ASiP^j **1-3** are already described in the main manuscript, here only the synthesis of **ASiP^j-H_2O_2** is described.

Synthesis of the probe ASiP^{j}-H_2O_2.

A solution of ASiP^{j} **1** (30 mg, 0.05 mmol) in anhydrous dichloromethane (5 mL) was treated with diisopropylethylamine (44 μL, 0.25 mmol) and pyridine (40 μL, 0.5 mmol), and the resulting mixture, after being stirred for 10 min at room temperature, was treated with 4-(pinacolboronate)-benzyl chloroformate (0.5 mmol). The reaction mixture was stirred at 45 °C for 24 h, and then it was diluted with dichloromethane and washed with 1 *N* HCl. The organic layer was evaporated and the residue was subjected to flash coloumn chromatography (eluent, CH_2Cl_2/MeOH = 95/5) to afford the product (3 mg, 8%) as a green solid. ^{1}H NMR ($CDCl_3$, 500 MHz, 298 K): δ 7.81 (d, J = 8.0 Hz, 2H), 7.38 (d, J = 8 Hz, 2H), 6.93 (s, 2H), 4.72 (s, 2H), 3.77–3.75 (m, br, 4H), 3.64 (br, 4H), 3.39 (s, 3H), 2.95–2.90 (m, br, 4H), 2.75 (br, 4H), 2.13–2.00 (m, 8H), 1.34 (s, 12H), 0.68 (s, 3H), 0.612 (s, 3H); ^{13}C NMR ($CDCl_3$, 125 MHz, 298 K): δ 155.2, 150.9, 144.3, 141.8, 141.4, 135.3, 133.4, 132.6, 126.3, 125.6, 125.5, 124.4, 122.8, 84.0, 65.5, 52.4, 51.8, 51.7, 41.1, 29.9, 28.9, 28.2, 28.0, 25.1, 21.0, 20.9, 20.7, 1.2, 0.2, −0.7, −1.1; HRMS (ESI$^+$): calcd for $C_{42}H_{53}BN_3O_4Si^+$ $[M]^+$ 702.3898; found 702.3903.

References

(1) (a) Albota, M. A.; Xu, C.; Webb, W. W. Appl. *Optics* **1998**, *37*, 7352. (b) Xu, C.; Webb, W. W. *J. Opt. Soc. Am. B* **1996**, *13*, 481.

(2) Ishiyama, M.; Miyazono, Y.; Sasamoto, K.; Ohkura, Y.; Ueno, K. *Talanta* **1997**, *44*, 1299; Tominaga, H. *et al. Anal. Commun.* **1999**, *36*, 47.

(3) Lukinavičius, G.; Umezawa, K.; Olivier, N.; Honigmann, A.; Yang, G.; Plass, T.; Mueller, V.; Reymond, L.; Corrêa, I. R., Jr.; Luo, Z.-G.; Schultz, C.; Lemke, E. A.; Heppenstall, P.; Eggeling, C.; Manley. S.; Johnsson, K. *Nat. Chem.*, **2013**, *5*, 132.

(4) Hannant, J.; Hedley, H. J.; Pate, J.; Walli, A; Farha Al-Said, A. S.; Galindo, A. M.; Connolly, A. B.; Horrocks, R. B.; Houlton, A.; Pike, R. A. *Chem. Commun.*, **2010**, *46*, 5870.

(5) Srinivasachari, S.; Fichter, K. M.; Reineke, T. M. *J. Am. Chem. Soc.*, **2008**, *130*, 4618.

(6) Maruyama, T.; Fujie, Y.; Oya, N.; Hosaka, E.; Kanazawa, A.; Tanaka, D.; Hattori, Y.; Motoyoshiya, J. *Tetrahedron*, **2011**, *67*, 6927.

(7) Butkevich, A. N.; Ta, H.; Ratz, M.; Stoldt, S.; Jakobs, S.; Belov, V. N.; Hell, S. W. *ACS Chem. Biol.,* **2018**, *13*, 475.

^{1}H and ^{13}C NMR spectra for selected dyes

^{1}H NMR ($CDCl_3$, 500 Hz, 298 K) of ASiP^{a} **1**

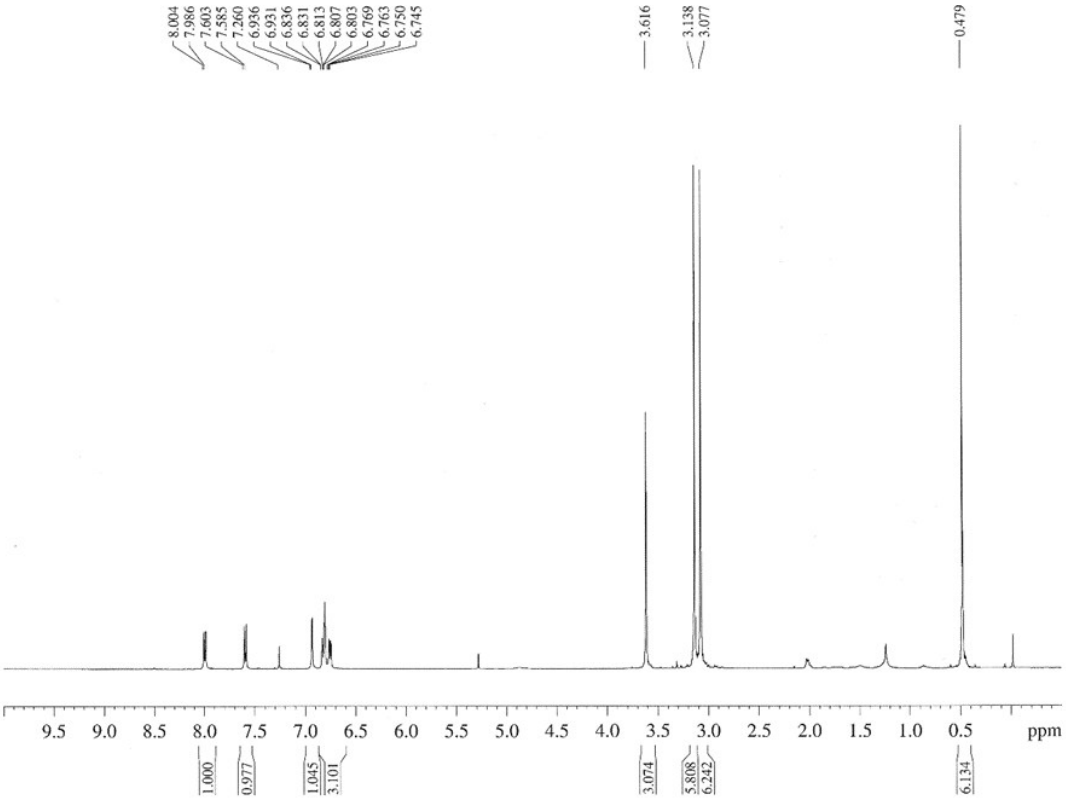

^{13}C NMR ($CDCl_3$, 125 MHz, 298 K) of ASiP^{a} **1**

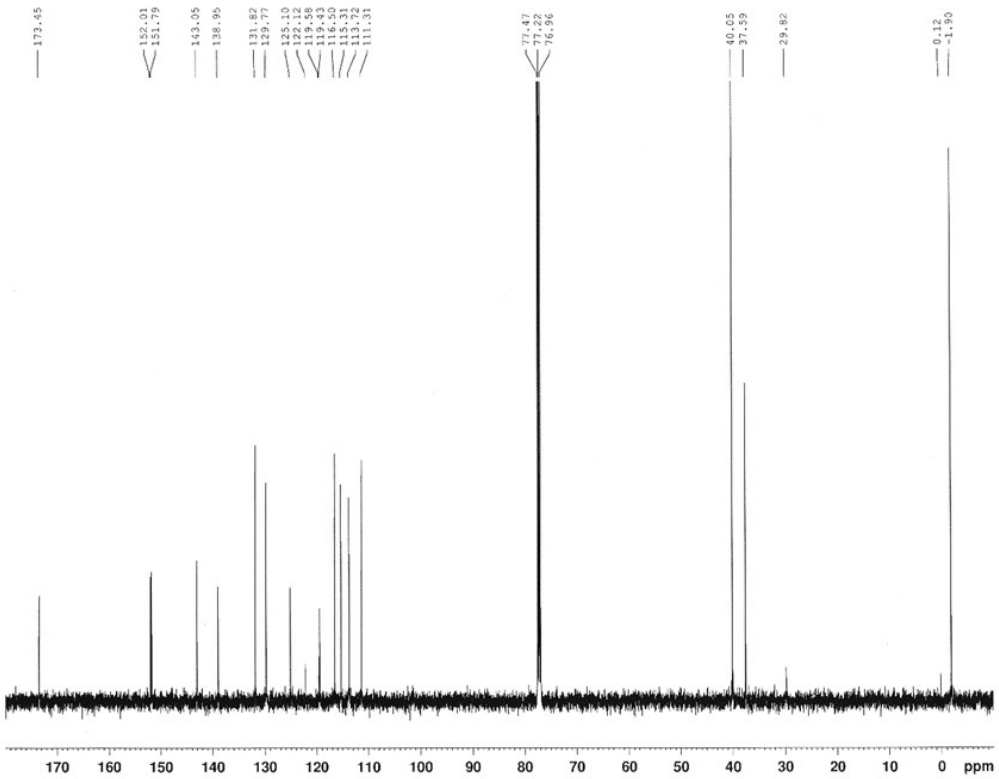

^{1}H NMR ($CDCl_3$, 300 Hz, 298 K) of ASiP^{a} **2**

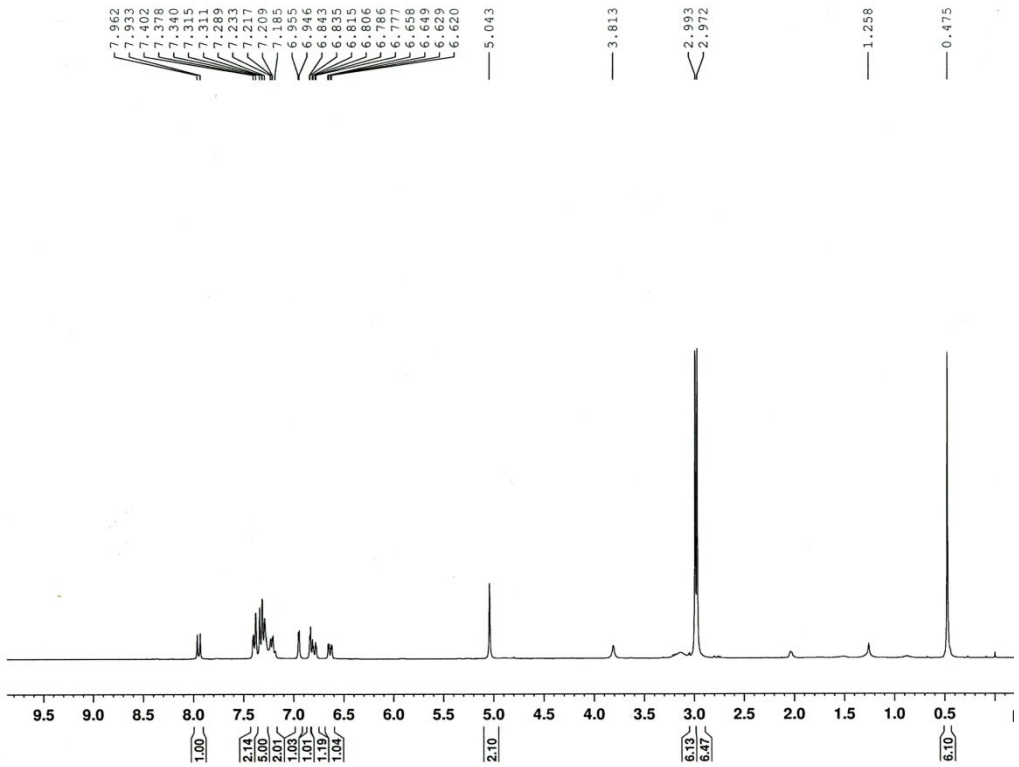

^{13}C NMR ($CDCl_3$, 75 MHz, 298 K) of ASiP^{a} **2**

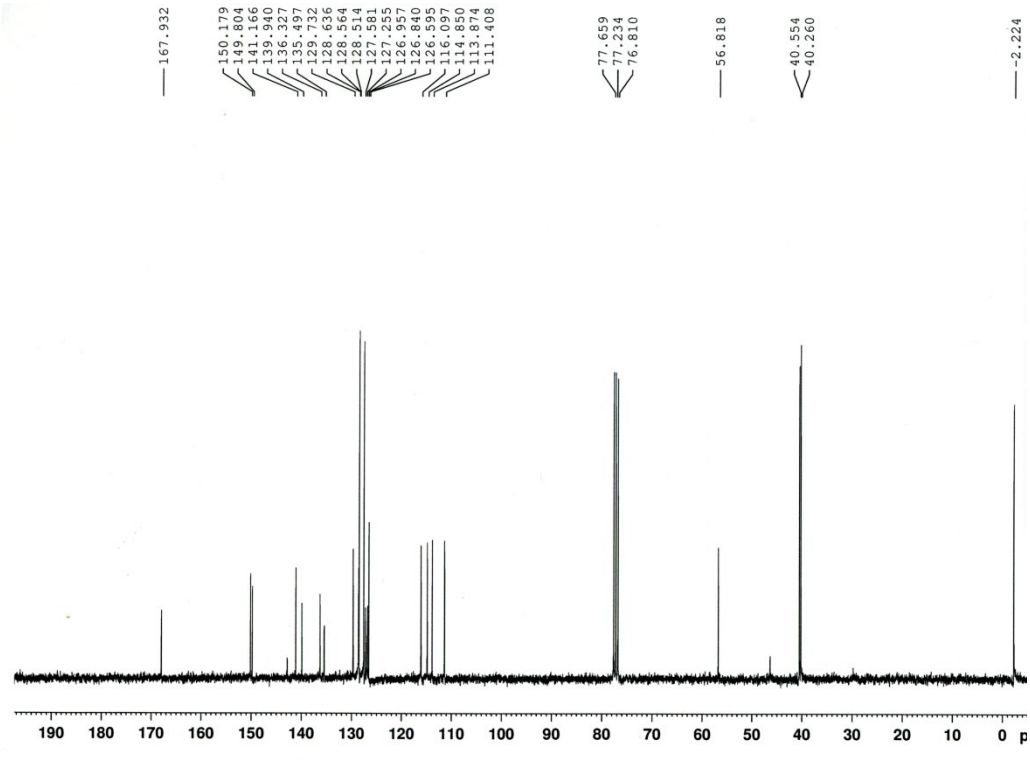

^{1}H NMR ($CDCl_3$, 300 Hz, 298 K) of ASiP^{a} **3**

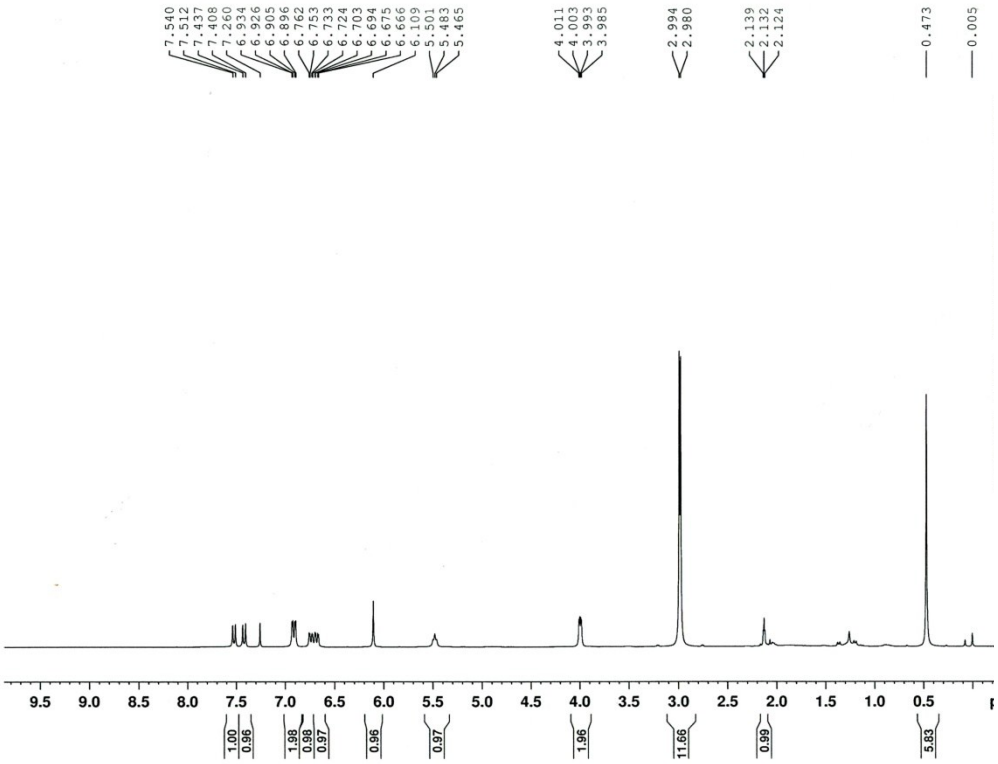

^{13}C NMR ($CDCl_3$, 125 MHz, 298 K) of ASiP^{a} **3**

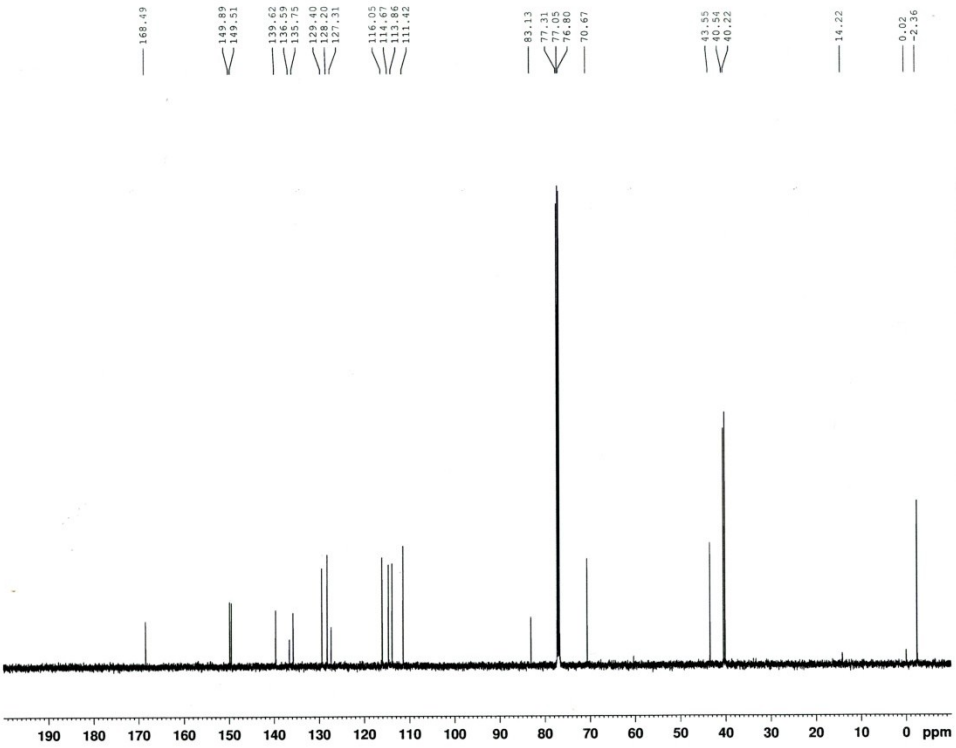

^{1}H NMR ($CDCl_3$, 300 Hz, 298 K) of ASiP^{a} **4**

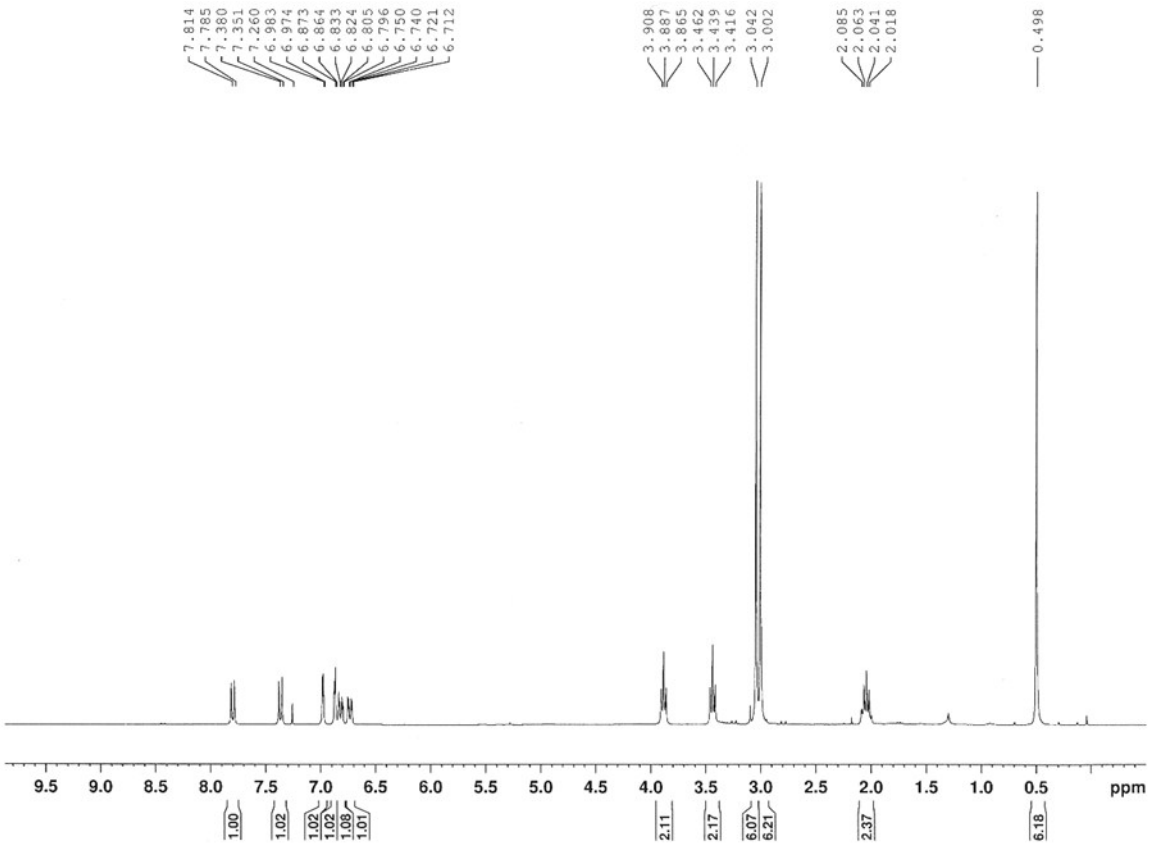

^{13}C NMR ($CDCl_3$, 75 MHz, 298 K) of ASiP^{a} **4**

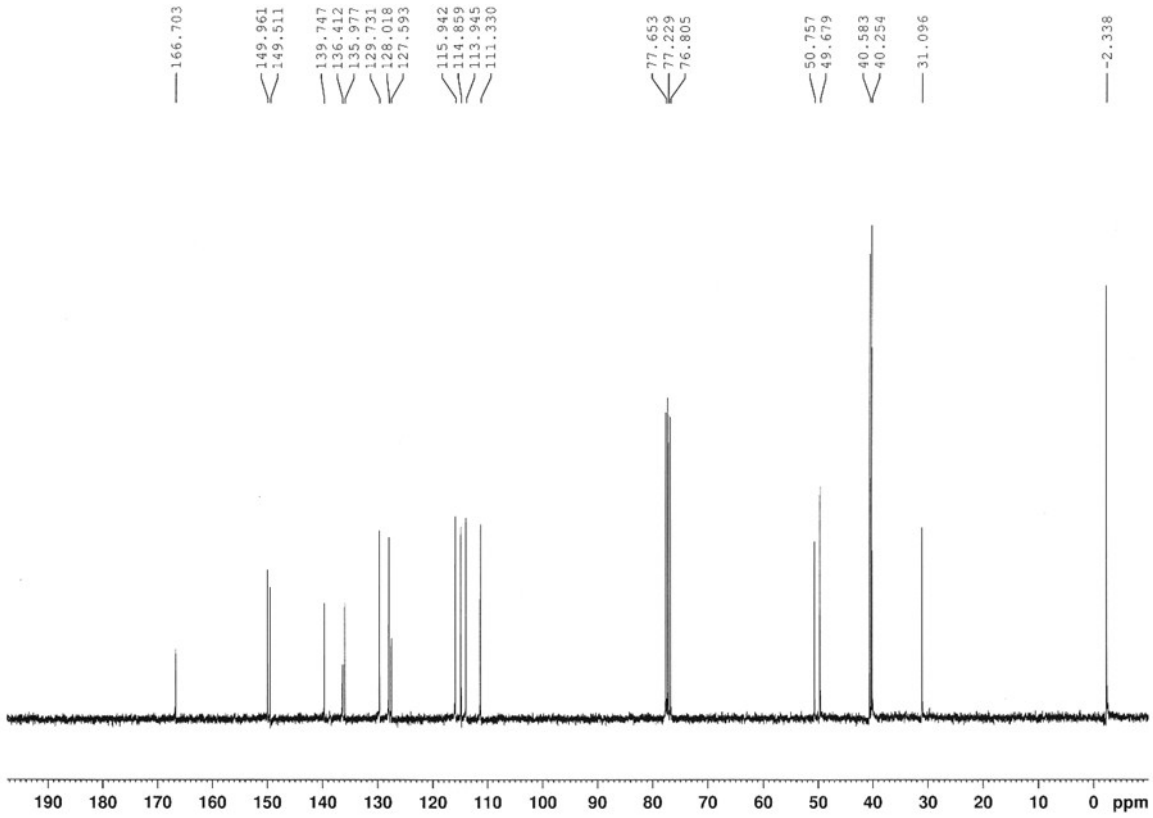

^{1}H NMR ($CDCl_3$, 500 Hz, 298 K) of ASiP^{a} **5**

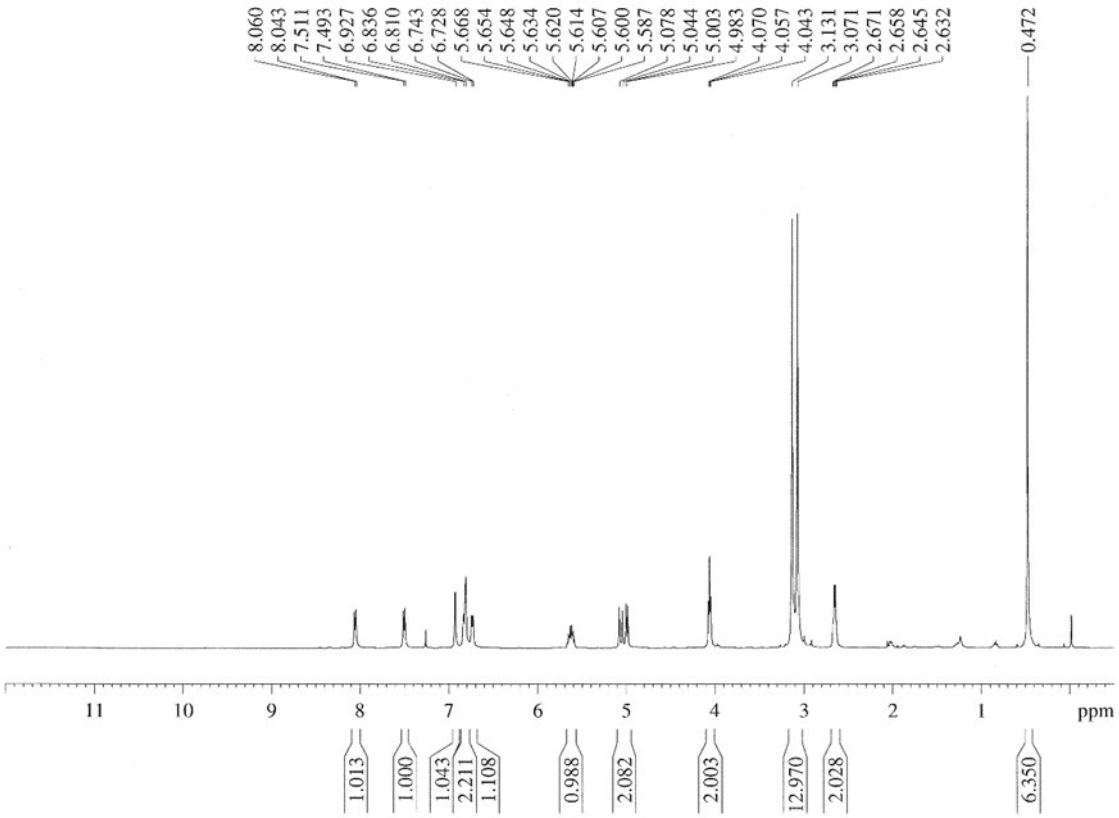

^{13}C NMR ($CDCl_3$, 125 MHz, 298 K) of ASiP^{a} **5**

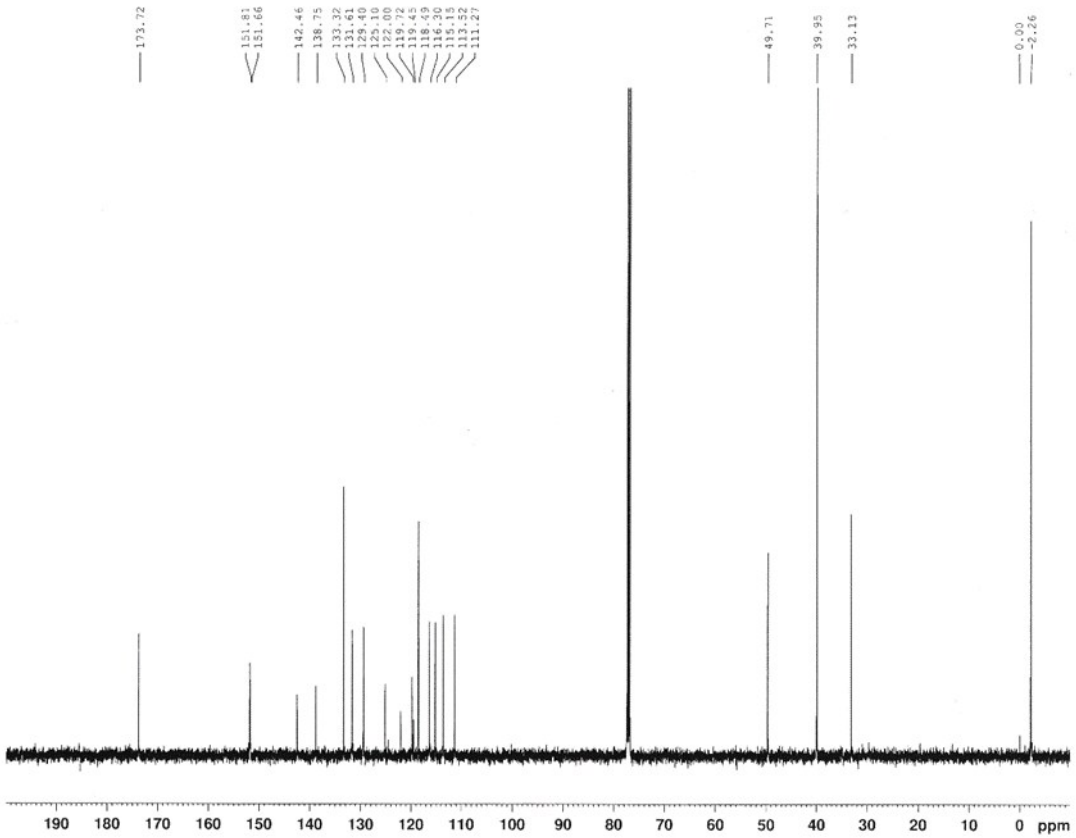

^{1}H NMR ($CDCl_3$, 500 Hz, 298 K) of ASiP^{a} **6**

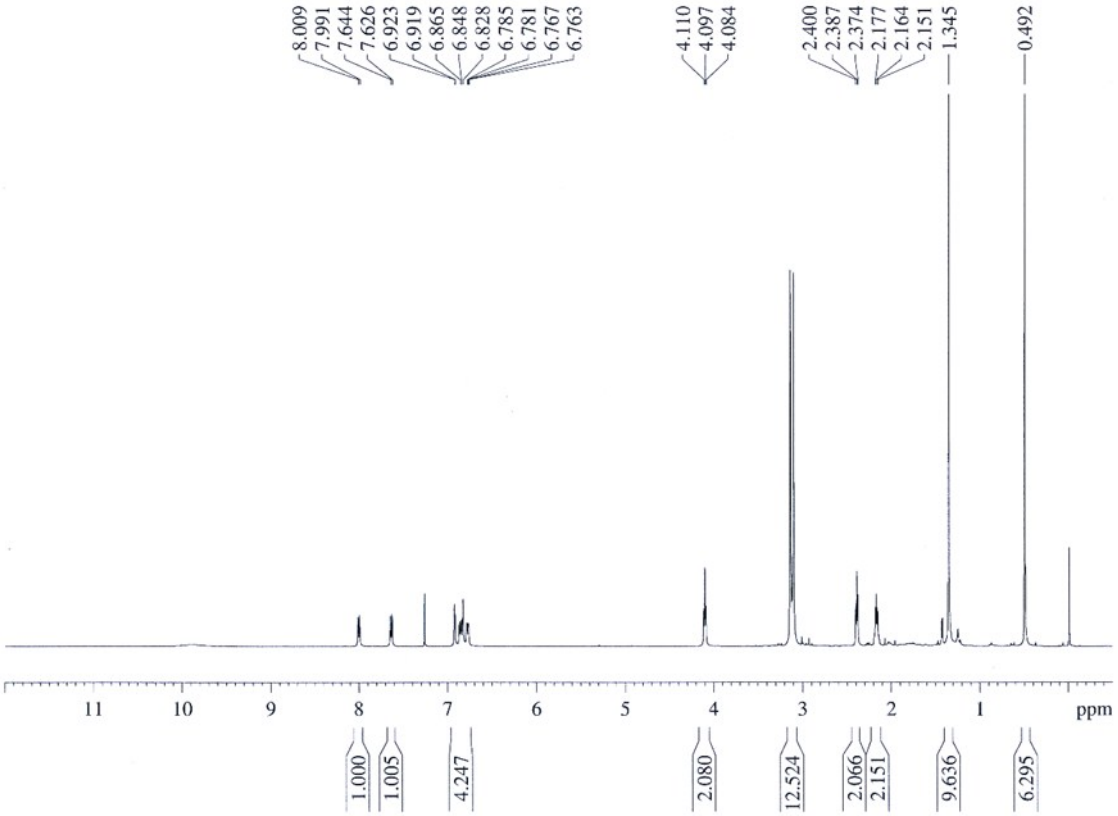

^{13}C NMR ($CDCl_3$, 125 MHz, 298 K) of ASiP^{a} **6**

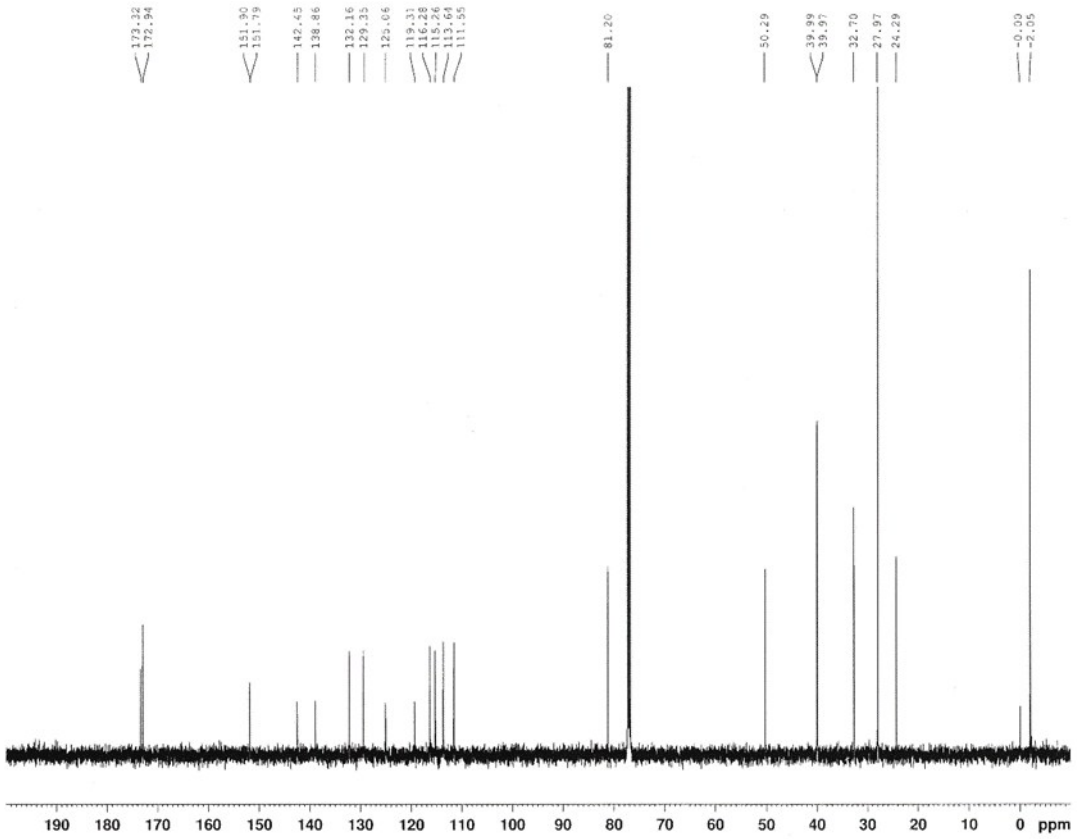

^{1}H NMR ($CDCl_3$, 500 Hz, 298 K) of ASiP^{a} **7**

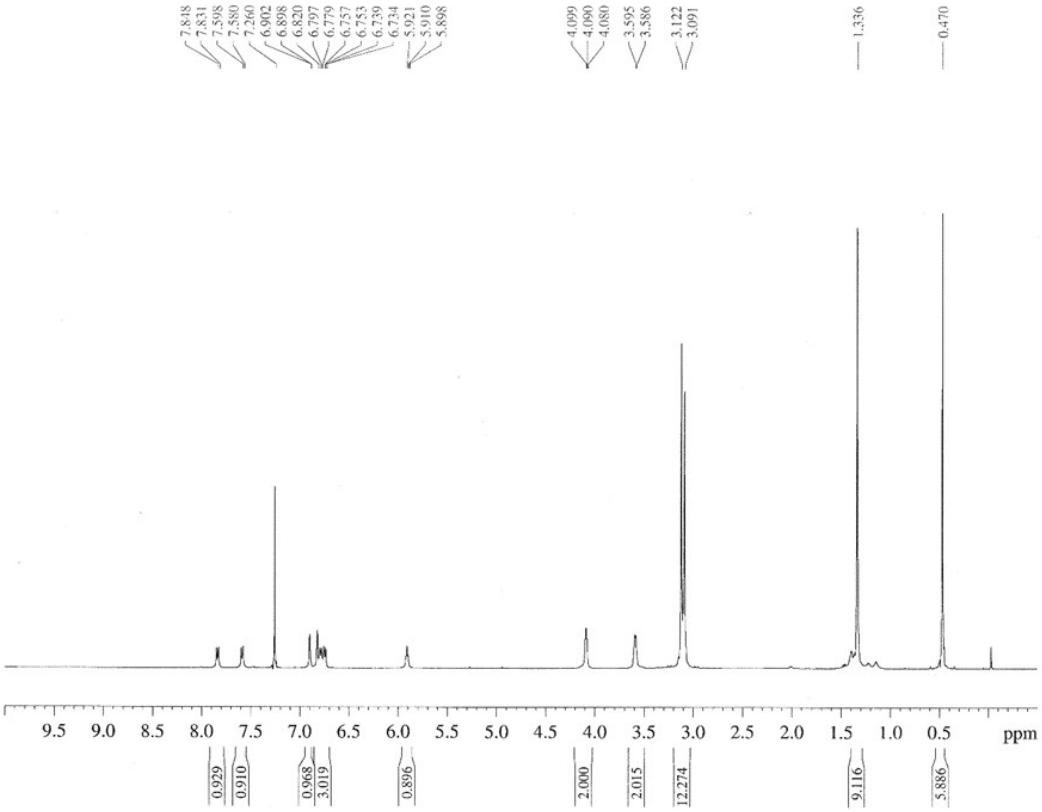

^{13}C NMR ($CDCl_3$, 125 MHz, 298 K) of ASiP^{a} **7**

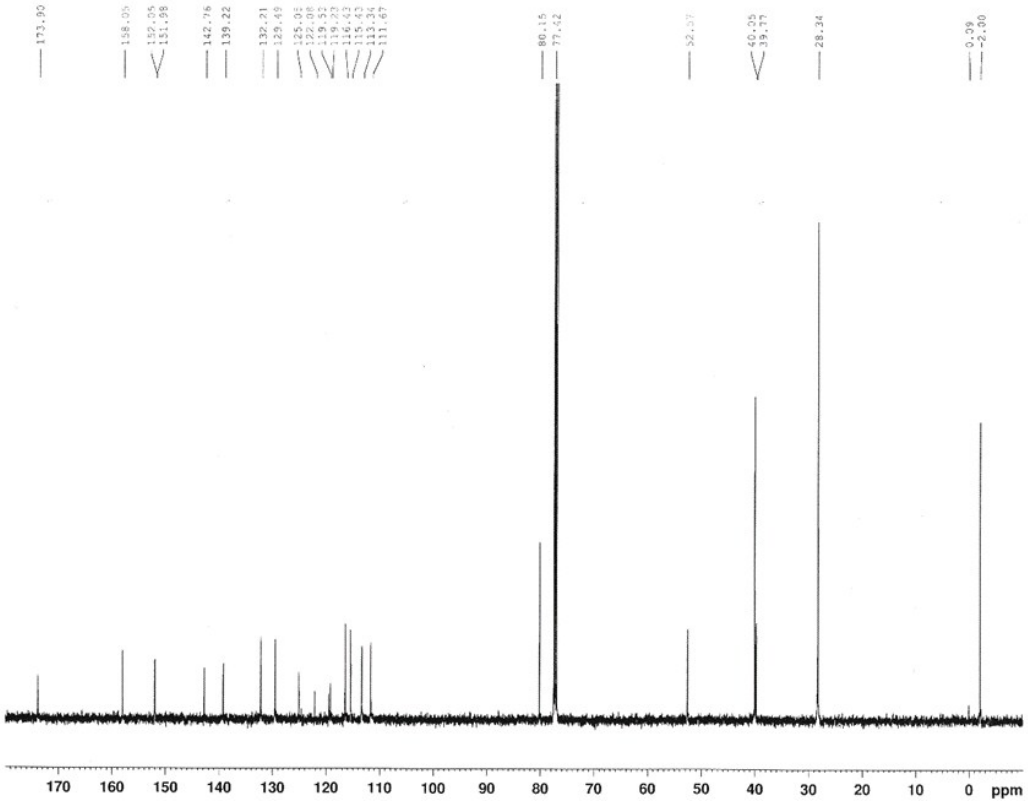

^{1}H NMR ($CDCl_3$, 300 Hz, 298 K) of ASiP^{a} **8**

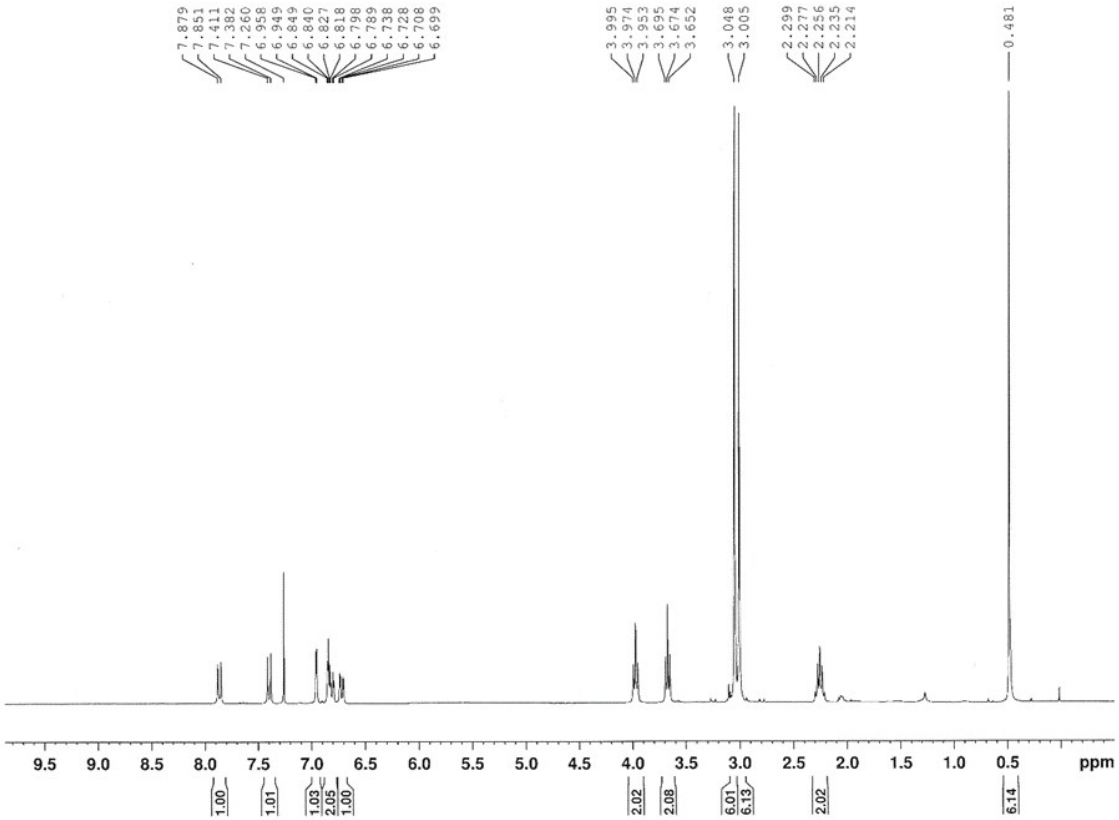

^{13}C NMR ($CDCl_3$, 75 MHz, 298 K) of ASiP^{a} **8**

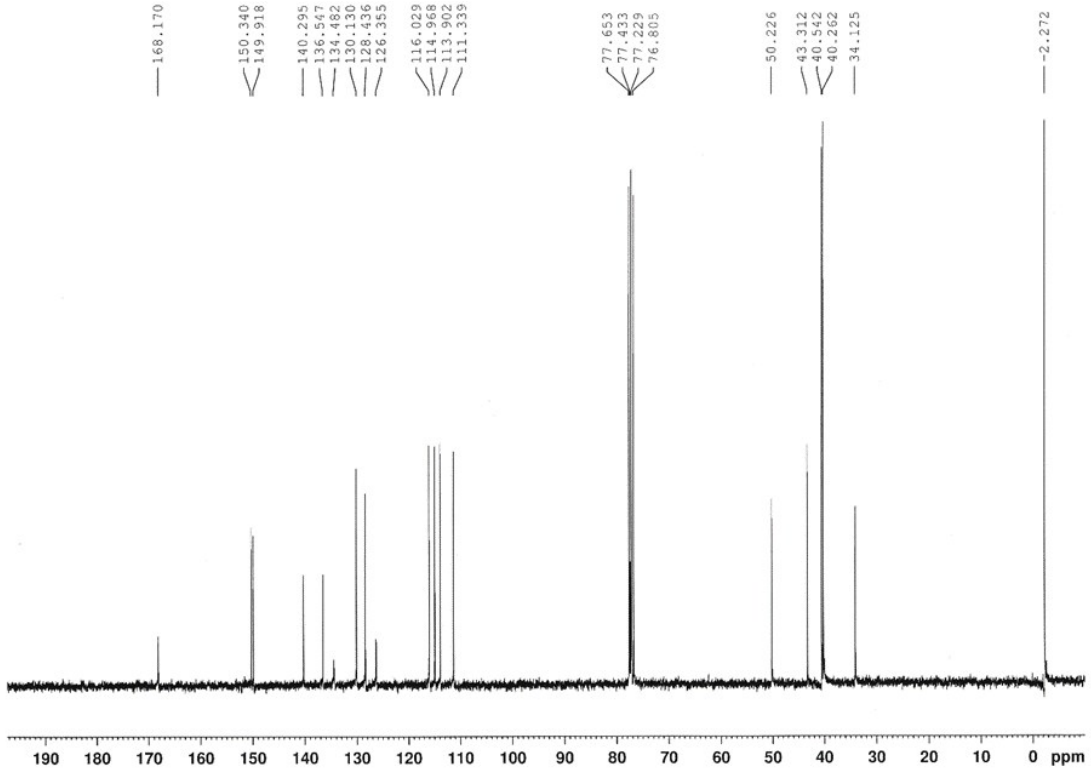

^{1}H NMR ($CDCl_3$, 300 Hz, 298 K) of ASiP^{a} **9**

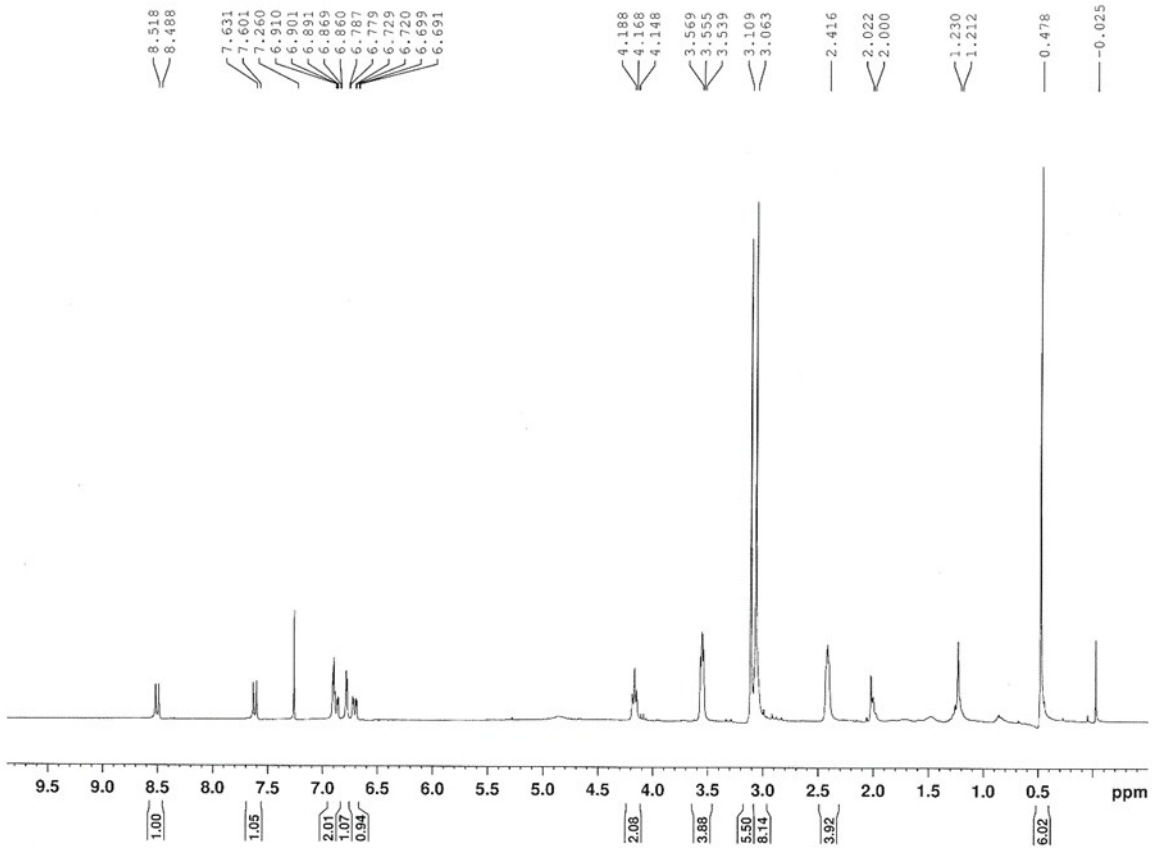

^{13}C NMR ($CDCl_3$, 125 MHz, 298 K) of ASiP^{a} **9**

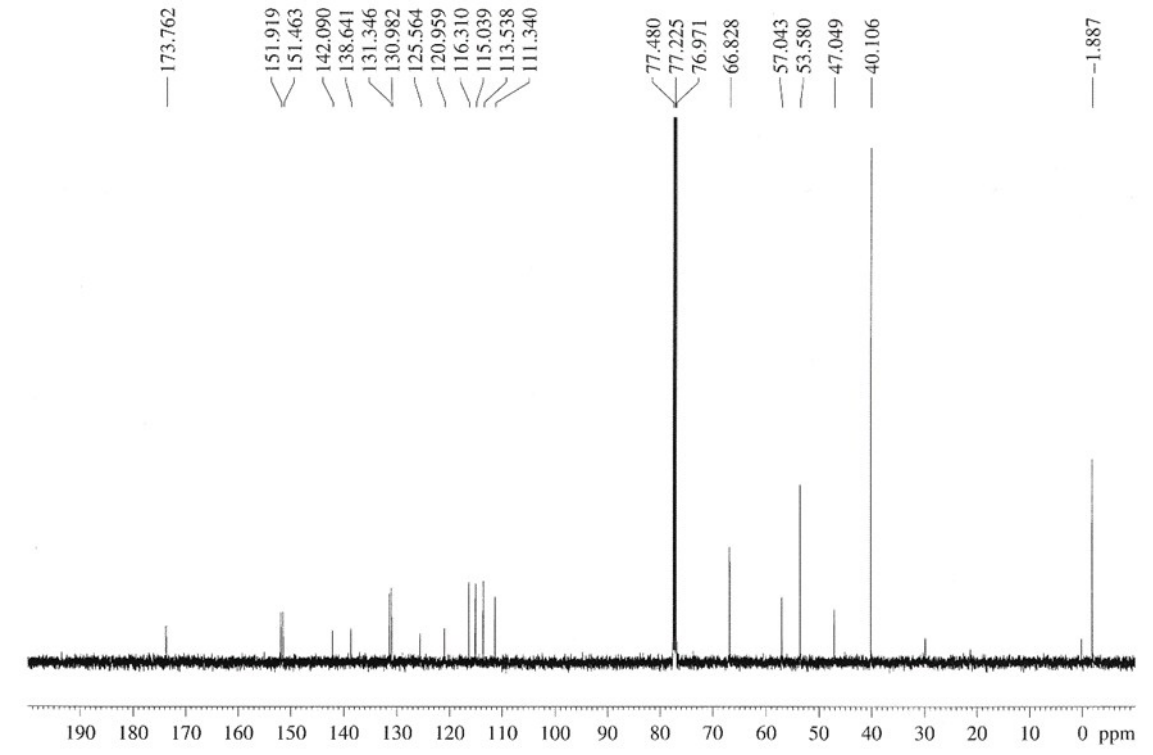

^{1}H NMR ($CDCl_3$, 500 Hz, 298 K) of ASiP^{a} **10**

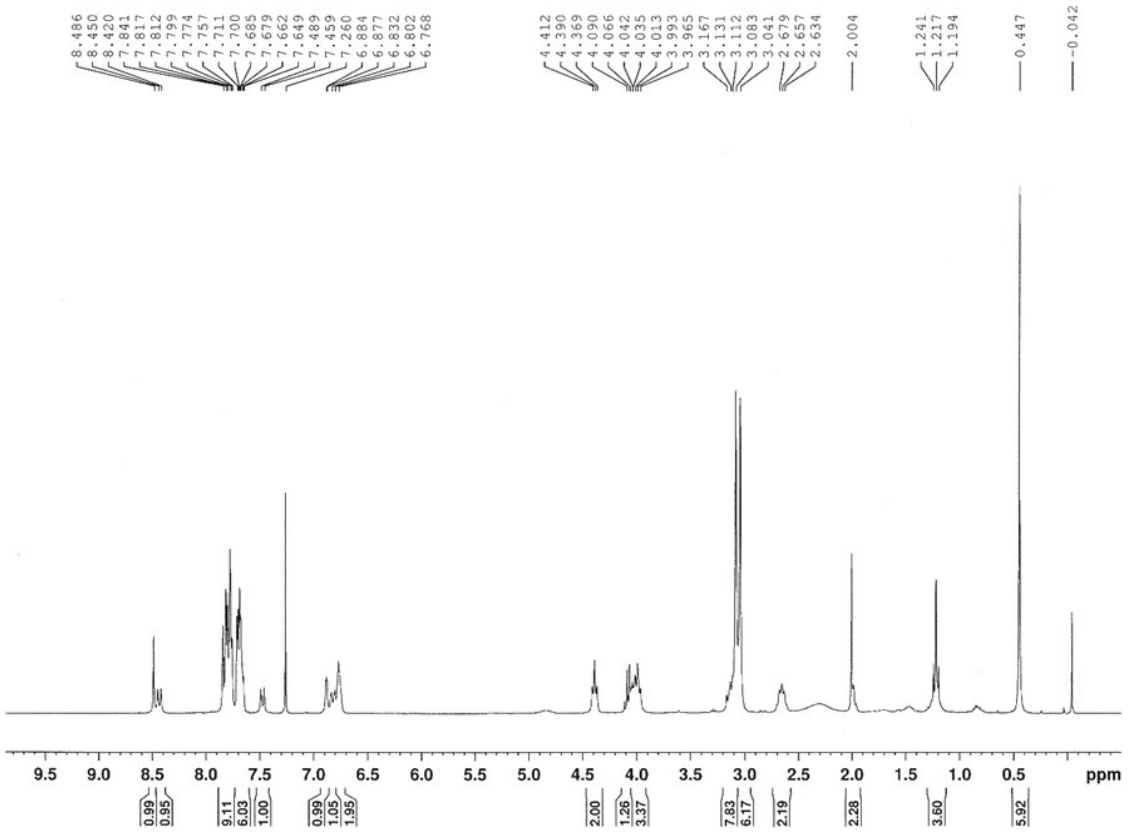

^{13}C NMR ($CDCl_3$, 125 MHz, 298 K) of ASiP^{a} **10**

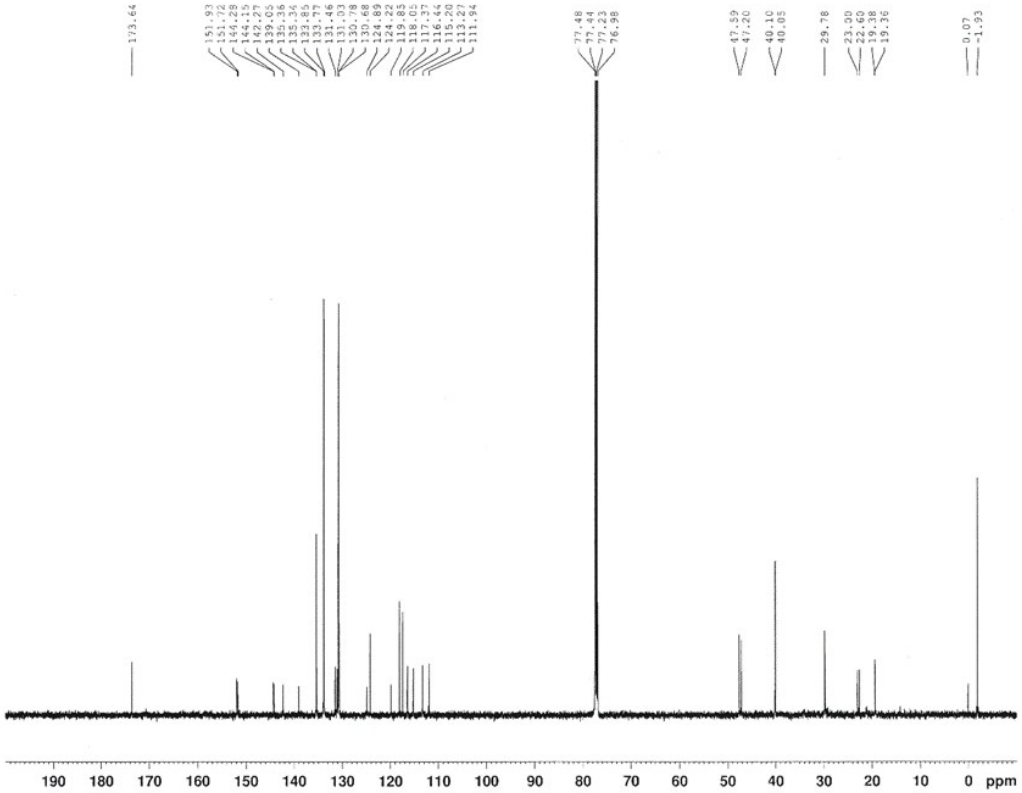

^{1}H NMR (CD_3CN, 500 MHz, 298 K) of NIR-ASiP^{a} **1**

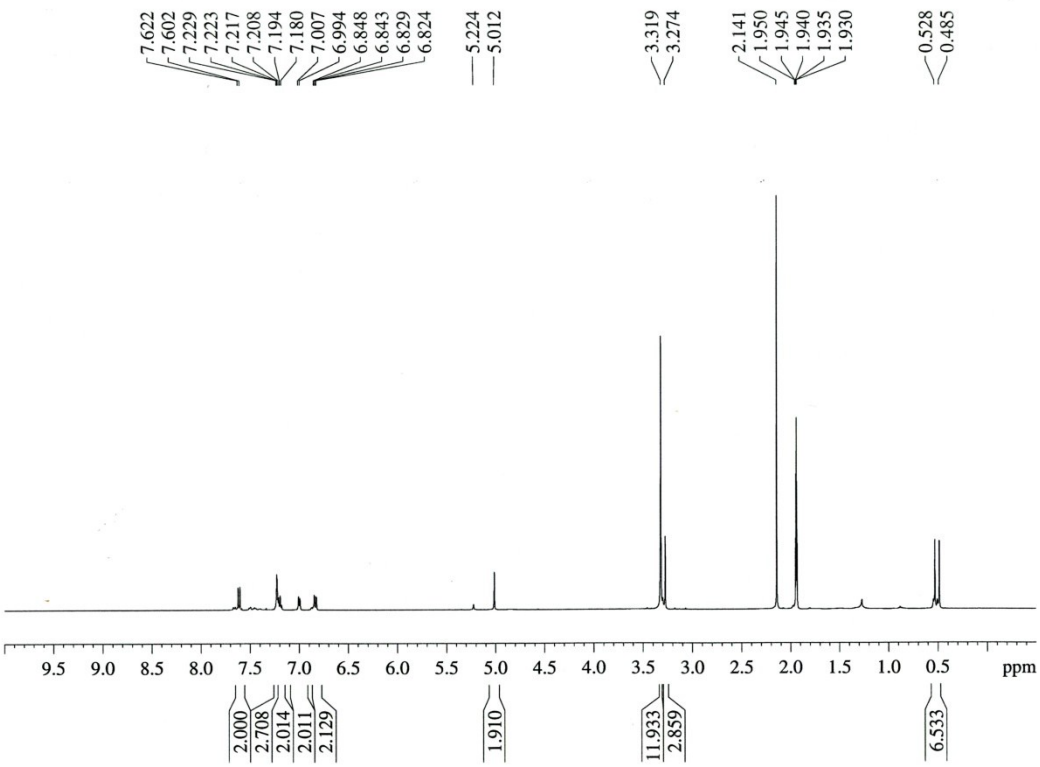

^{13}C NMR (CD_3OD, 125 MHz, 298 K) of NIR-ASiP^{a} **1**

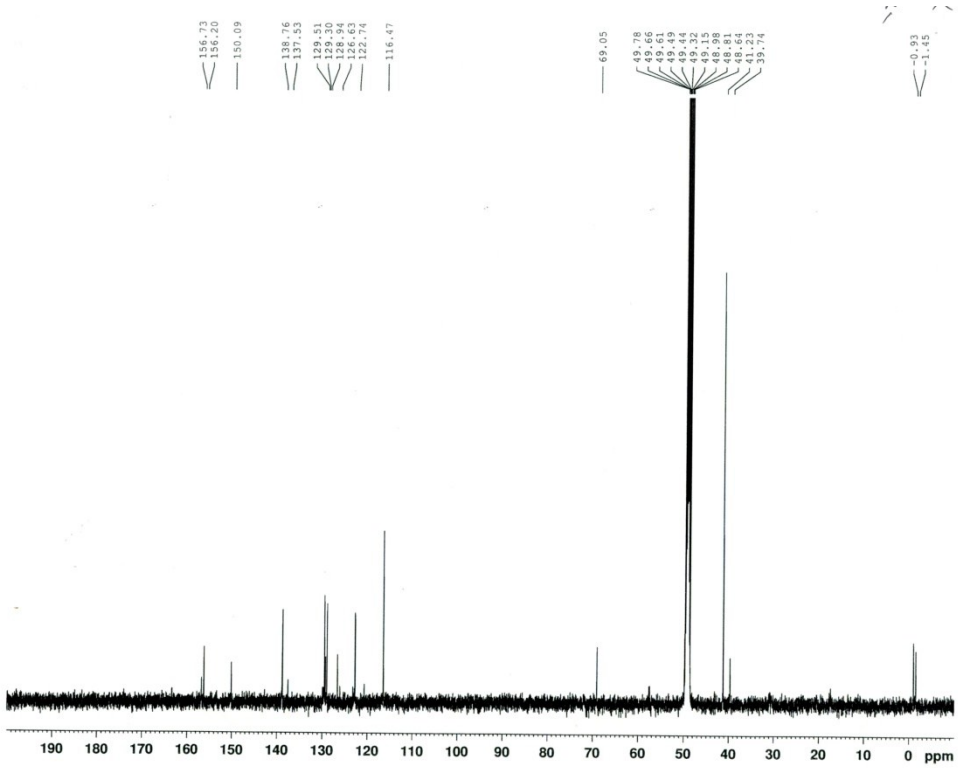

^{1}H NMR (CD_3OD, 500 MHz, 298 K) of NIR-ASiP^{a} **2**

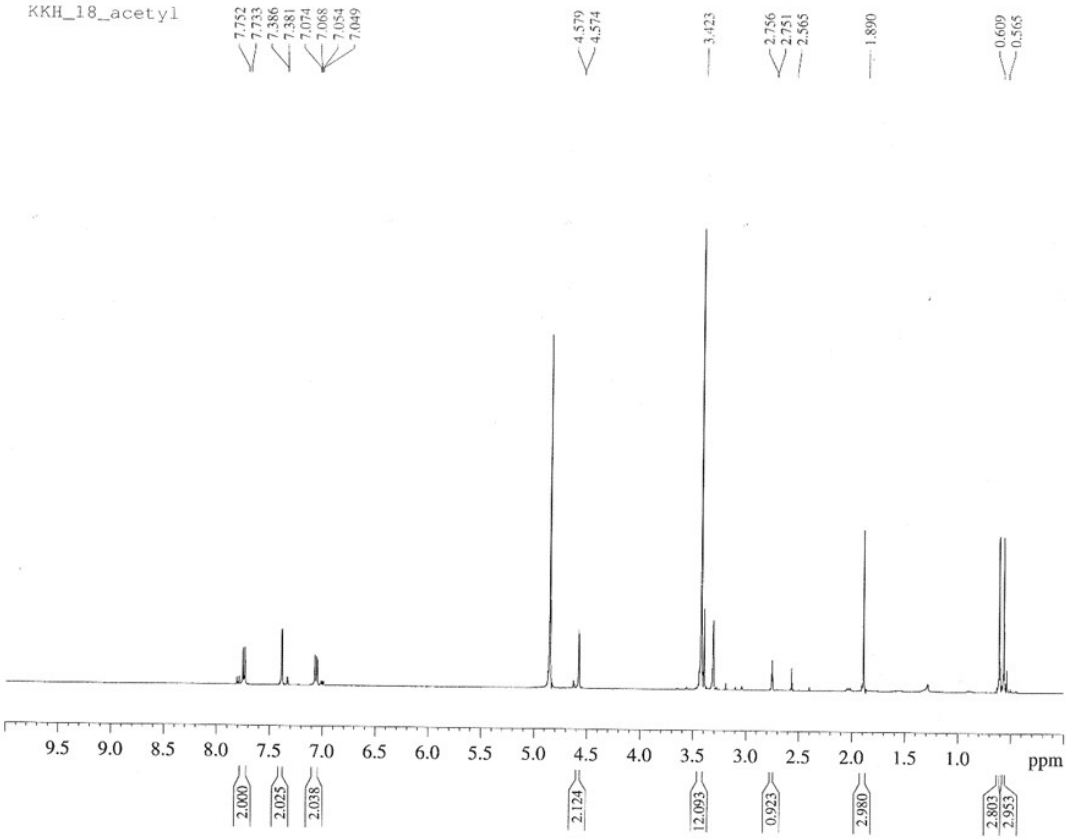

^{13}C NMR (CD_3OD, 125 MHz, 298 K) of NIR-ASiP^{a} **2**

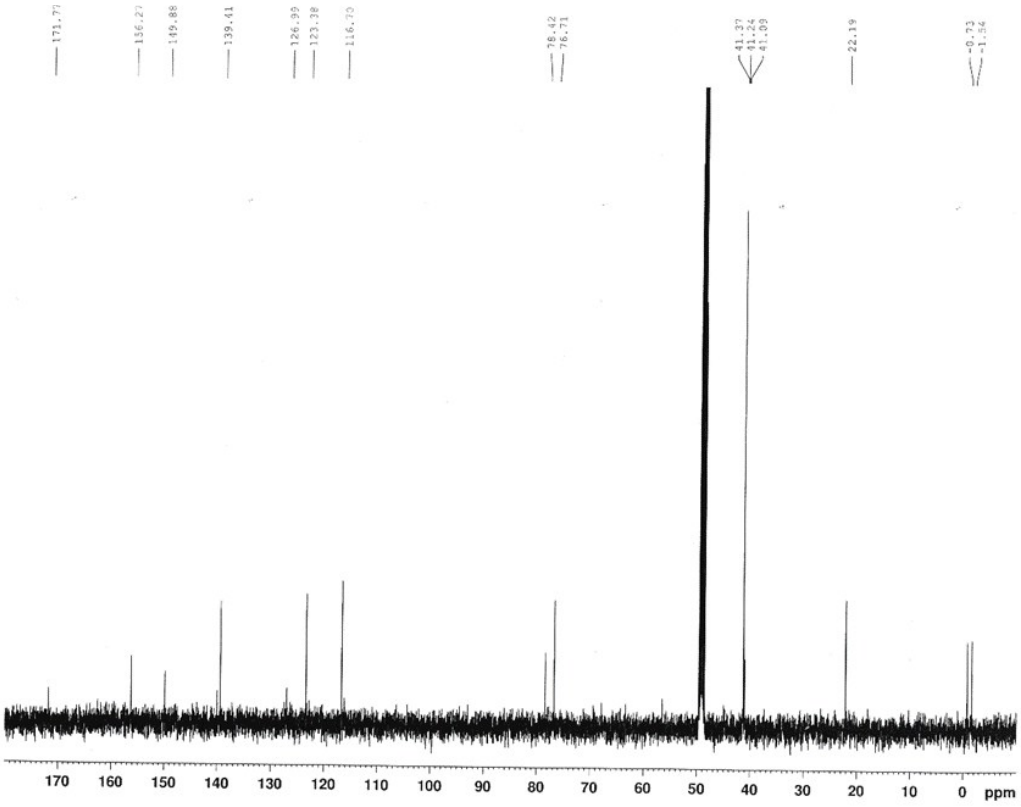

^{1}H NMR (CD_3OD, 500 MHz, 298 K) of NIR-ASiP^{a} **3**

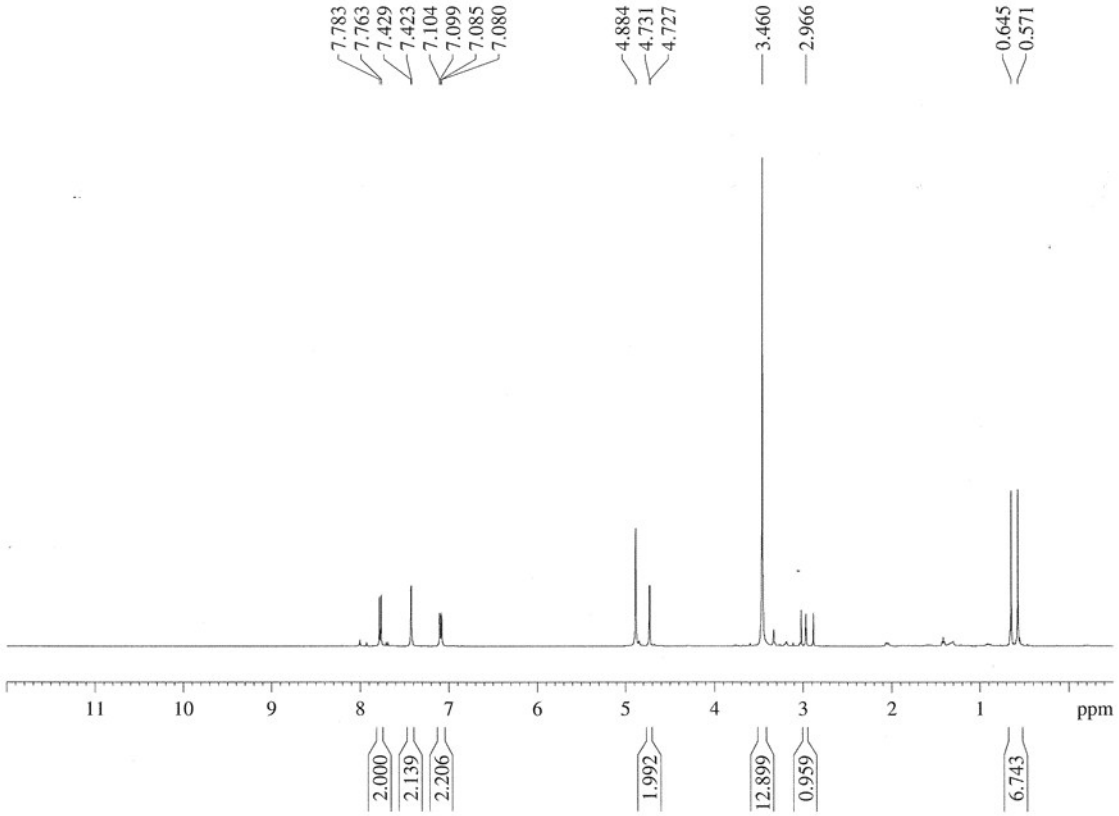

^{13}C NMR (CD_3OD, 125 MHz, 298 K) of NIR-ASiP^{a} **3**

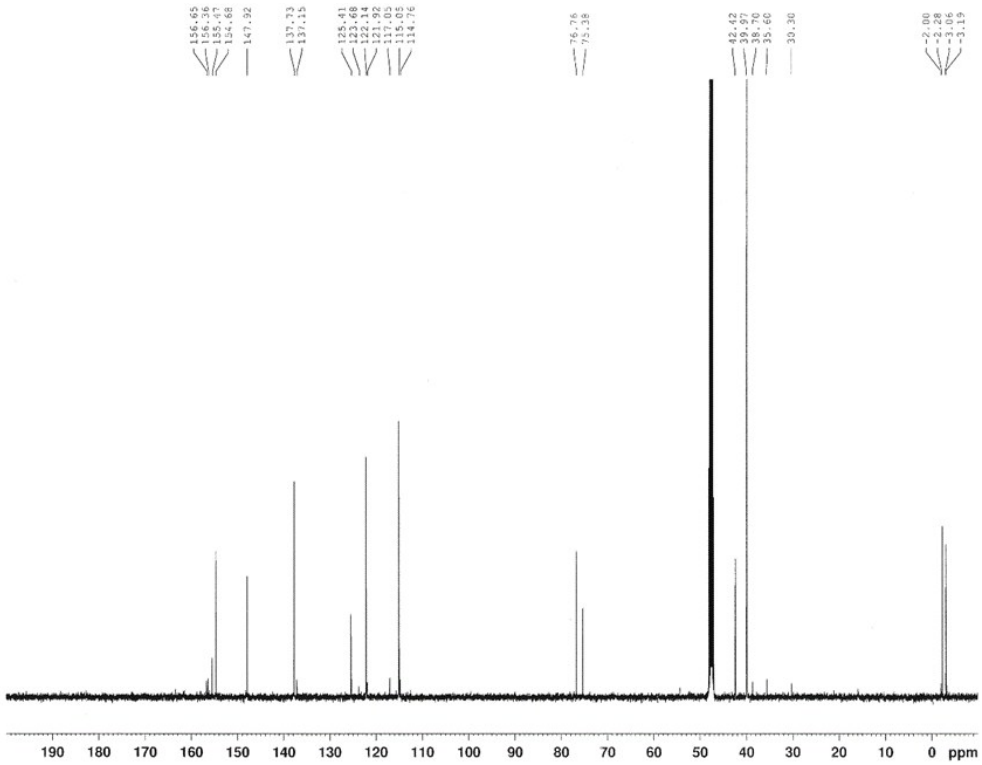

^{1}H NMR (CD_3OD, 500 MHz, 298 K) of NIR-ASiP^{a} **4**

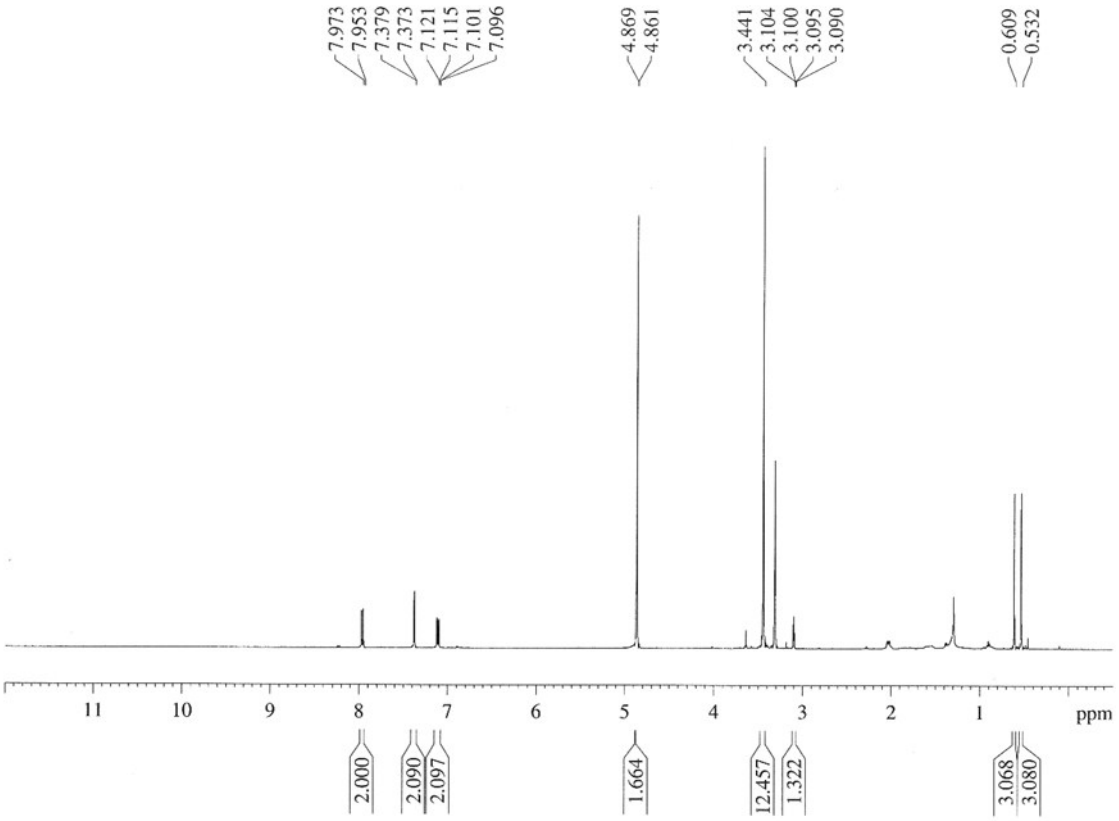

^{13}C NMR (CD_3OD, 125 MHz, 298 K) of NIR-ASiP^{a} **4**

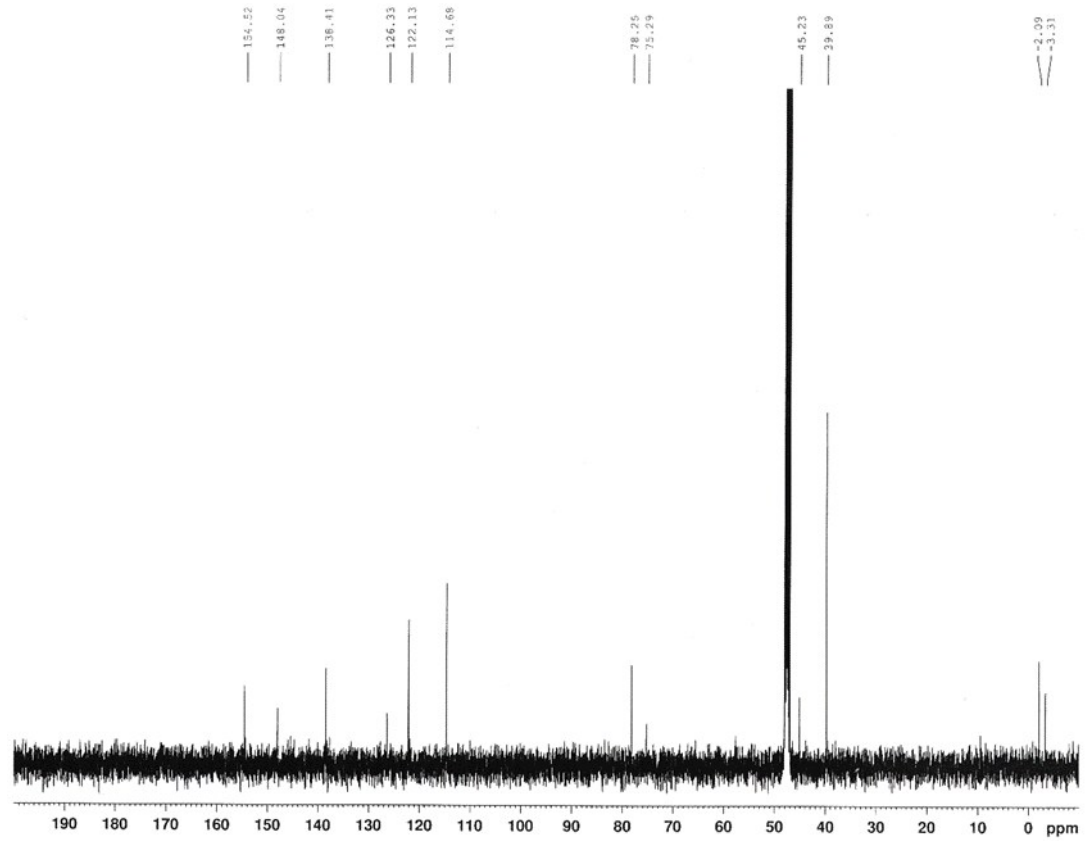

^{1}H NMR (CD_3OD, 500 MHz, 298 K) of NIR-ASiP^{a} **5**

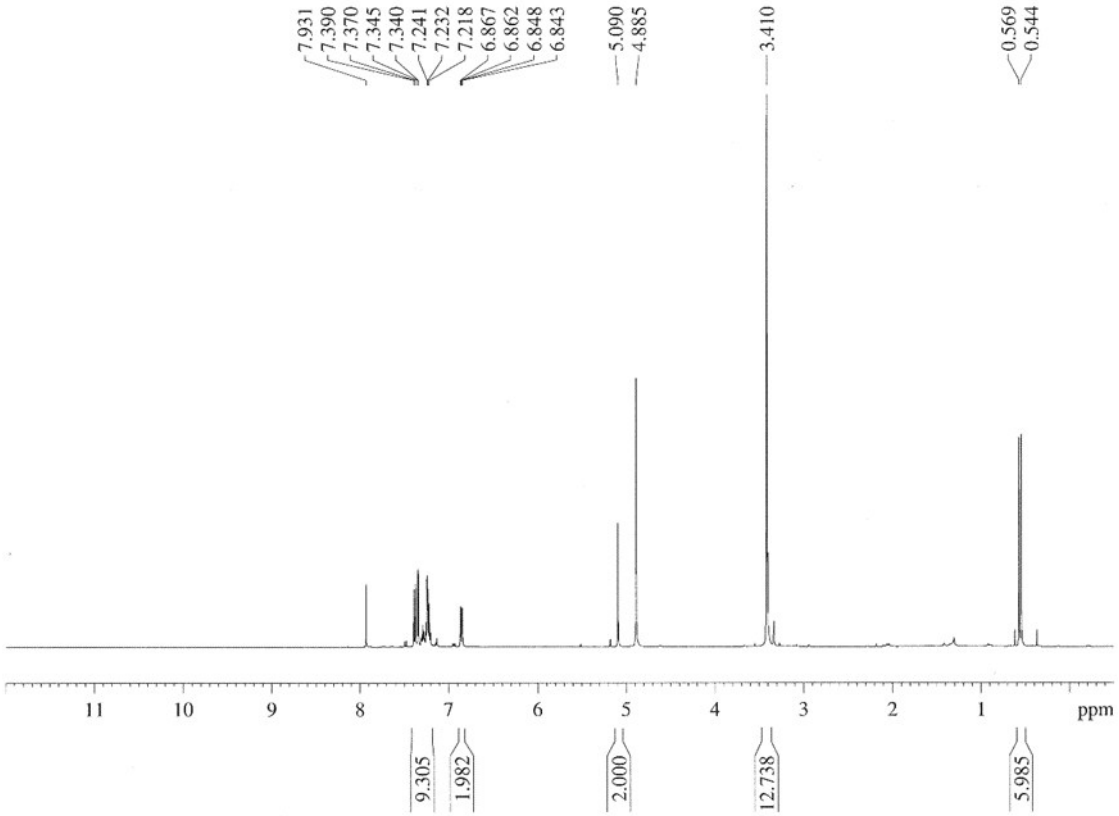

^{13}C NMR (CD_3OD, 125 MHz, 298 K) of NIR-ASiP^{a} **5**

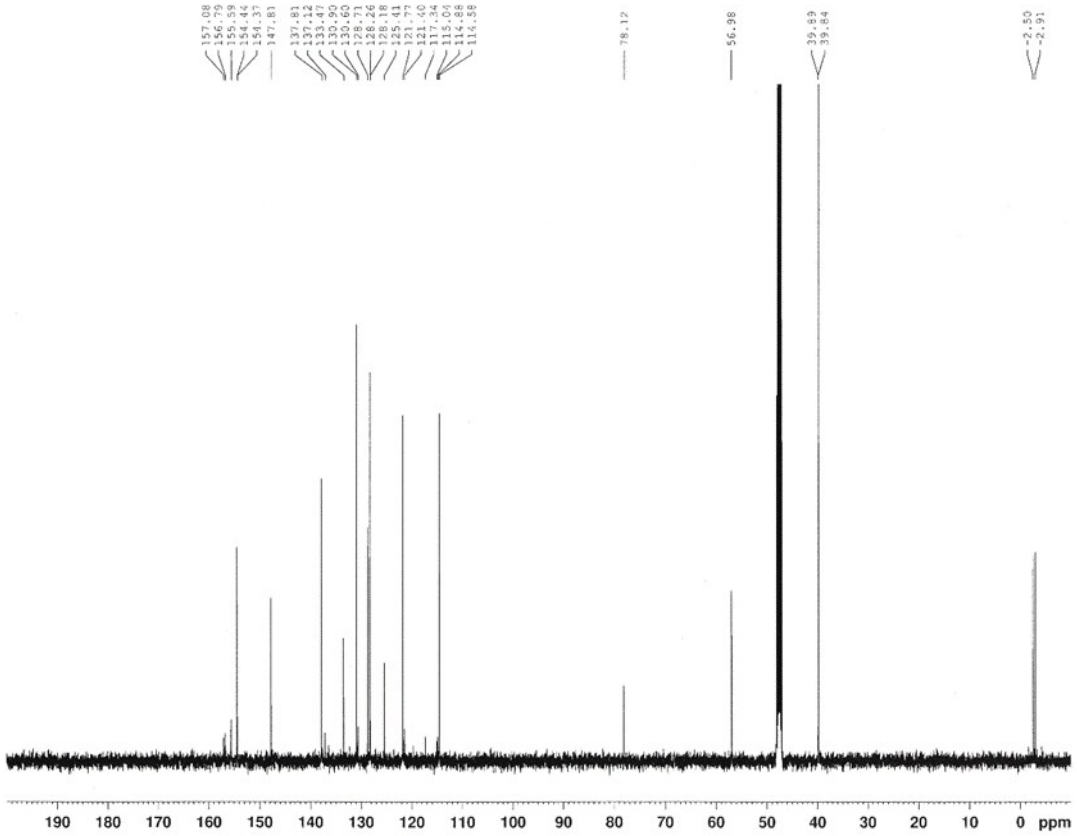

^{1}H NMR (CD_3OD, 500 MHz, 298 K) of NIR-ASiP^{a} **6**

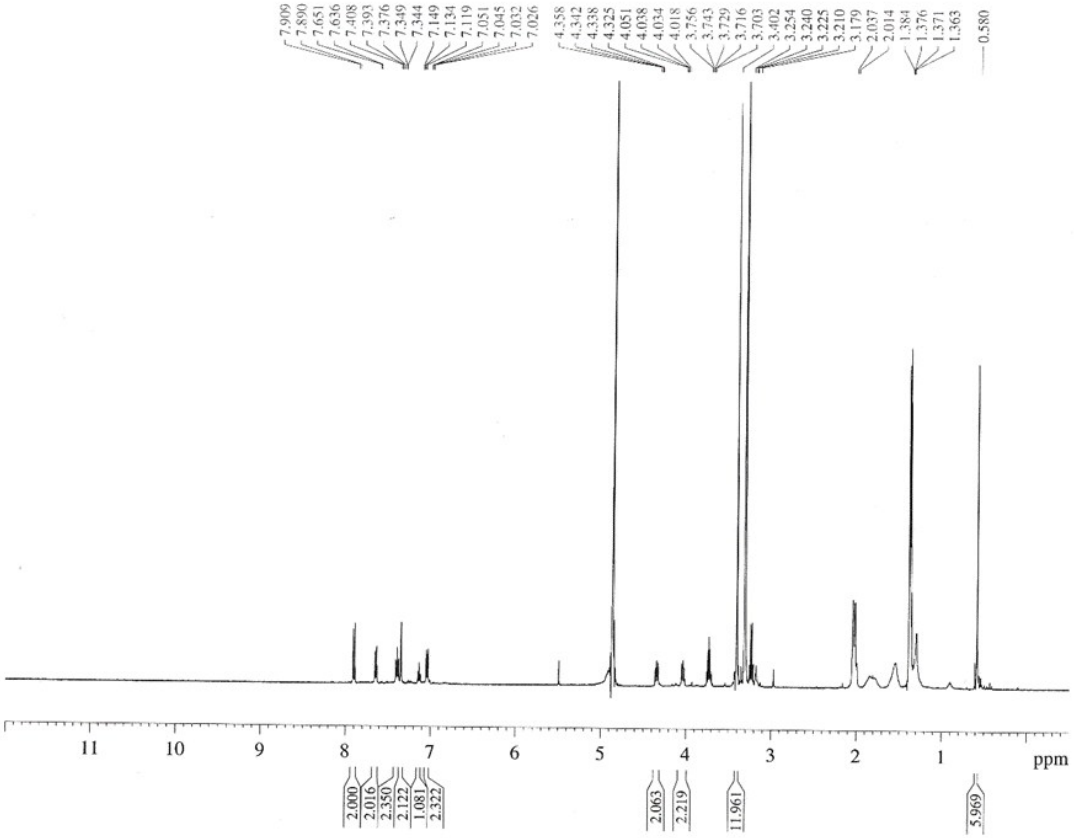

^{13}C NMR (CD_3OD, 125 MHz, 298 K) of NIR-ASiP^{a} **6**

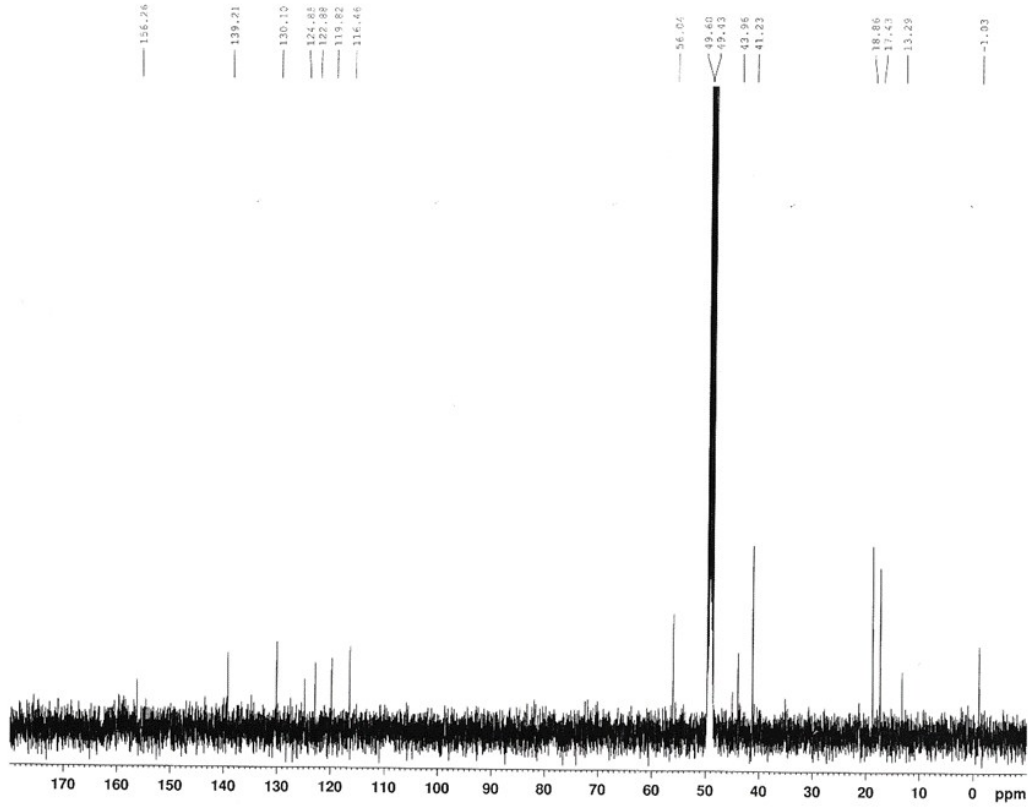

^{1}H NMR ($CDCl_3$, 300 MHz, 298K) of the julolidine-derived Si-xanthone **C**

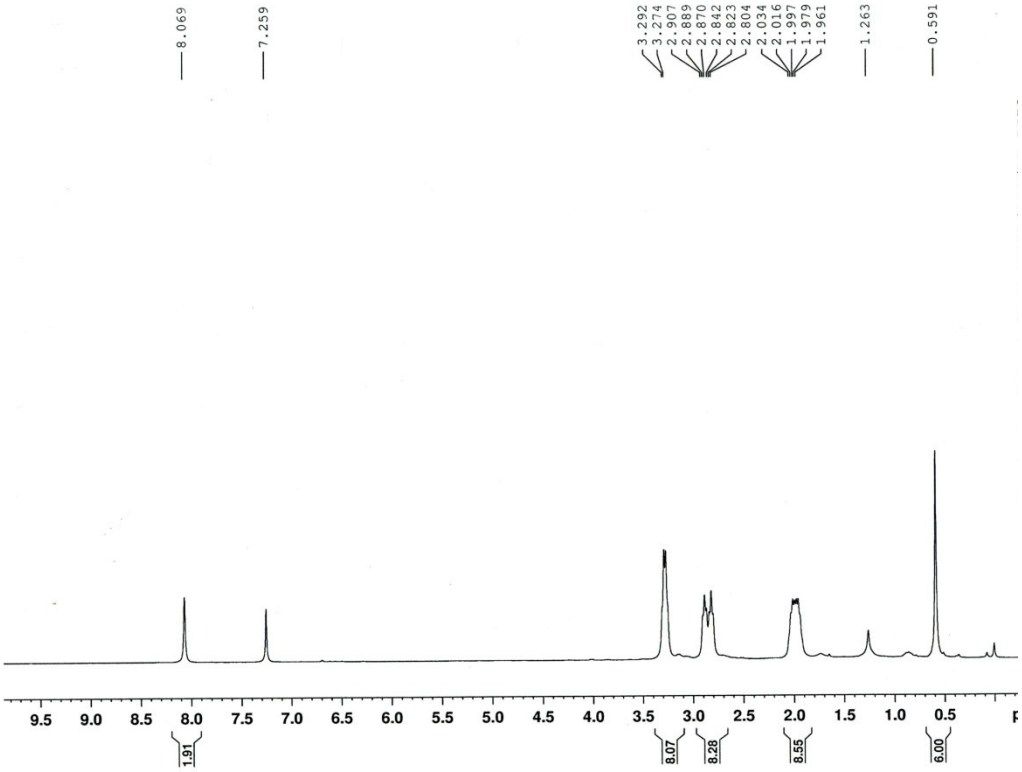

^{13}C NMR ($CDCl_3$, 125 MHz, 298 K) of the julolidine-derived Si-xanthone **C**

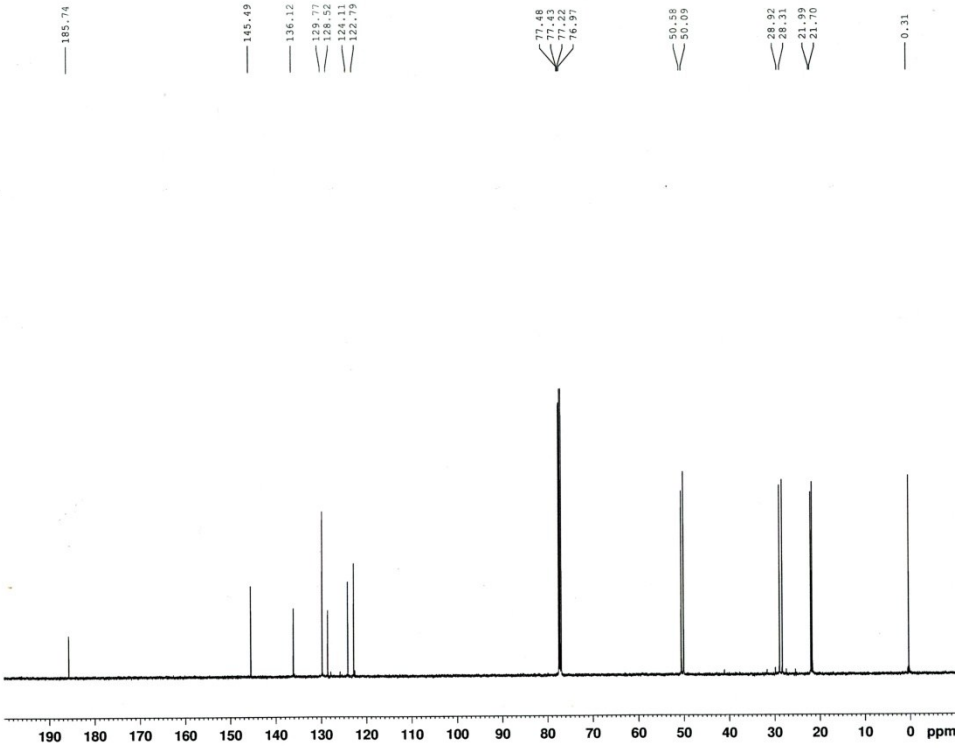

^{1}H NMR ($CDCl_3$, 500 MHz, 298K) of ASiP^{j} **1**

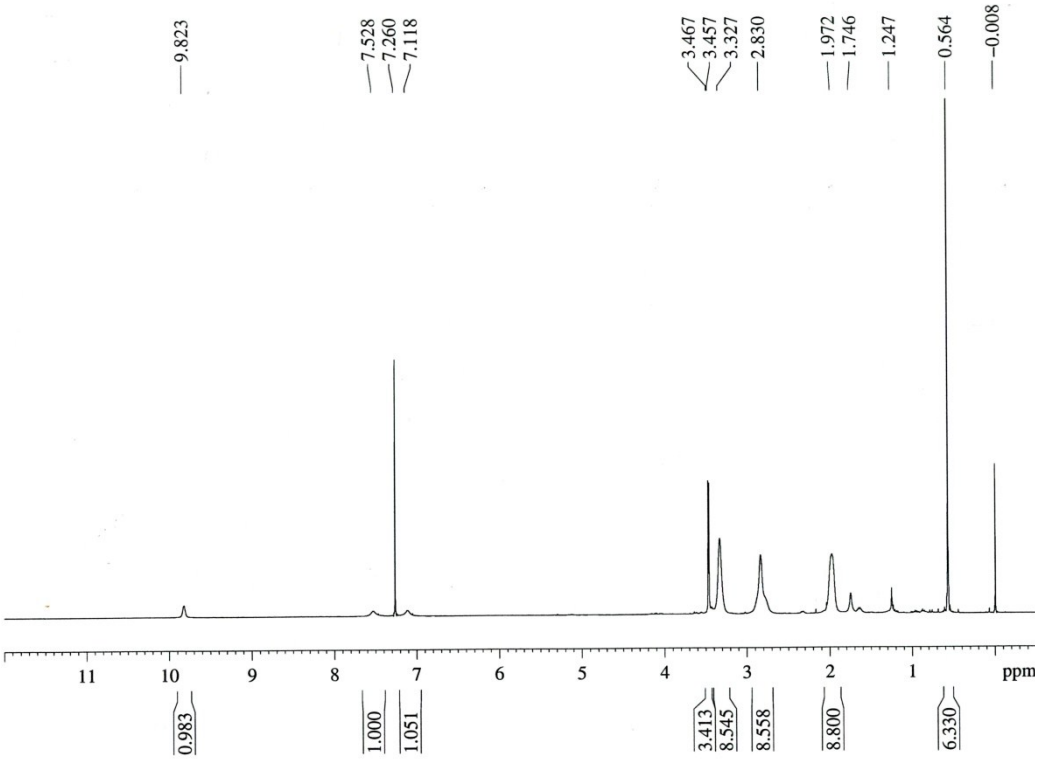

^{13}C NMR ($CDCl_3$, 125 MHz, 298 K) of ASiP^{j} **1**

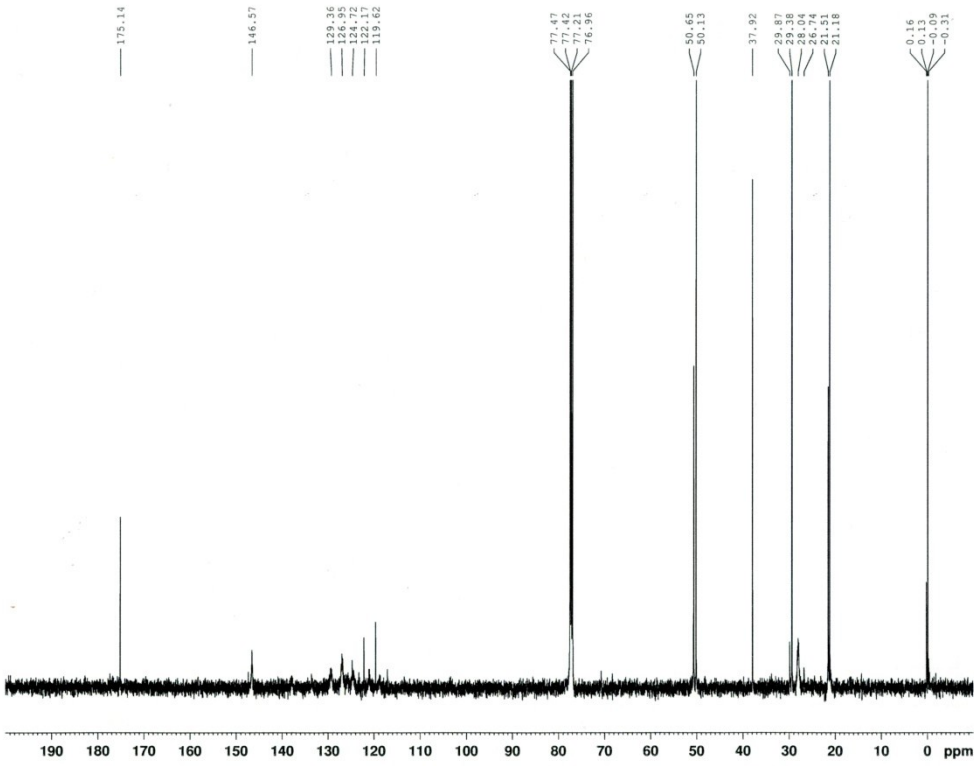

^{1}H NMR ($CDCl_3$, 500MHz, 298K) of ASiP^{j} **2**

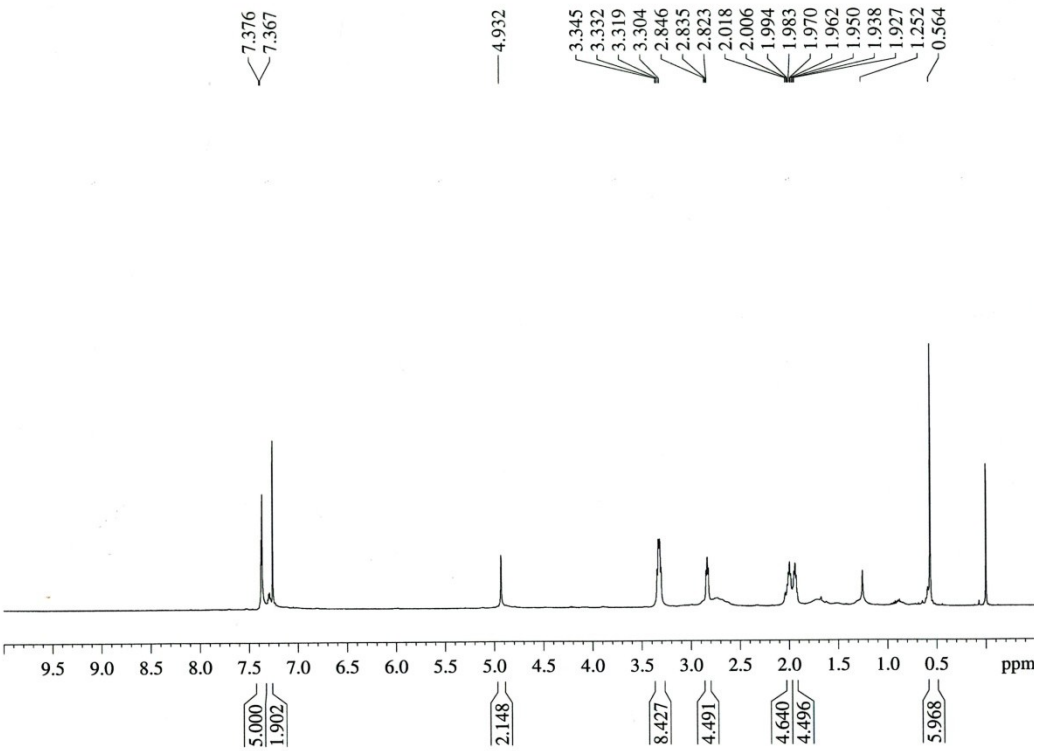

^{13}C NMR ($CDCl_3$, 75 MHz, 298 K) of ASiP^{j} **2**

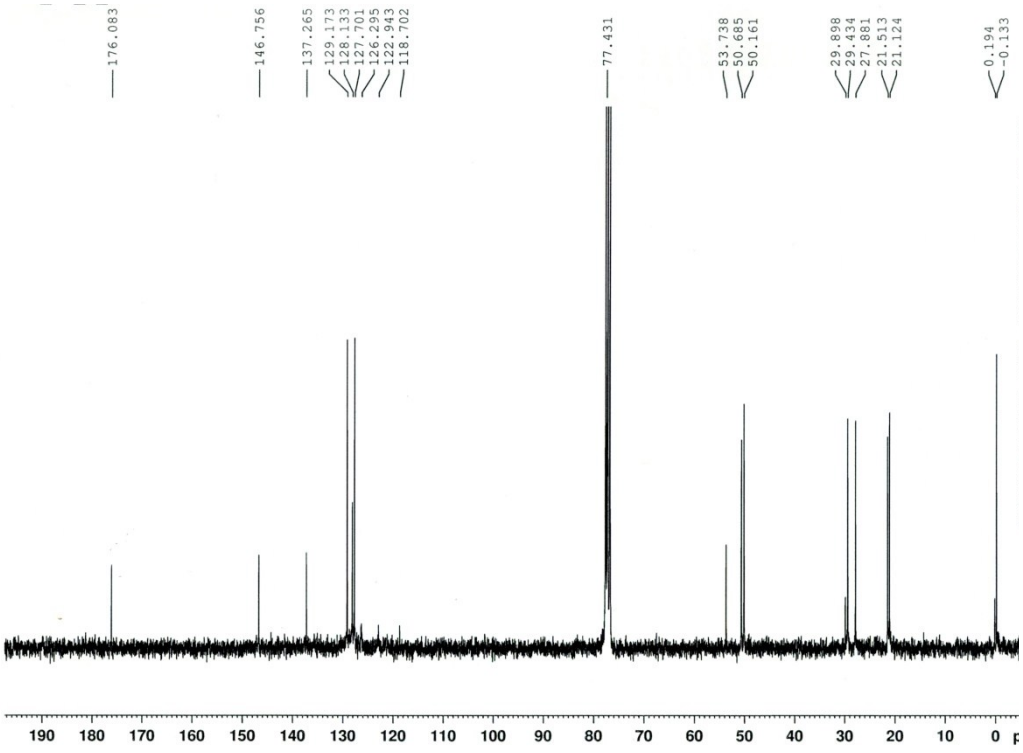

^{1}H NMR ($CDCl_3$, 300MHz, 298K) of ASiP^{i} **3**

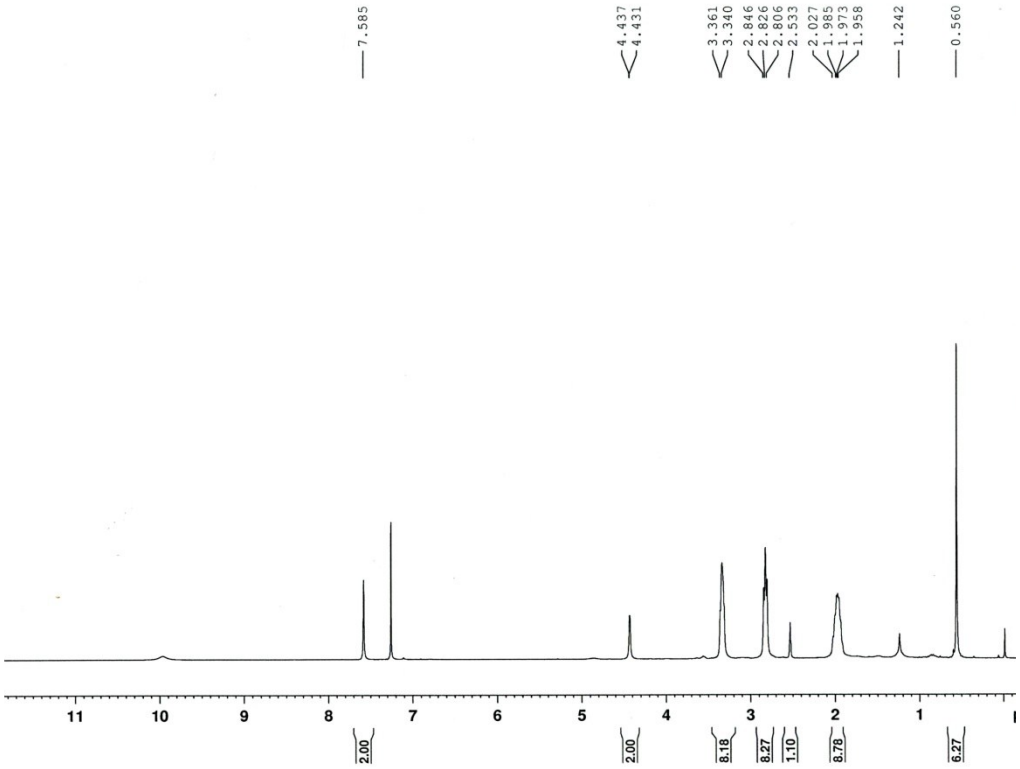

^{13}C NMR ($CDCl_3$, 125 MHz, 298 K) of ASiP^{i} **3**

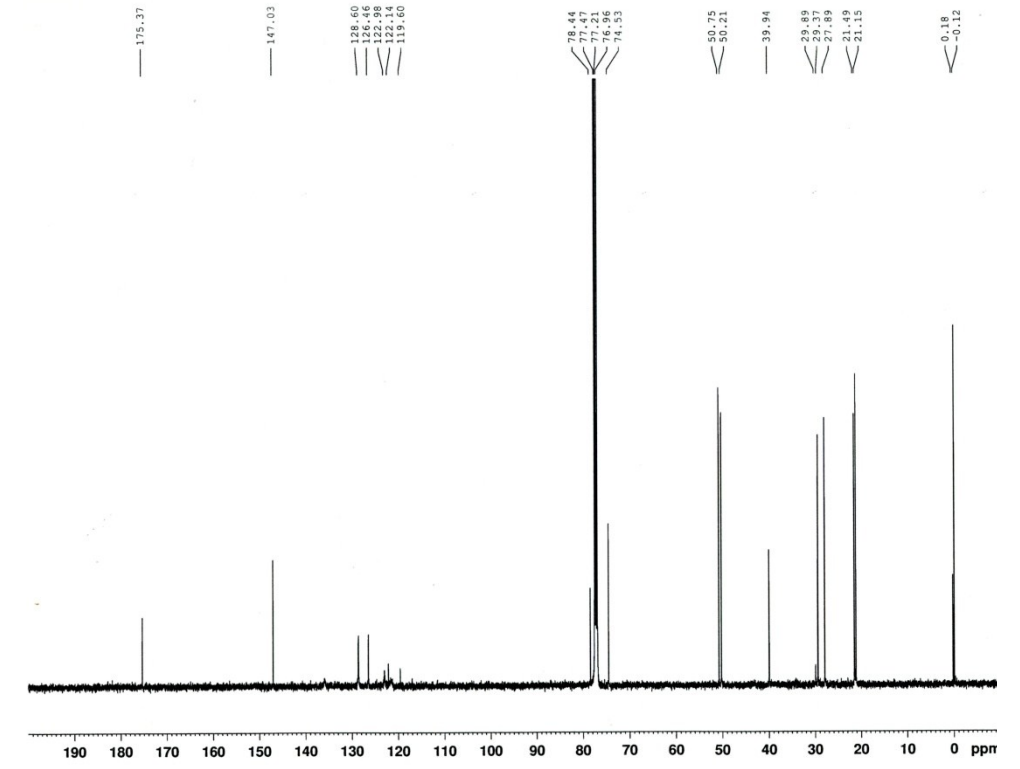

^{1}H NMR (CD_3OD, 500 MHz, 298 K) of NIR-ASiP^{j} **1**

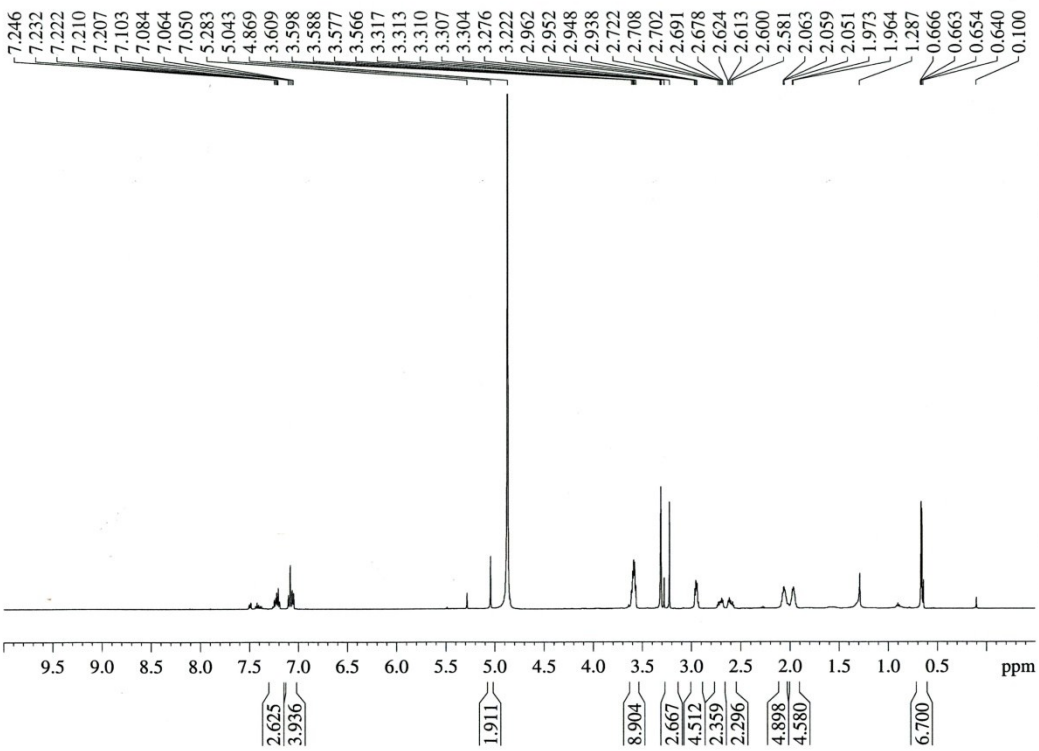

^{13}C NMR (CD_3OD, 125 MHz, 298 K) of NIR-ASiP^{j} **1**

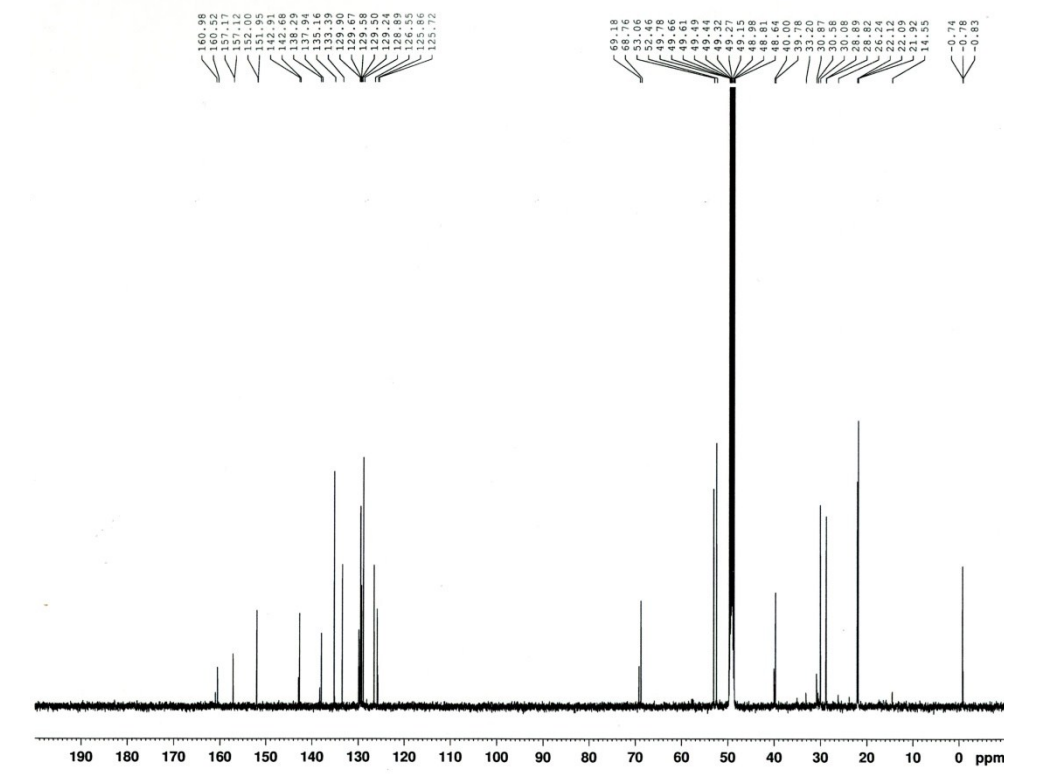

^{1}H NMR (CD_3OD, 500 MHz, 298 K) of NIR-ASiP^{j} **2**

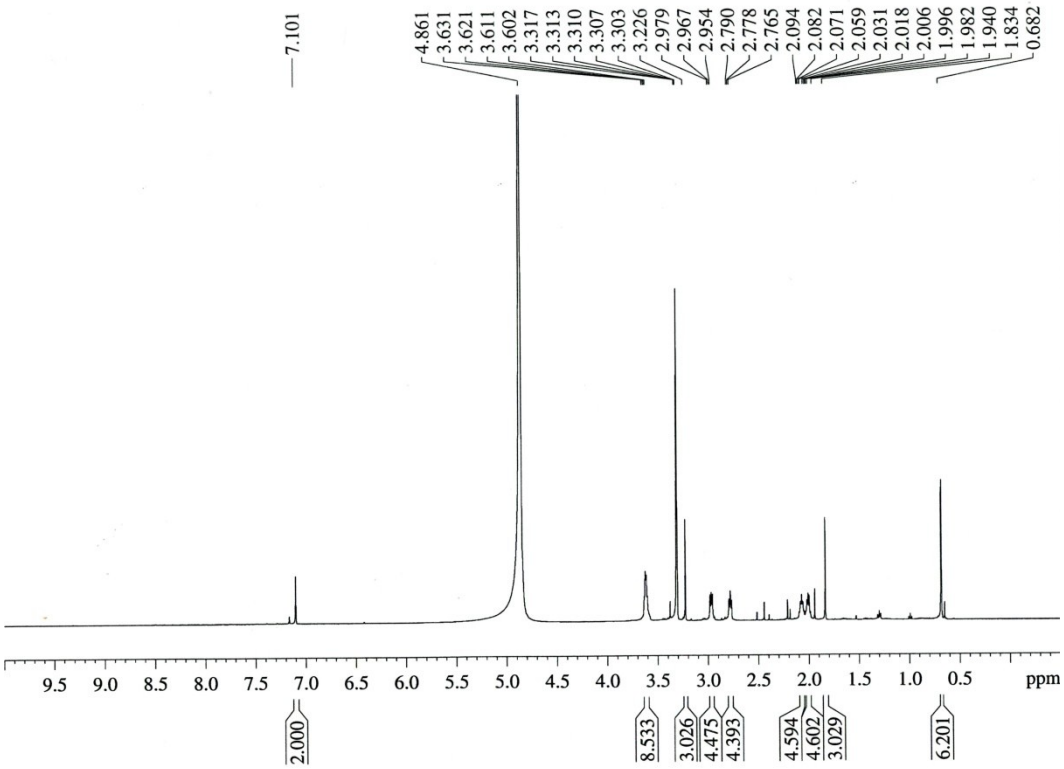

^{13}C NMR (CD_3OD, 125 MHz, 298 K) of NIR-ASiP^{j} **2**

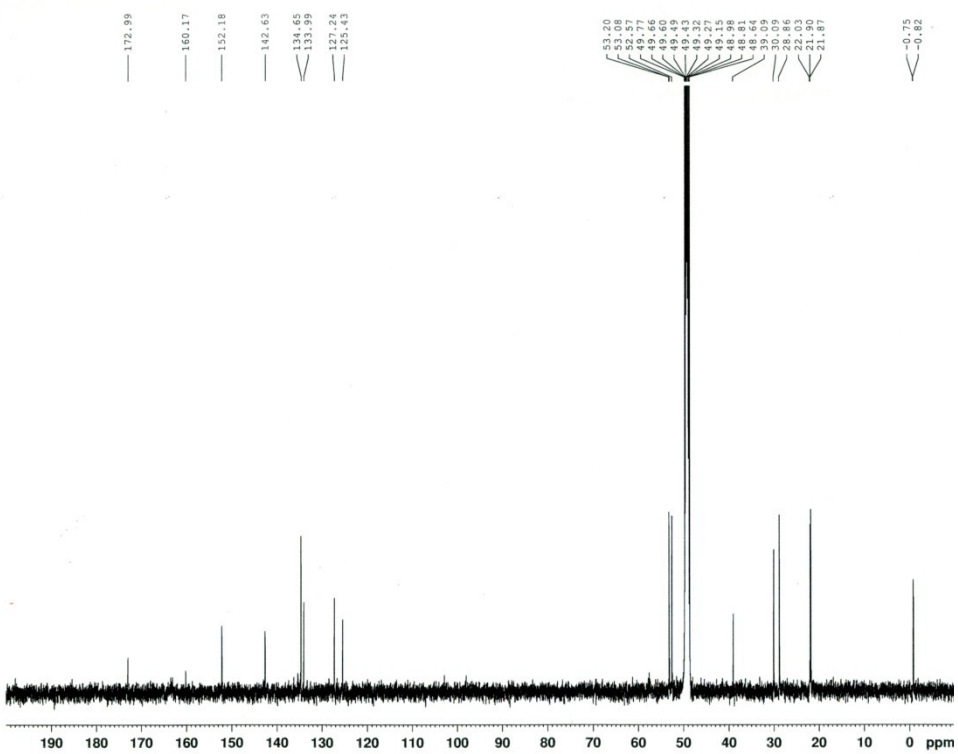

^{1}H NMR (CD_3OD, 500 MHz, 298 K) of NIR-ASiP^{j} **3**

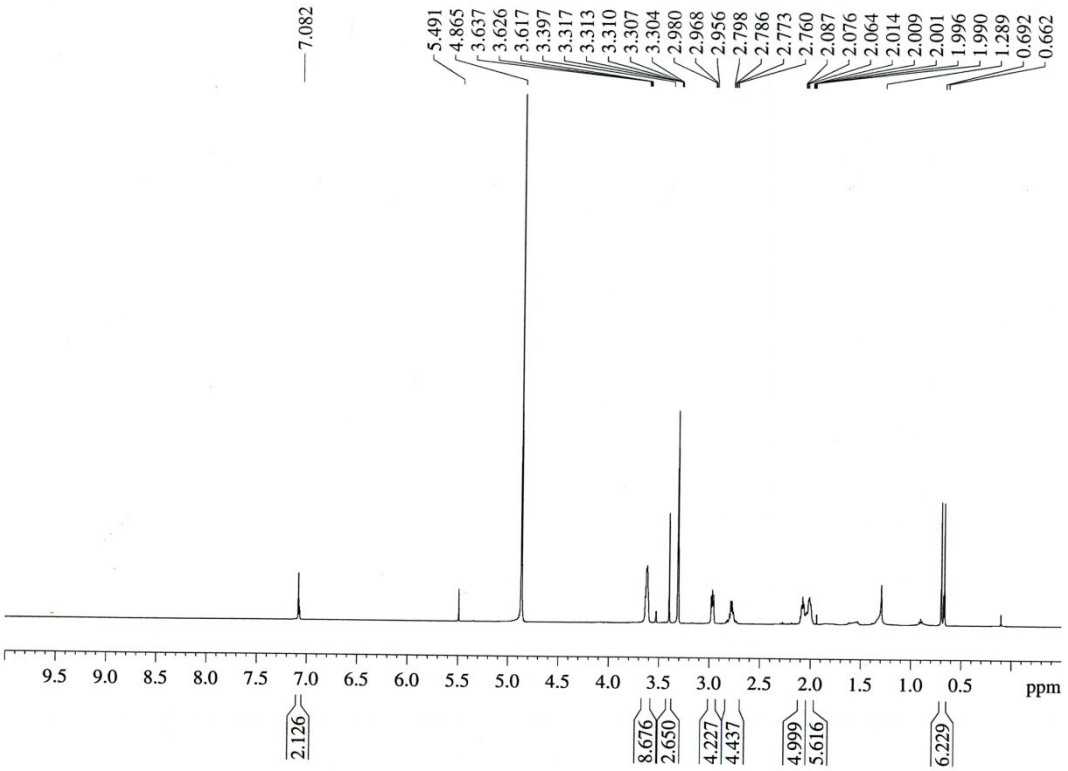

^{13}C NMR (CD_3OD, 125 MHz, 298 K) of NIR-ASiP^{j} **3**

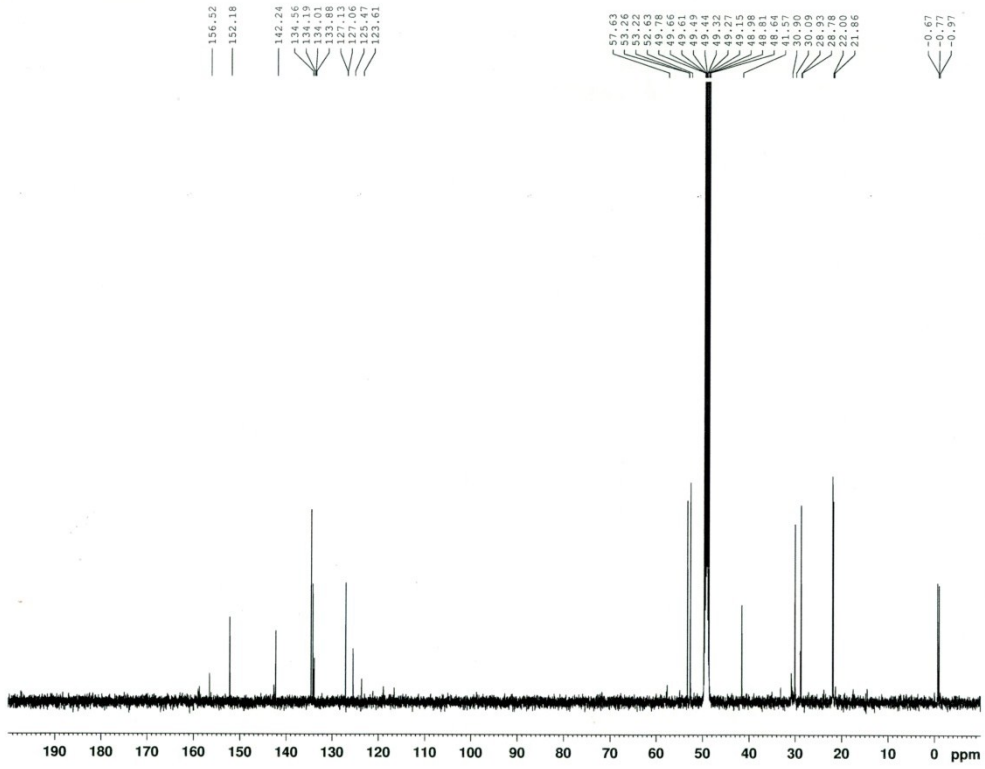

^{1}H NMR ($CDCl_3$, 500 MHz, 298 K) of **ASiP^{i}-H_2O_2**

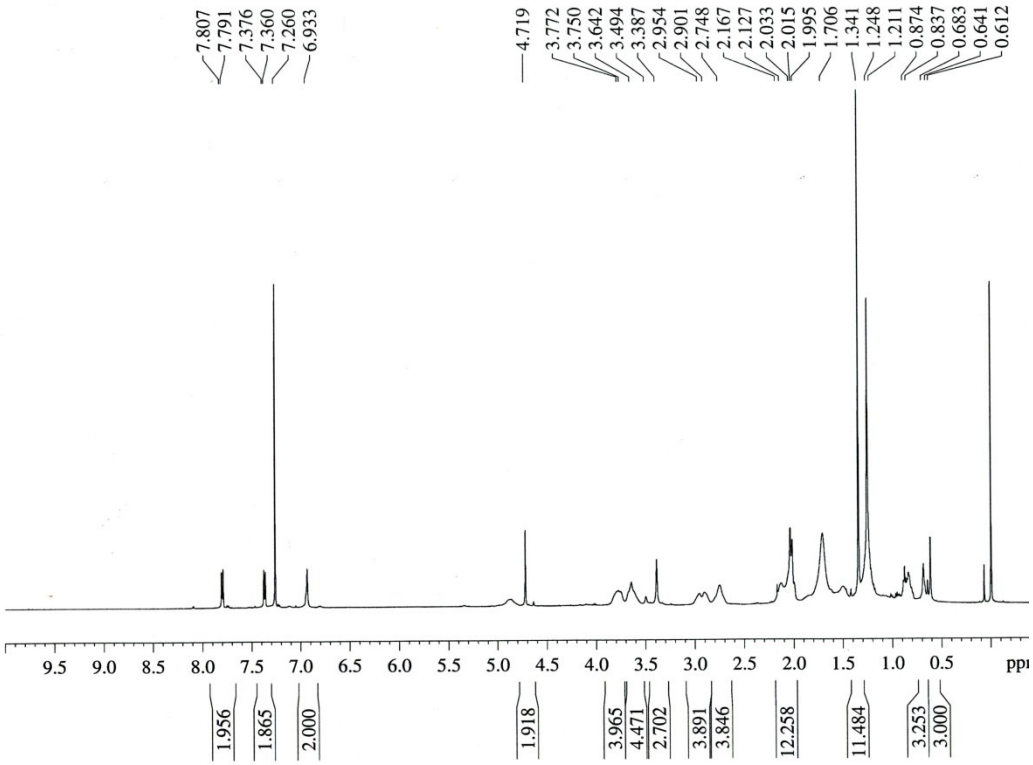

^{13}C NMR ($CDCl_3$, 125 MHz, 298 K) of **ASiP^{i}-H_2O_2**

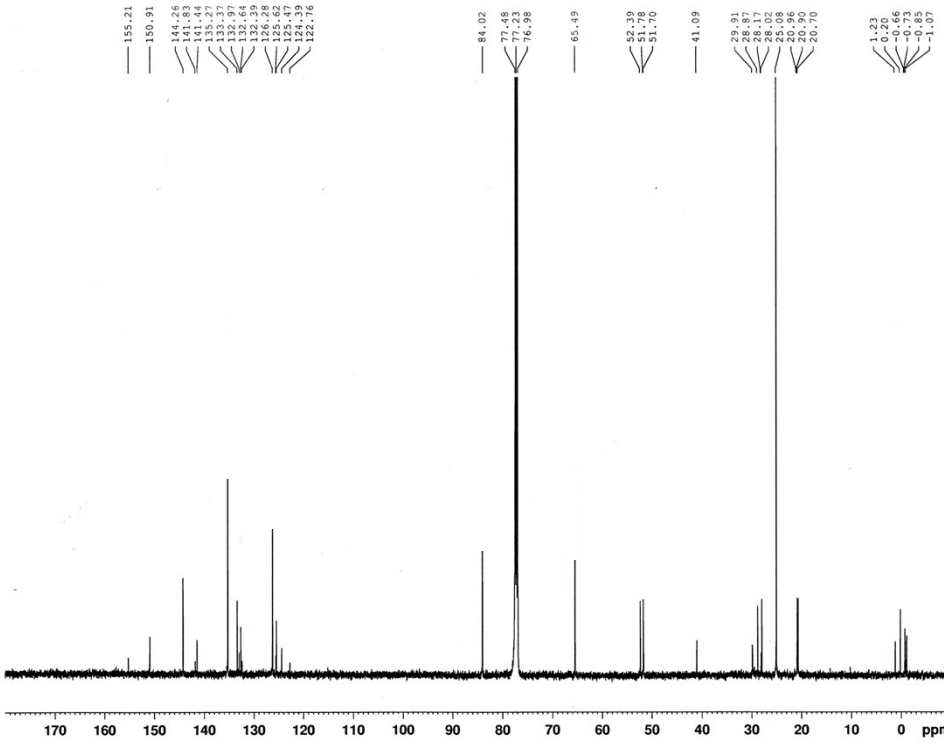

HR Mass-Spectra (ESI$^+$) for key dyes selected

HRMS (ESI$^+$) of ASiP^a **1**

```
[ Theoretical Ion Distribution ]
Molecular Formula : C20 H28 N3 Si
                    (m/z   338.2053, MW   338.5479, U.S.  9.5)
Base Peak :   338.2053, Averaged MW :   338.5455(a),   338.5467(w)

    m/z        INT.
  338.2053 100.0000**************************************************************
  339.2077  28.4102****************
  340.2064   7.1429****
  341.2074   1.1000*
  342.2095   0.1059
  343.2120   0.0070
  344.2148   0.0003
```

```
Data : 1-C20H28N3Si-HRFAB      Date : 17-Aug-2018 09:14
Instrument :  MStation
Sample : -
Note : -
Inlet : Direct      Ion Mode : FAB+
RT : 0.45 min      Scan# : (10,11)
Elements : C 20/0, H 28/0, N 3/0, Si 1/0
Mass Tolerance      : 3mmu
Unsaturation (U.S.) : -0.5 - 100.0

     Observed m/z   Int%      Err[ppm / mmu]    U.S.  Composition
1    338.2055   100.00      +0.7 /  +0.2     9.5   C20 H28 N3 Si

     339.2068    29.17
```

```
[ Mass Spectrum ]
Data : 1-C20H28N3Si-HRFAB      Date : 17-Aug-2018 09:14
Instrument :  MStation
Sample : -
Inlet : Direct      Ion Mode : FAB+
Spectrum Type : Normal Ion  [EF-Linear]
```

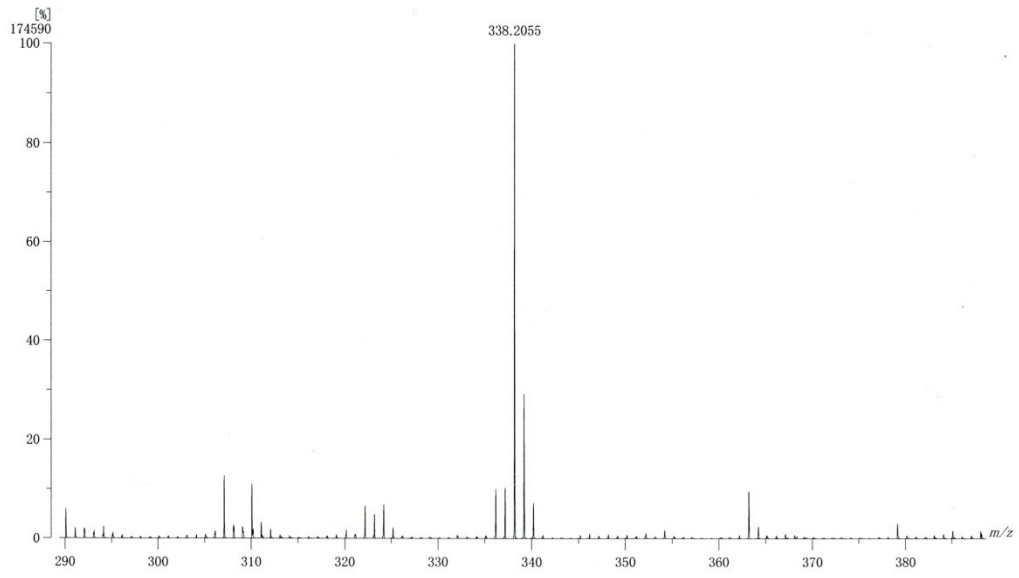

HRMS (ESI$^+$) of ASiP^a **2**

```
[ Theoretical Ion Distribution ]
Molecular Formula : C26 H32 N3 Si
                    (m/z   414.2366, MW   414.6457, U.S. 13.5)
Base Peak :   414.2366, Averaged MW :   414.6430(a),   414.6441(w)

    m/z        INT.
  414.2366 100.0000************************************************************
  415.2392  35.0836*********************
  416.2388   9.2244*****
  417.2396   1.6322*
  418.2415   0.1934
  419.2440   0.0163
  420.2467   0.0010
```

```
Data : 2-C26H32N3Si-HRFAB      Date : 17-Aug-2018 09:18
Instrument : MStation
Sample : -
Note : -
Inlet : Direct      Ion Mode : FAB+
RT : 0.15 min      Scan# : (4,5)
Elements : C 26/0, H 32/0, N 3/0, Si 1/0
Mass Tolerance      : 3mmu
Unsaturation (U.S.) : -0.5 - 100.0

     Observed m/z   Int%      Err[ppm / mmu]    U.S.  Composition
1    412.2207    10.38      -0.5 /  -0.2    14.5  C26 H30 N3 Si

2    414.2362   100.00      -0.8 /  -0.4    13.5  C26 H32 N3 Si

     415.2403    34.69
```

```
[ Mass Spectrum ]
Data : 2-C26H32N3Si-HRFAB      Date : 17-Aug-2018 09:18
Instrument : MStation
Sample : -
Inlet : Direct      Ion Mode : FAB+
Spectrum Type : Normal Ion  [EF-Linear]
```

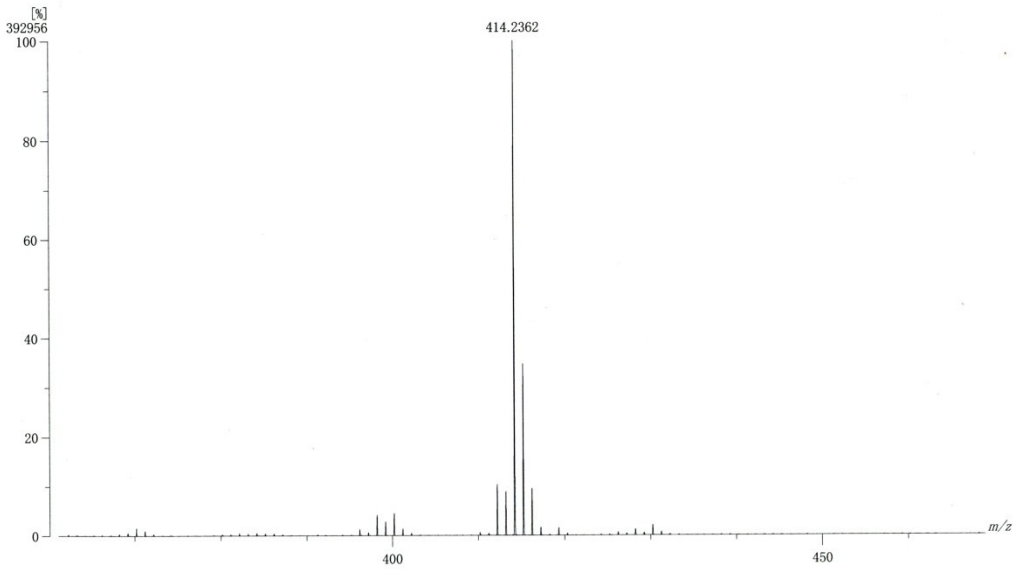

HRMS (ESI$^+$) of ASiP^a **3**

```
[ Theoretical Ion Distribution ]
Molecular Formula : C22 H28 N3 Si
                    (m/z   362.2053, MW   362.5699, U.S. 11.5)
Base Peak :   362.2053, Averaged MW :   362.5676(a),   362.5687(w)

     m/z        INT.
  362.2053 100.0000************************************************************
  363.2078  30.6346******************
  364.2068   7.7873*****
  365.2077   1.2624*
  366.2097   0.1313
  367.2123   0.0095
  368.2150   0.0005
```

```
Data : 3-C22H28N3Si-HRFAB      Date : 17-Aug-2018 09:22
Instrument :  MStation
Sample : -
Note : -
Inlet : Direct      Ion Mode : FAB+
RT : 0.55 min      Scan# : (12,13)
Elements : C 22/0, H 28/0, N 3/0, Si 1/0
Mass Tolerance      : 3mmu
Unsaturation (U.S.) : -0.5 - 100.0

      Observed m/z   Int%      Err[ppm / mmu]    U.S.  Composition
 1    362.2050   100.00      -0.7 /  -0.3    11.5  C22 H28 N3 Si

      363.2035    34.82

      379.1607    12.69

      399.1285    19.72
```

```
[ Mass Spectrum ]
Data : 3-C22H28N3Si-HRFAB      Date : 17-Aug-2018 09:22
Instrument :  MStation
Sample : -
Inlet : Direct      Ion Mode : FAB+
Spectrum Type : Normal Ion  [EF-Linear]
```

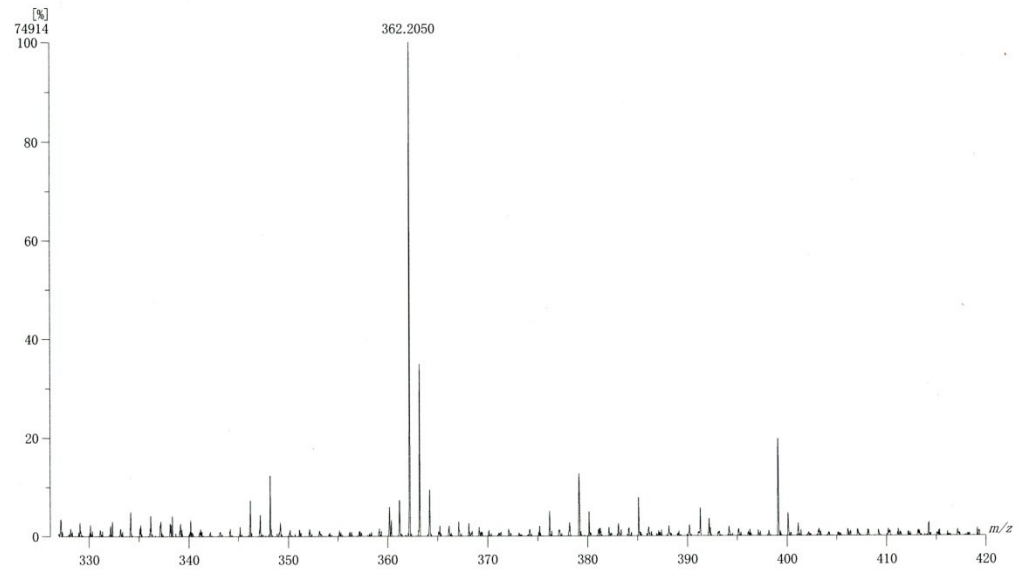

HRMS (ESI$^+$) of NIR-ASiP^a **1**

```
[ Theoretical Ion Distribution ]
Molecular Formula : C28 H34 N3 O2 Si
                    (m/z   472.2420, MW   472.6824, U.S. 14.5)
Base Peak :   472.2420, Averaged MW :   472.6794(a),   472.6804(w)

    m/z        INT.
  472.2420 100.0000************************************************************
  473.2447  37.3842***********************
  474.2446  10.4466******
  475.2457   1.9991*
  476.2475   0.2729
  477.2497   0.0285
  478.2521   0.0024
  479.2545   0.0002
```

```
Data : 4-C28H34N3O2Si-HRFAB      Date : 17-Aug-2018 09:26
Instrument :  MStation
Sample : -
Note : -
Inlet : Direct      Ion Mode : FAB+
RT : 0.40 min      Scan# : (9,10)
Elements : C 28/0, H 34/0, N 3/0, O 2/0, Si 1/0
Mass Tolerance      : 3mmu
Unsaturation (U.S.) : -0.5 - 100.0

     Observed m/z   Int%      Err[ppm / mmu]    U.S.  Composition
1     472.2422   100.00      +0.4 /  +0.2    14.5   C28 H34 N3 O2 Si

      473.2442    38.17

      474.2467    13.25
```

```
[ Mass Spectrum ]
Data : 4-C28H34N3O2Si-HRFAB      Date : 17-Aug-2018 09:26
Instrument :  MStation
Sample : -
Inlet : Direct      Ion Mode : FAB+
Spectrum Type : Normal Ion  [EF-Linear]
```

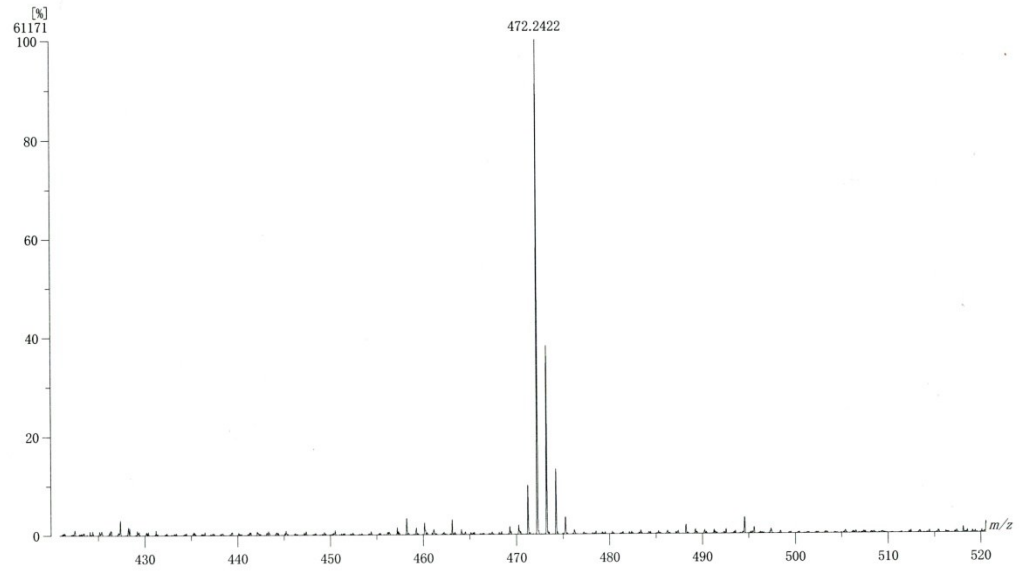

HRMS (ESI$^+$) of ASiP^j **1**

```
[ Theoretical Ion Distribution ]
Molecular Formula : C28 H36 N3 Si
                    (m/z   442.2679, MW   442.6994, U.S. 13.5)
Base Peak :   442.2679, Averaged MW :   442.6964(a),   442.6975(w)

    m/z        INT.
  442.2679 100.0000************************************************************
  443.2705  37.3080**********************
  444.2704  10.0172******
  445.2712   1.8417*
  446.2731   0.2308
  447.2755   0.0208
  448.2782   0.0014
```

Data : 5-C28H36N3Si-HRFAB Date : 17-Aug-2018 09:30
Instrument : MStation
Sample : -
Note : -
Inlet : Direct Ion Mode : FAB+
RT : 0.60 min Scan# : (13,14)
Elements : C 28/0, H 36/0, N 3/0, Si 1/0
Mass Tolerance : 3mmu
Unsaturation (U.S.) : -0.5 - 100.0

	Observed m/z	Int%	Err[ppm / mmu]	U.S.	Composition
1	440.2523	29.92	+0.2 / +0.1	14.5	C28 H34 N3 Si
2	442.2678	100.00	-0.1 / -0.1	13.5	C28 H36 N3 Si
	443.2632	30.27			
	444.2685	11.20			

[Mass Spectrum]
Data : 5-C28H36N3Si-HRFAB Date : 17-Aug-2018 09:30
Instrument : MStation
Sample : -
Inlet : Direct Ion Mode : FAB+
Spectrum Type : Normal Ion [EF-Linear]

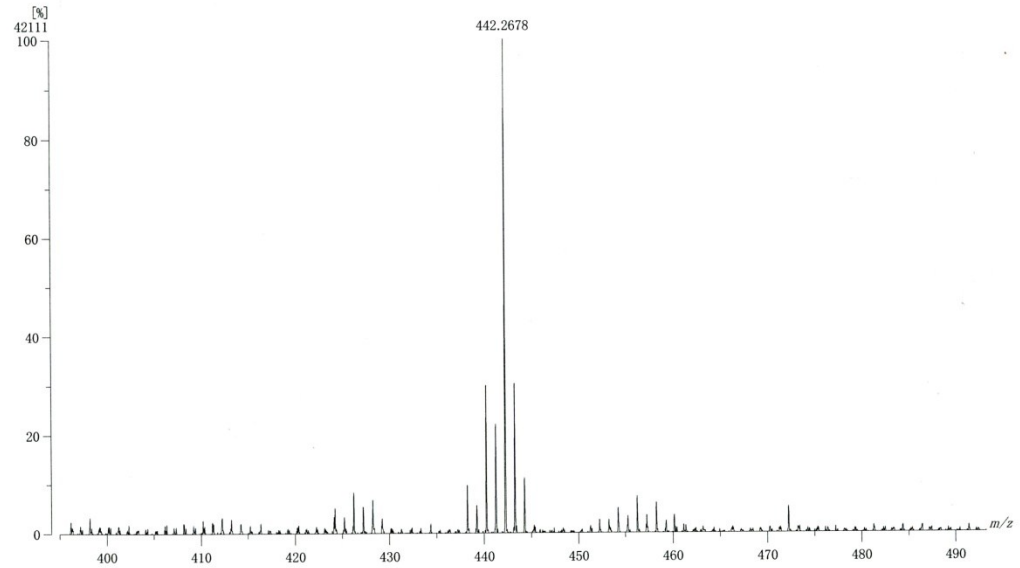

HRMS (ESI$^+$) of ASiP^j **2**

```
[ Theoretical Ion Distribution ]
Molecular Formula : C34 H40 N3 Si
                          (m/z    518.2992, MW    518.7972, U.S. 17.5)
Base Peak :    518.2992, Averaged MW :    518.7939(a),    518.7950(w)

     m/z        INT.
  518.2992 100.0000************************************************************
  519.3019  43.9814************************
  520.3024  12.6925*******
  521.3033   2.5822*
  522.3051   0.3734
  523.3074   0.0399
  524.3100   0.0033
  525.3128   0.0002
```

```
Data : 6-C34H40N3Si-HRFAB      Date : 17-Aug-2018 09:35
Instrument : MStation
Sample : -
Note : -
Inlet : Direct      Ion Mode : FAB+
RT : 0.55 min      Scan# : (12,13)
Elements : C 34/0, H 40/0, N 3/0, Si 1/0
Mass Tolerance      : 3mmu
Unsaturation (U.S.) : -0.5 - 100.0

     Observed m/z   Int%      Err[ppm / mmu]    U.S.  Composition
1    518.2989   100.00      -0.5 /  -0.3    17.5  C34 H40 N3 Si

     519.3014    41.19

     520.2899    14.66
```

```
[ Mass Spectrum ]
Data : 6-C34H40N3Si-HRFAB      Date : 17-Aug-2018 09:35
Instrument : MStation
Sample : -
Inlet : Direct      Ion Mode : FAB+
Spectrum Type : Normal Ion  [EF-Linear]
```

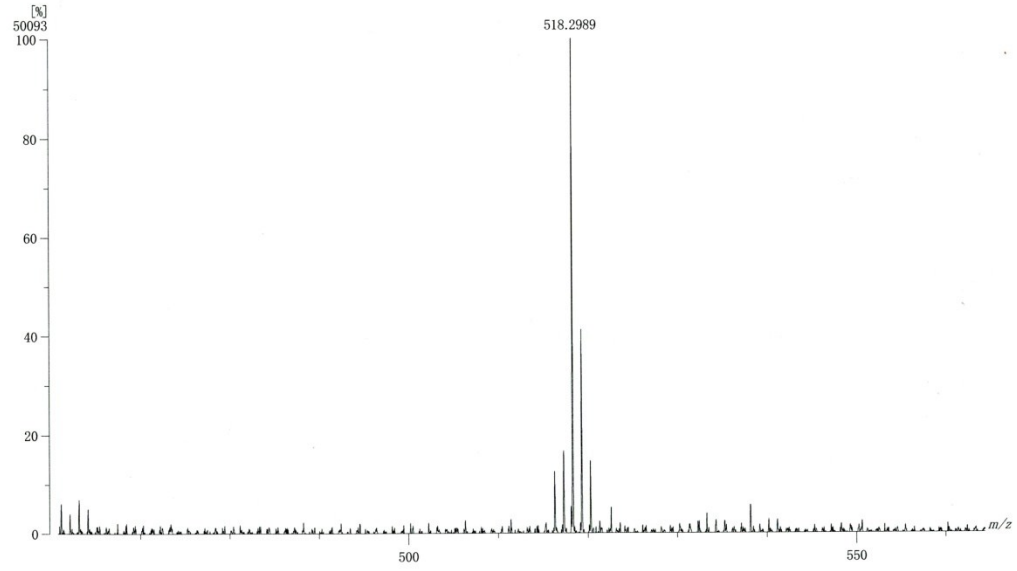

HRMS (ESI$^+$) of ASiP^j **3**

```
[ Theoretical Ion Distribution ]
Molecular Formula : C30 H36 N3 Si
                    (m/z   466.2679, MW   466.7214, U.S. 15.5)
Base Peak :   466.2679, Averaged MW :   466.7185(a),   466.7196(w)

    m/z        INT.
  466.2679 100.0000************************************************************
  467.2705  39.5325***********************
  468.2706  10.8595******
  469.2715   2.0691*
  470.2733   0.2730
  471.2757   0.0262
  472.2784   0.0019
  473.2812   0.0001
```

Data : 7-C30H36N3Si-HRFAB Date : 17-Aug-2018 09:39
Instrument : MStation
Sample : -
Note : -
Inlet : Direct Ion Mode : FAB+
RT : 0.55 min Scan# : (12,13)
Elements : C 30/0, H 36/0, N 3/0, Si 1/0
Mass Tolerance : 3mmu
Unsaturation (U.S.) : -0.5 - 100.0

	Observed m/z	Int%	Err[ppm / mmu]	U.S.	Composition
1	464.2526	20.38	+0.9 / +0.4	16.5	C30 H34 N3 Si
2	465.2593	20.51	-1.6 / -0.7	16.0	C30 H35 N3 Si
3	466.2677	100.00	-0.3 / -0.2	15.5	C30 H36 N3 Si
	467.2731	36.72			
	468.2702	10.12			

[Mass Spectrum]
Data : 7-C30H36N3Si-HRFAB Date : 17-Aug-2018 09:39
Instrument : MStation
Sample : -
Inlet : Direct Ion Mode : FAB+
Spectrum Type : Normal Ion [EF-Linear]

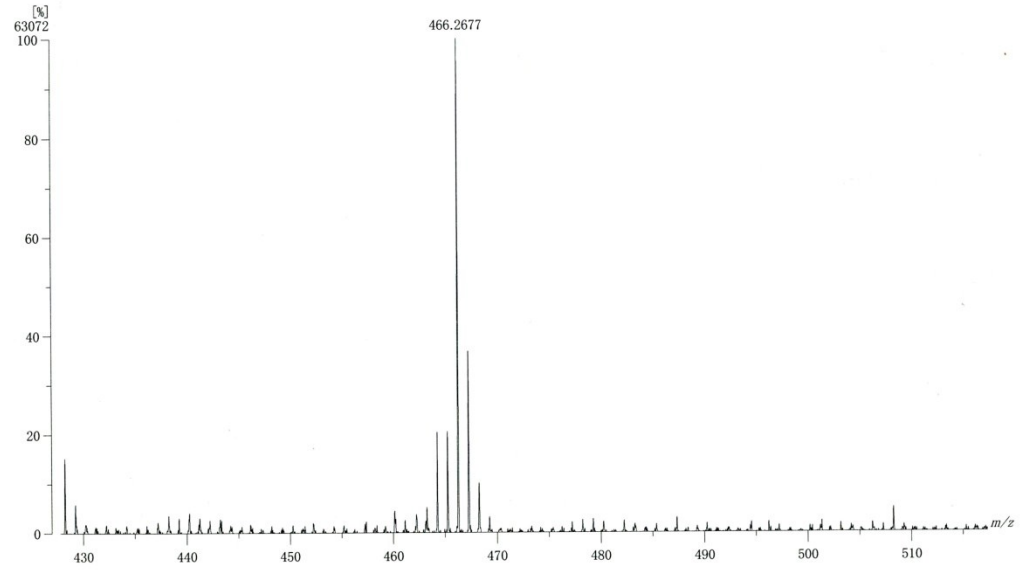

HRMS (ESI^{+}) of NIR-ASiP^{j} **1**

```
[ Theoretical Ion Distribution ]
Molecular Formula : C36 H42 N3 O2 Si
                    (m/z   576.3046, MW   576.8339, U.S. 18.5)
Base Peak :   576.3046, Averaged MW :   576.8303(a),   576.8313(w)

    m/z        INT.
  576.3046 100.0000************************************************************
  577.3074  46.2821*************************
  578.3081  14.1194********
  579.3092   3.0658**
  580.3110   0.4899
  581.3132   0.0606
  582.3155   0.0061
  583.3180   0.0005
```

```
Data : 8-C36H42N3O2Si-HRFAB      Date : 17-Aug-2018 09:43
Instrument :  MStation
Sample : -
Note : -
Inlet : Direct      Ion Mode : FAB+
RT : 0.55 min      Scan# : (12,13)
Elements : C 36/0, H 42/0, N 3/0, O 2/0, Si 1/0
Mass Tolerance      : 3mmu
Unsaturation (U.S.) : -0.5 - 100.0

     Observed m/z   Int%      Err[ppm / mmu]    U.S.  Composition
1    575.2974    21.45      +1.0 /  +0.6    19.0   C36 H41 N3 O2 Si

2    576.3042   100.00      -0.7 /  -0.4    18.5   C36 H42 N3 O2 Si

     577.3061    44.59

     578.3122    14.01
```

```
[ Mass Spectrum ]
Data : 8-C36H42N3O2Si-HRFAB      Date : 17-Aug-2018 09:43
Instrument :  MStation
Sample : -
Inlet : Direct      Ion Mode : FAB+
Spectrum Type : Normal Ion  [EF-Linear]
```

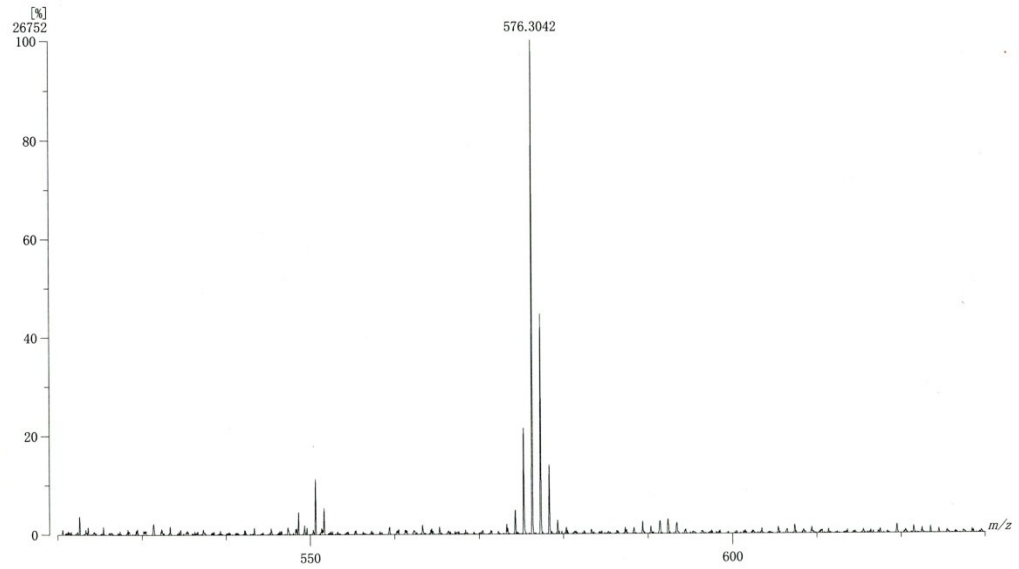

HRMS (ESI$^+$) of NIR-ASiP^j **2**

```
[ Theoretical Ion Distribution ]
Molecular Formula : C30 H38 N3 O Si
                        (m/z   484.2784, MW   484.7367, U.S. 14.5)
Base Peak :   484.2784, Averaged MW :   484.7334(a),   484.7345(w)

    m/z        INT.
  484.2784 100.0000************************************************************
  485.2811  39.5706************************
  486.2812  11.0750******
  487.2822   2.1525*
  488.2840   0.2956
  489.2863   0.0304
  490.2888   0.0025
  491.2914   0.0002
```

```
Data : 9-C30H38N3OSi-HRFAB      Date : 17-Aug-2018 09:47
Instrument :  MStation
Sample : -
Note : -
Inlet : Direct      Ion Mode : FAB+
RT : 0.50 min      Scan# : (11,12)
Elements : C 30/0, H 38/0, N 3/0, O 1/0, Si 1/0
Mass Tolerance      : 3mmu
Unsaturation (U.S.) : -0.5 - 100.0
```

	Observed m/z	Int%	Err[ppm / mmu]	U.S.	Composition
1	483.2710	26.25	+0.8 / +0.4	15.0	C30 H37 N3 O Si
2	484.2781	100.00	-0.7 / -0.3	14.5	C30 H38 N3 O Si
	485.2844	47.61			
	486.2882	12.84			
	487.3214	11.36			

```
[ Mass Spectrum ]
Data : 9-C30H38N3OSi-HRFAB      Date : 17-Aug-2018 09:47
Instrument :  MStation
Sample : -
Inlet : Direct      Ion Mode : FAB+
Spectrum Type : Normal Ion  [EF-Linear]
```

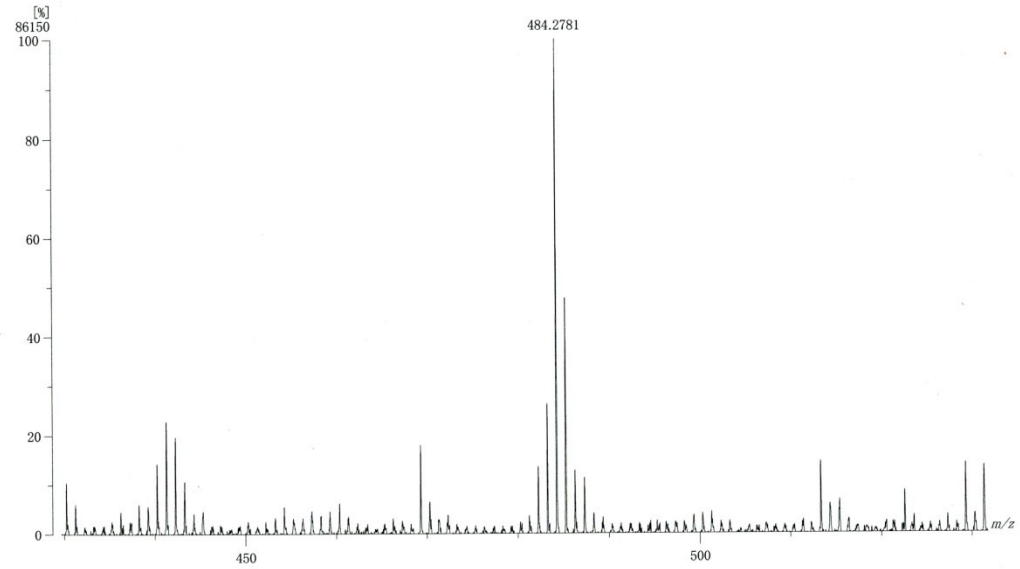

HRMS (ESI$^+$) of NIR-ASiP^j **3**

```
[ Theoretical Ion Distribution ]
Molecular Formula : C30 H35 F3 N3 O Si
                    (m/z   538.2502, MW   538.7081, U.S. 14.5)
Base Peak :   538.2502, Averaged MW :   538.7052(a),   538.7061(w)

    m/z       INT.
  538.2502 100.0000************************************************************
  539.2528  39.5706***********************
  540.2530  11.0750******
  541.2539   2.1525*
  542.2558   0.2956
  543.2580   0.0304
  544.2605   0.0025
  545.2631   0.0002
```

```
Data : 10-C30H35F3N3OSi-HRFAB      Date : 17-Aug-2018 09:51
Instrument :  MStation
Sample : -
Note : -
Inlet : Direct      Ion Mode : FAB+
RT : 0.50 min      Scan# : (11,12)
Elements : C 30/0, H 35/0, F 3/0, N 3/0, O 1/0, Si 1/0
Mass Tolerance      : 3mmu
Unsaturation (U.S.) : -0.5 - 100.0

     Observed m/z   Int%      Err[ppm / mmu]    U.S.  Composition
1    537.2419    18.33      -0.8 /  -0.4    15.0  C30 H34 F3 N3 O Si

2    538.2505   100.00      +0.6 /  +0.3    14.5  C30 H35 F3 N3 O Si

     539.2500    42.61

     540.2519    11.53
```

```
[ Mass Spectrum ]
Data : 10-C30H35F3N3OSi-HRFAB      Date : 17-Aug-2018 09:51
Instrument :  MStation
Sample : -
Inlet : Direct      Ion Mode : FAB+
Spectrum Type : Normal Ion  [EF-Linear]
```

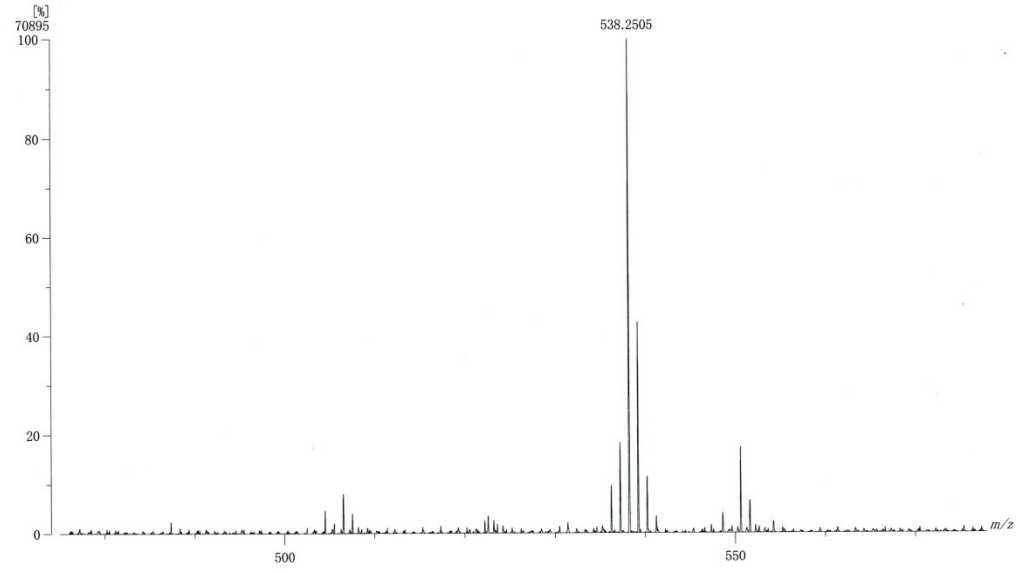

HRMS (ESI$^+$) of probe **ASiP^i-H_2O_2**

```
[ Theoretical Ion Distribution ]
Molecular Formula : C42 H53 N3 O4 Si B
                    (m/z   702.3898, MW   702.7970, U.S. 19.5)
Base Peak :   702.3906, Averaged MW :   702.7922(a),   702.7934(w)

    m/z        INT.
  701.3935  21.9518*************
  702.3906 100.0000****************************************************************
  703.3931  50.7731*******************************
  704.3941  16.7075**********
  705.3954   3.9938**
  706.3971   0.7283
  707.3992   0.1061
  708.4014   0.0128
  709.4038   0.0013
  710.4062   0.0001
```

```
Data : 11-C42H53BN3O4Si-HRFAB      Date : 17-Aug-2018 09:55
Instrument :  MStation
Sample : -
Note : -
Inlet : Direct      Ion Mode : FAB+
RT : 0.80 min      Scan# : (17,18)
Elements : C 42/0, H 53/0, N 3/0, O 4/0, Si 1/0, B 1/0
Mass Tolerance      : 3mmu
Unsaturation (U.S.) : -0.5 - 100.0

     Observed m/z   Int%      Err[ppm / mmu]    U.S. Composition
         700.3800   14.57

         701.3922   39.01

     1   702.3903  100.00      +0.7 /  +0.5    19.5  C42 H53 N3 O4 Si B

         703.4031   58.12

         704.4001   18.90
```

```
[ Mass Spectrum ]
Data : 11-C42H53BN3O4Si-HRFAB      Date : 17-Aug-2018 09:55
Instrument :  MStation
Sample : -
Inlet : Direct      Ion Mode : FAB+
Spectrum Type : Normal Ion  [EF-Linear]
```

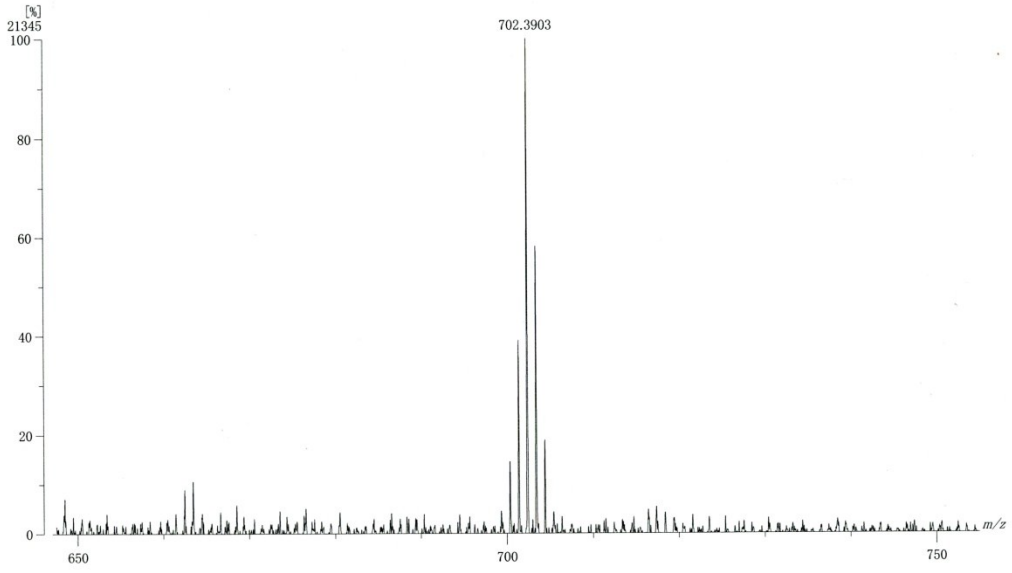

LCMS analysis data for selected compounds

(The left data are MS values; the smaller peak came from m/2z)

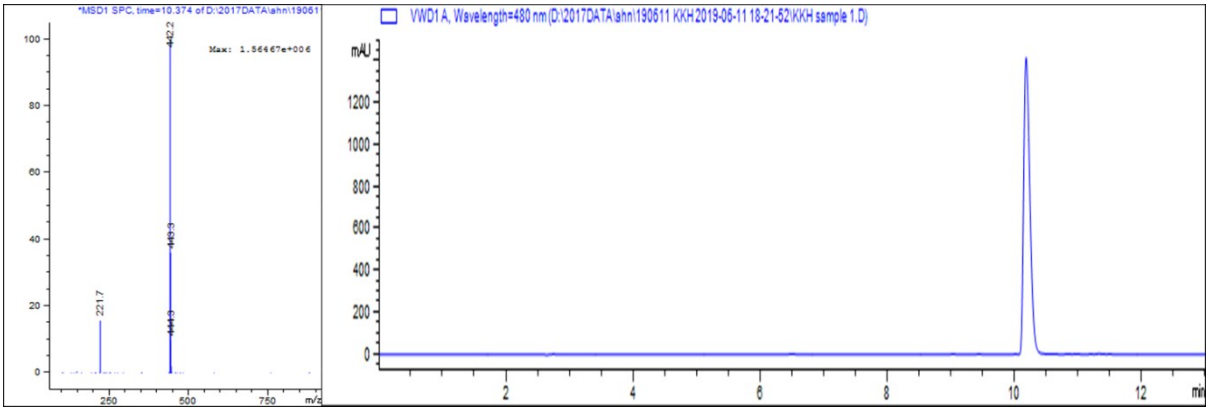

LCMS of ASiP^j **1**

LCMS of ASiP^j **2**

LCMS of ASiP^j **3**

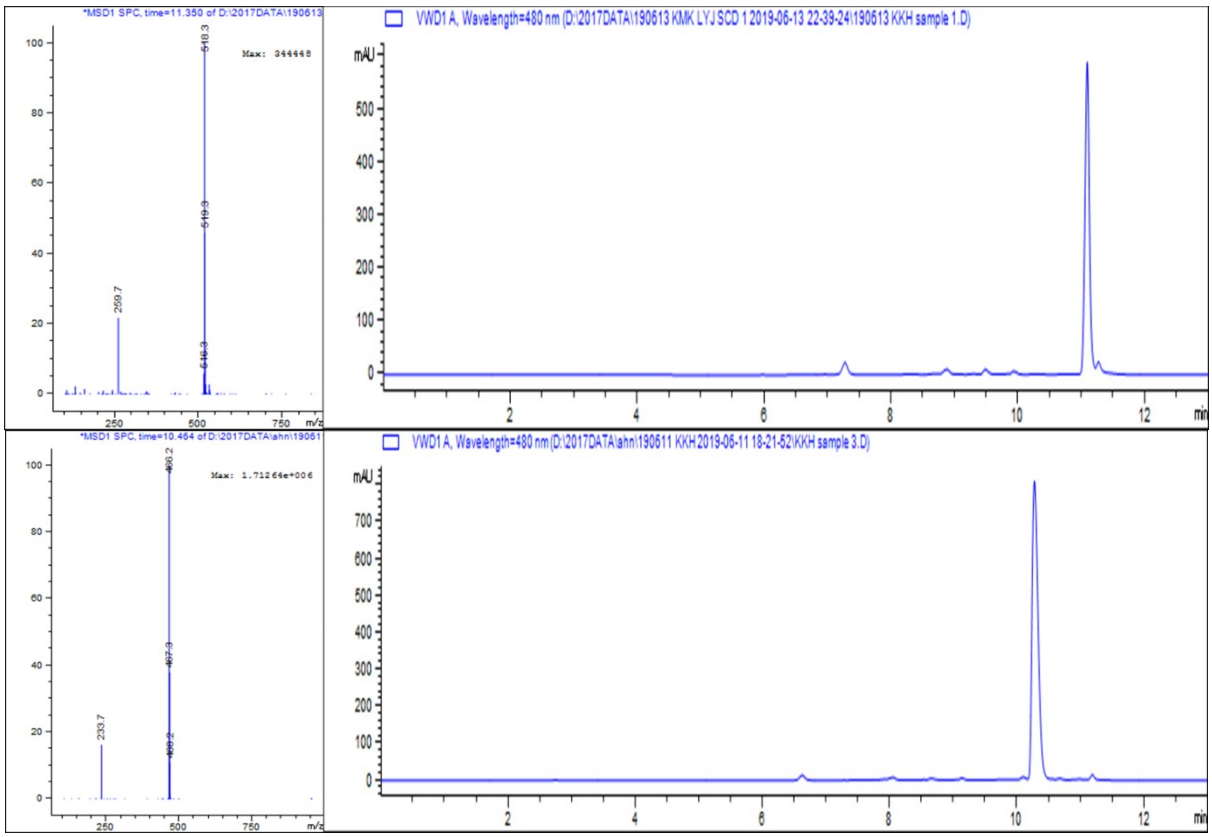

LCMS of NIR-ASiP^{j} **1**

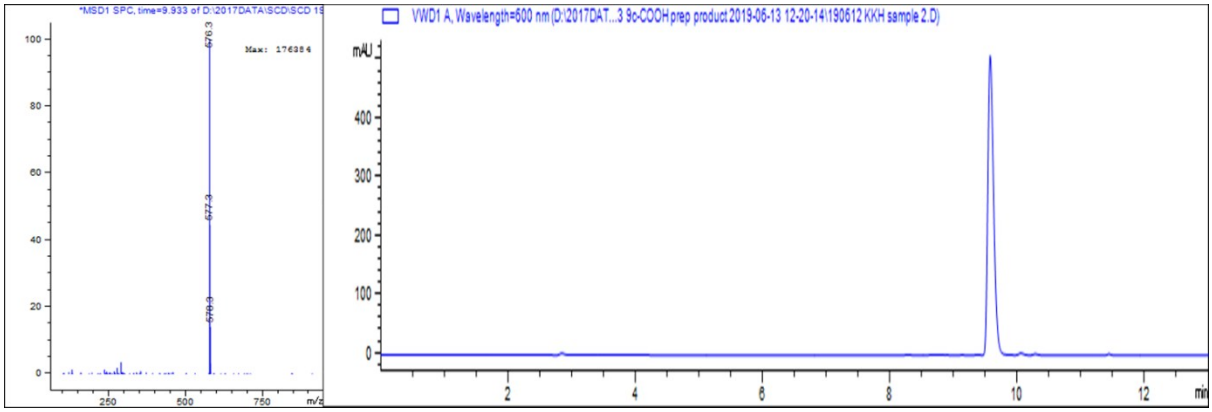

LCMS of NIR-ASiP^{j} **2**

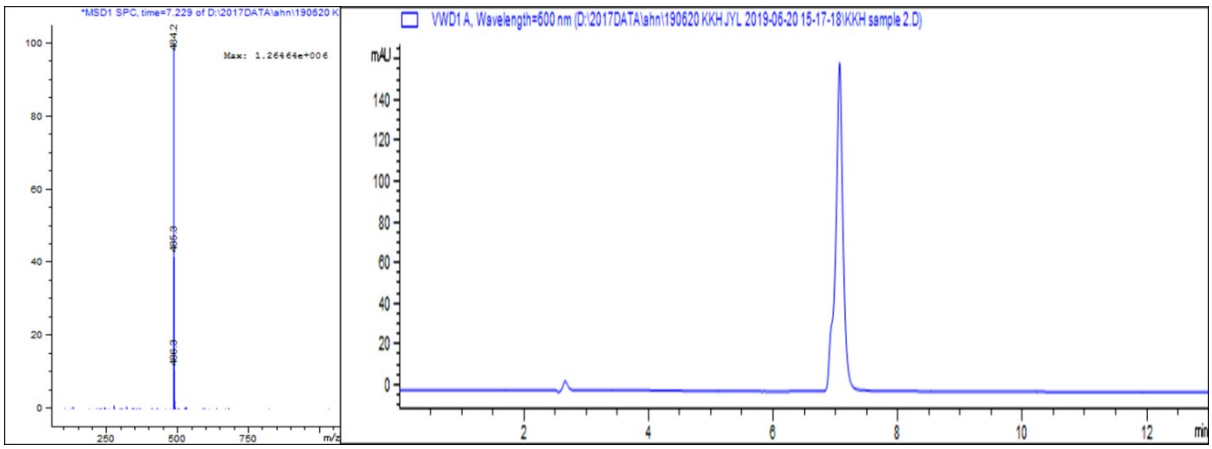

LCMS of NIR-ASiP^{j} **3**